ФИЗИКА ЭЛЕМЕНТАРНЫХ ЧАСТИЦ И АТОМНОГО ЯДРА
2014. Т. 45. ВЫП. 2

ISOTROPIC AND ANISOTROPIC DARK ENERGY MODELS

*B. Saha**

Joint Institute for Nuclear Research, Dubna

INTRODUCTION 586

DARK ENERGY 587

DARK ENERGY MODELS 590

- Λ-Term 591
- Quintessence 591
- k-Essence 592
- Chaplygin Gas 592
- Modified Chaplygin Gas 593
- Phantom-Type Dark Energy 593
- Oscillating Dark Energy 593
- Model with Interaction between Dark Energy and Dark Matter 594
- Scalar–Tensor Models of Dark Energy 595
- Models with Tachyon Matter 595
- Quintom Models of Dark Energy 595
- The Weyl–Eddington–Einstein Affine Gravity 596
- EoS Parameter as Dark Energy 596
- Models with Spinor Field 596

COSMOLOGICAL MODELS 598

- Spatially Homogeneous and Isotropic Models 598
- Spatially Homogeneous and Anisotropic Models 599
- Isotropic but Spatially Inhomogeneous Models 602
- Models with Two Ignorable Coordinates 602

BIANCHI TYPE-VI MODELS WITH A VARIABLE DECELERATION PARAMETER 603

- Solution to the Field Equations 605

*E-mail: bijan@jinr.ru; http://bijansaha.narod.ru

Physical Aspects of Dark Energy Model 607
BIANCHI TYPE-VI_0 MODELS WITH A VARIABLE EoS 612
Solution to the Field Equations 612
Physical Aspects of Dark Energy Model 614
BIANCHI TYPE-V SPACE–TIME WITH VARIABLE EoS PARAMETER 618
Solution to the Field Equations 619
Physical Aspects of Dark Energy Model 620
BIANCHI TYPE-III SPACE–TIME WITH VARIABLE EoS PARAMETER 624
Solution to the Field Equations 625
Physical Aspects of Dark Energy Model 626
BIANCHI TYPE-I COSMOLOGICAL MODELS 630
Model with Constant Deceleration Parameter 631
LRS BI Model with Dominance Dark Energy 636
INTERACTING TWO-FLUID SCENARIO IN FRW MODEL 643
Noninteracting Two-Fluid Model 644
Interacting Two-Fluid Scenario 650
Physical Acceptability and Stability of Solutions 654
CONCLUDING REMARKS ON THE RESULTS 656
REFERENCES 658

ФИЗИКА ЭЛЕМЕНТАРНЫХ ЧАСТИЦ И АТОМНОГО ЯДРА
2014. Т. 45. ВЫП. 2

ISOTROPIC AND ANISOTROPIC DARK ENERGY MODELS

B. Saha[*]

Joint Institute for Nuclear Research, Dubna

The evolution of the Universe filled with dark energy (DE) with or without perfect fluid is discussed. In doing so, we consider a number of cosmological models, namely Bianchi type I, III, V, VI_0, VI, and FRW one. For the anisotropic cosmological models we have used proportionality condition as an additional constraint. The exact solutions to the field equations in quadrature are found in the case of a BVI model. It was found that the proportionality condition used here imposed severe restriction on the energy–momentum tensor, namely, it leads to isotropic distribution of matter.

Anisotropic BVI_0, BV, BIII, and BI DE models with variable EoS parameter ω have been investigated by using a law of variation for the Hubble parameter. In this case the matter distribution remains anisotropic, though, depending on the concrete model, there appear different restrictions on the components of energy–momentum tensor. That is why we need an extra assumption such as a variational law for the Hubble parameter. It is observed that, at the early stage, the EoS parameter ω is positive, i.e., the Universe was matter-dominated at the early stage but at later time the Universe is evolving with negative values, i.e., the present epoch. DE model presents the dynamics of EoS parameter ω whose range is in good agreement with the acceptable range by the recent observations.

A spatially homogeneous and anisotropic locally rotationally symmetric Bianchi-I space–time filled with perfect fluid and anisotropic DE possessing dynamical energy density is studied. In the derived model, the EoS parameter of DE $(\omega^{(\mathrm{de})})$ is obtained as time varying and it is evolving with negative sign which may be attributed to the current accelerated expansion of Universe. The distance modulus curve of derived model is in good agreement with SNLS type Ia supernovae for high red-shift value which in turn implies that the derived model is physically realistic.

A system of two fluids within the scope of a spatially flat and isotropic FRW model is studied. The role of the two fluids, either minimally or directly coupled in the evolution of the dark energy parameter, has been investigated. In doing so, we have used three different *ansatzs* regarding the scale factor that gives rise to a variable decelerating parameter. It is observed that, in the noninteracting case, both the open and the flat Universes can cross the phantom region whereas in the interacting case only the open Universe can cross the phantom region. The stability and acceptability of the obtained solution are also investigated.

Обсуждается эволюция Вселенной, наполненной темной энергией с идеальной жидкостью или без нее. Мы рассмотрим несколько космологических моделей, а именно модели типа Бианки I, III, V, VI_0, VI и модель Фридмана–Робертсона–Уокера (FRW). Для анизотропных моделей в качестве дополнительного условия использовано условие пропорциональности. В случае Бианки типа VI найдено точное решение полевых уравнений в квадратурах. Показано, что условие пропорциональности в этом случае налагает жесткое ограничение на тензор энергии-импульса — оно приводит к изотропному распределению вещества.

[*]E-mail: bijan@jinr.ru; http://bijansaha.narod.ru

Анизотропные модели темной энергии типа Бианки VI_0, V, III и I с переменным параметром уравнения состояния ω были изучены с использованием вариационного принципа для параметра Хаббла. В этих моделях распределение вещества остается анизотропным, но в зависимости от конкретной модели возникают различные ограничения на компоненты энергии-импульса. По этой причине и понадобится дополнительное условие типа вариационного принципа для параметра Хаббла. Было обнаружено, что в начальной стадии эволюции параметр уравнения состояния ω положителен, т. е. на этой стадии Вселенная преимущественно заполнена веществом, а на поздней стадии эволюции параметр ω становится отрицательным, что соответствует настоящей эпохе. Модель темной энергии показывает динамику параметра ω, область изменения которого находится в хорошем соответствии с наблюдениями.

Изучено пространственно-однородное и анизотропное локально вращательно-симметричное пространство-время типа Бианки I, заполненное идеальной жидкостью и анизотропной темной энергией с меняющейся плотностью. В этой модели параметр уравнения состояния $(\omega^{(\mathrm{de})})$ меняется со временем и эволюционирует с отрицательным знаком, что может быть связано с ускоренным расширением Вселенной. Полученные результаты находятся в большом соответствии с наблюдательными данными.

В рамках пространственно плоской и изотропной модели FRW изучена система двух жидкостей. Выяснена их роль при прямой или минимальной связи в эволюции параметра темной энергии. При этом сделаны три предположения относительно масштабного фактора, которые порождают параметр замедления, зависящий от времени. Показано, что в случае минимальной связи открытые и плоские модели могут пересекать фантомную область, тогда как в случае прямого взаимодействия только открытая модель может сделать это. Также были изучены допустимость и устойчивость полученных решений.

PACS: 98.80.Cq

INTRODUCTION

Cosmology is a discipline to understand the nature of origin, evolution, large scale structure, and ultimate fate of the Universe. Being that, it is perhaps the oldest discipline of the world. From the very beginning of mankind, looking at the sky people were eager to know, where do they come from and who is behind these all. Many leaves it with God, while a few goes forward to get a logical answer. In their quest for knowledge they modeled the Universe in accord with the information they have at hand.

The start of scientific cosmology took place as early as in 1543 with Nicholas Copernicus suggesting the heliocentric model of the Universe. Further development of scientific cosmology is connected with the scientists like Galileo Galilei and Johannes Kepler, who provided both observational and theoretical support to this cause. The Isaac Newton took this mission forward. But the biggest boost for cosmology came in the 1920s with the theoretical works by A. Einstein, A. Friedmann, W. de Sitter and observations by E. Hubble.

Nevertheless, only after World War II ended, it moved from a speculative science to the much firmer ground of prediction, observation and verification. And it is because only then astronomers and astrophysicists took advantage of a powerful array of new tools and technologies. For the first time, astronomers began to make comprehensive studies of the sky at wavelengths other than the

visible. At the same time, they began to use rockets to lift their instruments far above the Earth surface. Eventually, they succeeded in placing instruments in space that brought dramatic confirmation of the Big Bang hypothesis — and pointed to yet stranger features of the Universe. And each of new findings, every single discovery of astrophysics poses an even greater challenge to the cosmologists to give theoretical explanation of these observations.

In this review, we plan to discuss the problem of late time acceleration and its possible solutions within the scope of both isotropic and anisotropic cosmological models.

The review is organized as follows: in Sec. 1, we give a brief review of dark energy; in Sec. 2, dark energy models are discussed; in Sec. 3, a short description of cosmological models is given; in Sec. 4, we study the Bianchi type-VI cosmological model; in Sec. 5, Bianchi type-VI_0 cosmological model filled with dark energy is investigated; in Sec. 6, Bianchi type-V model is studied; in Sec. 7, we study the Bianchi type-III dark energy model; in Sec. 8, the Bianchi type-I cosmological models are studied; in Sec. 9, we consider the isotropic and homogeneous FRW models and in Sec. 10, we give concluding remarks of the results obtained.

1. DARK ENERGY

In the early 20th century the common world-view held that the Universe is static — more or less the same throughout eternity. Even Albert Einstein supported this long-standing idea, and in order to get the steady state Universe he introduced cosmological constant in his famous system. So, when in 1922 the Russian meteorologist and mathematician Alexander Friedmann had published a set of possible mathematical solutions that gave a nonstatic Universe [68, 69], Einstein rejected it noting that this model was indeed a mathematically possible solution to the field equations. This model has gained big popularity only after the works of Robertson and Walker and became known as FRW model. This model describes a homogeneous and isotropic Universe. By homogeneity we mean that space has the same metric properties (measures) in all points, whereas by isotropy we mean that the space has the same measures in all directions. This idea of expanding Universe suggested the presence of an initial singularity, which means the finiteness of time.

Though the idea of an expanding Universe was supported both theoretically and experimentally, it was strongly believed that the Universe is expanding with deceleration. So, in 1998, when it was found that the Universe is expanding with acceleration, it comes like a bolt from the blue. The observations of type Ia supernova (SNeIa) in 1998 established that our Universe is currently accelerating [112, 113, 120] and recent observations of SNeIa of high confidence level [43, 121, 189] have further confirmed this. In addition, measurements of the

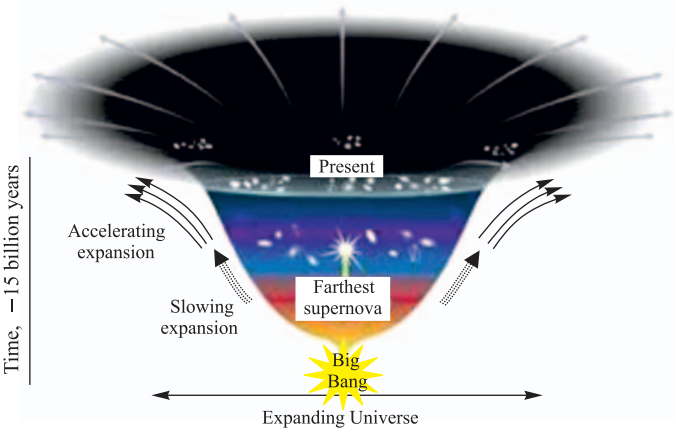

Fig. 1. Expansion of the Universe in the presence of a dark energy (Credit: Nasa; http://science.nasa.gov)

cosmic microwave background (CMB) [16] and large scale structure (LSS) [185] strongly indicate that our Universe is dominated by a component with negative pressure, dubbed as dark energy. In Fig. 1, the expansion of the Universe in the presence of a dark energy is shown.

Dark energy is a form of matter (energy) not observable in laboratory and it does not interact with electromagnetic radiation. These facts played decisive role in naming this object. In contrast to dark matter

— dark energy is uniformly distributed over the space;

— it does not intertwine under the influence of gravity in all scales;

— it has a strong negative pressure of the order of energy density.

Based on these properties, cosmologists have suggested a number of dark energy models, those are able to explain the current accelerated phase of expansion of the Universe.

What Dark Energy is? More is unknown than is known. We know how much dark energy there is because we know how it affects the Universe expansion. Other than that, it is a complete mystery. But it is an important mystery.

The Wilkinson Microwave Anisotropy Probe (WMAP) measures the composition of the Universe. The top chart shows a pie chart of the relative constituents today. A similar chart (bottom) shows the composition at 380,000 years old (13.7 billion years ago) when the light WMAP observes emanated. The composition varies as the Universe expands: the dark matter and atoms become less dense as the Universe expands, like an ordinary gas, but the photon and neutrino particles also lose energy as the Universe expands, so their energy density decreases faster than the matter. They formed a larger fraction of the Universe

13.7 billion years ago. It appears that the dark energy density does not decrease at all, so it now dominates the Universe even though it was a tiny contributor 13.7 billion years ago.

WMAP satellite experiment suggests 73% content of the Universe in the form of dark energy, 23% in the form of non-baryonic dark matter and the rest 4% in the form of the usual baryonic matter as well as radiation. The corresponding picture is given in Fig. 2.

Figure 3 shows the present accelerated mode of expansion and the future fate of the Universe depending on which way it evolves.

Thus, we see that the dark energy is really a very important component of the Universe and needs to be explained theoretically.

One explanation for dark energy is that it is a property of space. Albert Einstein was the first to realize that empty space is not nothing. Space has amazing properties, many of which are just begin-

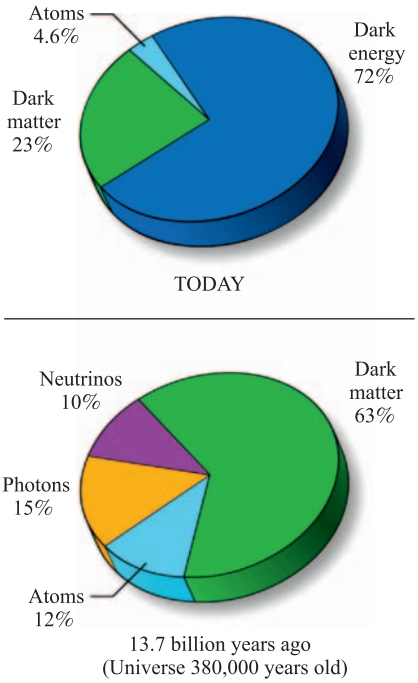

Fig. 2. Expansion of the Universe in the presence of a dark energy (Credit: Nasa/WMAP Science Team; http://www.gsfc.nasa.gov)

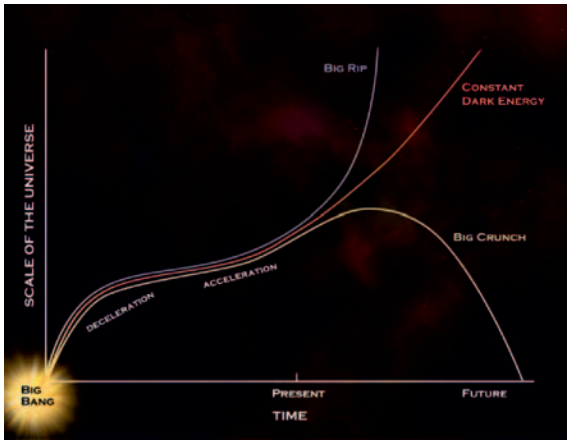

Fig. 3. The present day acceleration and future fate of the Universe (Credit: Wikipedia)

ning to be understood. The first property that Einstein discovered is that it is possible for more space to come into existence. Then one version of Einstein's gravity theory, the version that contains a cosmological constant, makes a second prediction: *empty space* can possess its own energy. Because this energy is a property of space itself, it would not be diluted as space expands. As more space comes into existence, more of this energy-of-space would appear. As a result, this form of energy would cause the Universe to expand faster and faster. Unfortunately, no one understands why the cosmological constant should even be there, much less why it would have exactly the right value to cause the observed acceleration of the Universe.

Another explanation for how space acquires energy comes from the quantum theory of matter. In this theory, *empty space* is actually full of temporary (*virtual*) particles that continually form and then disappear. But when physicists tried to calculate how much energy this fact would give empty space, the answer came out wrong — wrong by a lot. The number came out 10^{120} times too big. It is hard to get an answer to be so bad. So the mystery continues.

The third explanation for dark energy is that it is a new kind of dynamical energy fluid or field, something that fills all of space but something whose effect on the expansion of the Universe is the opposite of that of matter and normal energy. Some theorists have named this *quintessence*, after the fifth element of the Greek philosophers. But, if quintessence is the answer, we still do not know what it is like, what it interacts with, or why it exists. So the mystery continues.

Another possibility is that Einstein's theory of gravity is not correct. That would not only affect the expansion of the Universe, but it would also affect the way that normal matter in galaxies and clusters of galaxies behaved. This fact would provide a way to decide if the solution to the dark energy problem is a new gravity theory or not: we could observe how galaxies come together in clusters. But if it does turn out that a new theory of gravity is needed, what kind of theory would it be? How could it correctly describe the motion of the bodies in the Solar System, as Einstein's theory is known to do, and still give us the different prediction for the Universe that we need? There are candidate theories, but none are compelling. So the mystery continues.

2. DARK ENERGY MODELS

Given the fact that dark energy fills almost 3/4 of the Universe and there is no unambiguous answer to the question what dark energy is, cosmologists propose dark energy models in regular intervals. At present there are several candidates to explain this phenomenon of late time acceleration. In what follows we review a few of them.

2.1. Λ-Term. To ensure the sustainable cosmological solution to the gravitational field equations, Einstein introduced a fundamental constant, known as the cosmological constant, or Λ-term in the system [54, 55]. After Hubble experimentally confirmed that the Universe is expanding, Einstein returned to the original form equation, saying at the same time that the modification, which he did, was the biggest blunder of his life. The Λ-term made a temporary comeback in the late 60s of last century. Finally after the pioneer paper by A. Guth [78] on inflationary cosmology, researchers began to study the models with Λ-term with growing interest. An excellent overview of the cosmological constant can be found in [109].

With its introduction, the Einstein field equations take the form

$$G_\mu^\nu = R_\mu^\nu - \frac{1}{2}\delta_\mu^\nu R = -\varkappa T_\mu^\nu - \delta_\mu^\nu \Lambda. \tag{2.1}$$

In 1998, two groups [112, 120] independently showed that our Universe expands with acceleration confirming the existence of dark energy. The simplest form of dark energy is a positive cosmological constant. Introduction of a positive Λ-term corresponding to a universal repulsive force, leads to the present mode of the accelerated expansion. But it is accompanied by such theoretical problems as the fine-tuning, and coincidence problem [197] which states why the density of dark energy and dust matter density is currently comparable to, or why the Universe began to expand rapidly only right now. Another problem, which is associated with accelerated expansion, is a problem of eternal acceleration. Introduction of a negative Λ-term corresponding to an additional gravitational force can solve this problem [34]. Models with Λ-terms of the opposite sign were considered in [128, 137, 154].

2.2. Quintessence. The discovery that the expansion of the Universe is accelerating has promoted the search for new types of matter that can behave like a cosmological constant by combining positive energy density and negative pressure. Quintessence is a hypothetical form of dark energy, which is thought to be the fifth fundamental force. While the cosmological constant stays constant throughout time, quintessence changes over time due its dynamic character which is given by the equation of state. This is the most common type of dark energy [32, 138, 168, 210] with equation of state

$$p_{\mathrm{q}} = w_{\mathrm{q}} \varepsilon_{\mathrm{q}}, \tag{2.2}$$

with this ratio being a constant. Such an equation of state is well known, namely, when $w \in [0, 1]$, it describes a perfect fluid. With $w = -1$, it describes a typical cosmological constant (Λ-term) [109, 137, 167]. So if the Universe, filled with mostly similar substance, expands with acceleration, the condition $w < -1/3$ must be held. Usually, the constant w varies between -1 and $-1/3$, i.e.,

$w \in [-1, -1/3]$. This limitation is attributed to the following fact. The rigorous definition of w (both for the equilibrium state and for small perturbations) implies that when $w < 1$ the propagation velocity of small perturbations (for instance, the sound) in quintessence exceeds the speed of light and, hence, the inequality leads to violation of the causality principle. Many quintessence models behave like a tracker field that partially solves the cosmological constant problem [210]. In these models, the quintessence field has a density which closely tracks (but is less than) the radiation density until matter-radiation equality, which triggers quintessence to start having characteristics similar to dark energy, eventually dominating the Universe.

2.3. k-Essence. A key challenge for theoretical physics is to address the cosmic consequence problem: why does the dark energy component have a tiny energy density compared to the expectation based on the quantum field theory and why does the cosmic acceleration begin at such a late stage in the evolution of the Universe? Most dark energy candidates require extraordinary fine-tuning of the initial energy.

The purpose of introducing k-essence is to provide a dynamical explanation which does not require the fine-tuning of initial condition or mass parameters and which is decidedly nonanthropic.

A further property of k-essence is that, because of the dynamical attractor behavior, cosmic evolution is insensitive to initial conditions.

The k-essence component has the property that it only behaves as a negative pressure component after the matter-radiation equality, so that it can only overtake the matter density and induce cosmic acceleration after the matter has dominated the Universe for certain period. In general, k-essence is defined as a scalar field with noncanonical kinetic energy and can be given by the Lagrangian

$$L_{\mathrm{k}} = K(\phi)p(X), \quad X = \frac{1}{2}\nabla_\mu\phi\nabla^\mu\phi, \tag{2.3}$$

where $K(\phi) > 0$.

2.4. Chaplygin Gas. In order to combine these two different physical concepts as dark matter and dark energy, and thus reduce the two physical parameters in one, a rather exotic equation of state [91] was proposed

$$p_{\mathrm{ch}} = -\frac{A}{\varepsilon_{\mathrm{ch}}}. \tag{2.4}$$

In this paper, the authors described the transition of a Universe filled with dust in the rapidly expanding Universe. The model proposed in [91], was generalized in the works [17, 25]. Generalized Chaplygin gas model is given by the equation of state

$$p_{\mathrm{ch}} = -\frac{A}{\varepsilon_{\mathrm{ch}}^{\alpha}}, \tag{2.5}$$

where A is a positive constant and $0 < \alpha \leqslant 1$. Note that the original Chaplygin gas was introduced into aerodynamics [37]. There are quite a good number of works on this model [2, 11, 12, 15, 18, 19, 22, 24, 27, 44, 48, 58, 59, 73, 75, 76, 79, 80, 88, 96, 105, 107, 136, 170, 182].

2.5. Modified Chaplygin Gas. Modified Chaplygin gas (MCG) is the generalization of generalized Chaplygin gas $p = -B/\varepsilon^{\gamma}$ with the addition of a barotropic term $p = A\varepsilon$ and given by the EoS

$$p = A\varepsilon - \frac{B}{\varepsilon^{\alpha}}, \tag{2.6}$$

where A and B are the positive constants, and $0 \leqslant \alpha \leqslant 1$. The MCG parameters α and B have been constrained by the cosmic microwave background (CMB) data. The MCG is able to explain the cosmic accelerated expansion, and the EoS of MCG is valid from radiation era to Λ-CDM model.

2.6. Phantom-Type Dark Energy. Until recently it was assumed that the standard cosmological source of dark energy must have a small negative pressure, such that $-\varepsilon < p < 0$, and under no condition the pressure should exceed the mysterious barrier $p = -\varepsilon = -\Lambda$, which corresponds to cosmological constant. In this case only strong energy condition may be violated:

$$\varepsilon + 3p > 0, \quad \varepsilon + p > 0, \tag{2.7}$$

and the subsequent could follow one of the two scenarios: the Asymptotic Emptiness and the Big Crunch.

The phantom is dark energy with a strong negative pressure. It can be modeled by a scalar field with a negative kinetic energy given by the Lagrangian

$$L = \frac{k}{2}\partial_{\mu}\varphi\partial^{\mu}\varphi - V(\varphi), \tag{2.8}$$

where $k = -1$ corresponds to the phantom; while $k = 1$, to the standard scalar field. Here $V(\varphi)$ is a potential. The most striking result that is attributed to the phantom is that the energy density grows proportionally to the scale factor. Thus, in contrast to the standard sources, when the increase of the energy density corresponds to the reduction of the scale factor, in this case the energy density's increase is accompanied by the Universe expansion. This leads to the appearance of singularities in the future known as *Big Rip*. In this case the Universe becomes infinite during a finite time [46, 51]. Note that, in case of $w < -1$, Eq. (2.2) too gives rise to a phantom matter.

2.7. Oscillating Dark Energy. The discovery of positive accelerations gives rise to a number of problems. One of the most baffling of those is the problem of eternal acceleration [125]. A positive Λ-term, as well as the most dark energy models proposed so far, leads to the regime of eternal acceleration. In [181],

the authors proposed a cosmological model of a cyclic Universe experiencing periodical expansions and contractions. Every cycle begins with a Big Bang, terminates with a Big Crunch only to begin with a Big Bang again. The expansion phase of each cycle contains the eras of radiation, matter and quintessence. The last one corresponds to the modern accelerated mode of expansion.

In the paper [62], a cosmological model has been investigated, where the effective potential $V(\phi)$ might be negative for some values of ϕ. In this case the cyclic model of the Universe is realized. One of the simplest way to achieve cyclic models is to introduce a negative Λ-term together with some potential to the system [34, 128, 154]. Note that the models considered in [128, 154, 161] give both cyclic (also known as nonperiodic solutions, as the volume scale is strictly positive and when the volume scale tends to zero, there occurs a physical singularity, though the solution can be mathematically continued and enter into a new cycle) and oscillatory (positive in each space-time point) solutions. We have also proposed a model of quintessence with modified equation of state [138]

$$p = W(\varepsilon - \varepsilon_{\rm cr}), \quad W \in (-1, 0), \quad (2.9)$$

with $\varepsilon_{\rm cr}$ being some critical energy density. The model gives rise to cyclic or oscillatory Universe. Setting $\varepsilon_{\rm cr} = 0$, one obtains ordinary quintessence. As one sees from (2.9), the pressure is negative as long as $\varepsilon > \varepsilon_{\rm cr}$. Since with the expansion of the Universe the energy density decreases, at some moment of time ε becomes less than $\varepsilon_{\rm cr}$, i.e., $\varepsilon < \varepsilon_{\rm cr}$. This leads to the positive pressure and the contraction of the Universe. The corresponding behavior of energy density and pressure is given in Fig. 4.

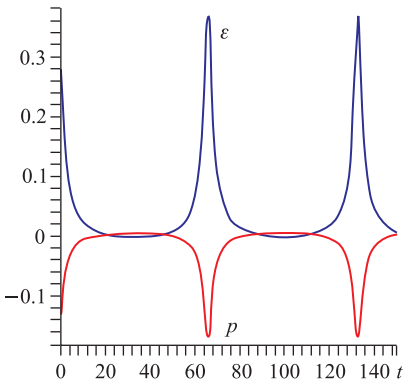

Fig. 4. Energy density and pressure of a quintessence with a modified equation of state oscillate

Oscillating dark energy with a periodic equation of state in two equivalent formulations was considered in [106]. It was shown that such a model assumes a natural unification of initial inflation with modern accelerating mode of expansion. Model with oscillating dark energy was also studied in [101].

2.8. Model with Interaction between Dark Energy and Dark Matter. Experimental checks conducted within the solar system impose strict constraints on the possibility of nonminimal interaction between dark energy and dark matter [200]. Nevertheless, a possibility of additional (nongravitational) interaction between them without a contradiction with the experimental data, appears due to the unknown nature of the dark matter as the main fraction of that background.

Moreover, it was established that the models with interacting dark energy are in good agreement with the modern observation data [108, 110]. It leads to the appearance of a number of papers offering the models with interacting dark matter and dark energy [42, 74].

2.9. Scalar–Tensor Models of Dark Energy. Scalar–tensor theory of gravitation is an alternative to or generalization of Einstein's theory of gravitation, where a scalar field is present in addition to the tensor field. It was proposed almost half a century ago in a series of papers [28, 64, 90], and even at present time remains important for explaining the accelerating expansion phase, especially in the inflation and quintessence scenarios. The main assumption of this theory is a connection between the matter and the scalar and gravitational fields φ and $g_{\mu\nu}$ via some effective metrics $\tilde{g}_{\mu\nu} = A^2(\varphi)g_{\mu\nu}$. In the paper [70], a scalar–tensor model of dark energy with a new degree of physical freedom has been considered. It is argued that the scalar field φ of graviton is responsible for the change of gravitational one. Scalar–tensor models of ordinary and phantom matter were studied in [71]. Similar models for Bianchi type-I space–time were constructed in [61]. In that paper dynamical behavior of metric functions was described for three different interactions.

2.10. Models with Tachyon Matter. The idea of tachyon is not new, and after a series of works [171, 172] the tachyon models found their application in cosmology. They were not observed experimentally and a few of them, rolling tachyon, for example, posses a very interesting equation of state, where the tachyon parameters exhibit smooth variations within the interval $(-1, 0)$. This very fact makes the tachyon one of the candidates for dark energy [35, 45, 174, 175, 180]. There are a number of tachyon dark energy models. One of the most effective models was proposed in [169]. It is defined by using cosmological diagnostic pairs (r, s) called the statefinders:

$$r = \frac{\partial^3 a/\partial t^3}{aH^3}, \quad s = \frac{r-1}{3(q-1/2)}, \tag{2.10}$$

where q is the deceleration parameter, and a is the scale factor of FRW space–time. Since different cosmological models related to the dark energy yield qualitatively different trajectories on the $r - s$ plane, the proposed diagnostics can help to distinguish between these models.

2.11. Quintom Models of Dark Energy. In order to understand the behavior of dark energy state equation (2.2) with $w > -1$ in the past and with $w < -1$ at present, quintom model of dark energy was proposed [63]. Quintom model is a dynamic model of dark energy and compared to the other models of dark energy it defines the cosmic evolution in a different way. One of the characteristics of quintom model is the fact that its equation of state can smoothly pass the value of $w = -1$ [30]. In contrast to (2.2), where w is a constant, in quintom model it

depends on time and can be given by the EoS

$$w(t) = -r - \frac{s}{t^2}, \tag{2.11}$$

where r and s are some parameters. Many authors have used quintom model in order to generate a bouncing Universe. Spinor description of quintom model was given in [31].

2.12. The Weyl–Eddington–Einstein Affine Gravity. Recently the Weyl–Eddington–Einstein affine gravity proposed by Weyl [199], Eddington [52, 53], and Einstein [56, 57] was further developed by Filippov and coauthors [47, 65–67]. In these papers the authors, based on the ideas of Weyl, Eddington, and Einstein, proposed an affine theory of gravity for D-dimensional space–time with symmetric connections. It was shown that such a theory can predict dark energy (the cosmological constant as a first approximation), a neutral massive (or tachyonic) vector field, and massive (or tachyonic) scalar fields. It was also shown that these fields couple only to gravity and may generate dark matter and/or inflaton. Further details of the theory, such as the nature of the scalar and vector fields, can describe massive particle, tachyon and phantom, depending on the concrete choice of the geometric Lagrangian.

2.13. EoS Parameter as Dark Energy. In addition to the models mentioned above recently attempt to describe dark energy by using a time-dependent parameter of equation of state [4, 5, 114, 115, 153, 166, 201] has been taken. In some of these models, it is assumed that the deceleration parameter is a constant. This yields two types of solutions — one of which is in the form of power function; while the second, exponential. These solutions describe the expanding nonsingular and singular Universes, respectively. The range of values for the equation of state w in both cases is in good agreement with recent observational data, namely: (i) SNe Ia data in 2003 [93], (ii) SNe Ia data collaborated with CMBR anisotropy and galaxy clustering statistics in 2004 [185], and (iii) a combination of cosmological datasets coming from CMB anisotropies, luminosity distances of high red-shift-type Ia supernovae and galaxy clustering 2009 [82, 94].

2.14. Models with Spinor Field. Recently, cosmological models with spinor field are widely studied by various authors [6, 127, 128, 154, 159, 160, 190]. One of the main objectives of [127, 128, 154, 159, 160] was to find regular solutions of the equations. In some cases, especially in the presence of a negative cosmological constant (Λ-term), which plays the role of the additional gravitational field, we were able to obtain regular solutions. It was also found that the introduction of a nonlinear spinor field leads to a rapid expansion of the Universe. This very fact allows us to consider the spinor field as a possible candidate for explaining the accelerated expansion phase. In connection with this, there appear a number of works [119, 139–141], where the spinor field is considered as an alternative model of dark energy.

Thus, it can be concluded that a suitable choice of spinor field nonlinearity
(i) *accelerates the isotropization process* [128, 131, 154];
(ii) *gives rise to a singularity-free Universe* [128, 129, 131, 154];
(iii) *generates late-time acceleration* [119, 139–142, 179].

Given the role that spinor field can play in the evolution of the Universe, question that naturally pops up is: if the spinor field can redraw the picture of evolution caused by perfect fluid and dark energy, then is it possible to simulate perfect fluid and dark energy by means of a spinor field? Affirmative answer to this question was given in a number of papers [95, 143–146]. In those papers, the authors have shown that different types of perfect fluid and dark energy can be described by nonlinear spinor field.

In [143], two types of nonlinearity were used, one occurs as a result of self-action and the other resulted from the interaction between the spinor and scalar fields. It was shown that the case with induced nonlinearity is the partial one and can be derived from the case with self-action. The description of generalized Chaplygin gas and modified quintessence in terms of spinor field and the study of the evolution of the Universe filled with nonlinear spinor field within the scope of a Bianchi type-I and FRW cosmological model were given in [144–146].

It was found that the spinor field Lagrangian

$$L_{\mathrm{sp}} = \frac{i}{2}\left[\Psi\gamma^{\mu}\nabla_{\mu}\Psi - \nabla_{\mu}\bar{\Psi}\gamma^{\mu}\Psi\right] - \nu S^{1+W} \tag{2.12}$$

simulates various types of matter depending on the value of W, namely:

$$W = 0 \quad \text{(dust)}, \tag{2.13a}$$
$$W = 1/3 \quad \text{(radiation)}, \tag{2.13b}$$
$$W \in (1/3,\, 1) \quad \text{(hard Universe)}, \tag{2.13c}$$
$$W = 1, \quad \text{(stiff matter)}, \tag{2.13d}$$
$$W \in (-1/3,\, -1) \quad \text{(quintessence)}, \tag{2.13e}$$
$$W = -1 \quad \text{(cosmological constant)}, \tag{2.13f}$$
$$W < -1 \quad \text{(phantom matter)}, \tag{2.13g}$$
$$W > 1 \quad \text{(ekpyrotic matter)}. \tag{2.13h}$$

Spinor field Lagrangian that describes a Chaplygin gas is given by (2.5).

In account of it the spinor field Lagrangian now reads

$$L_{\mathrm{sp}} = \frac{i}{2}\left[\Psi\gamma^{\mu}\nabla_{\mu}\Psi - \nabla_{\mu}\bar{\Psi}\gamma^{\mu}\Psi\right] - (A + \lambda K^{(1+\gamma)/2})^{1/(1+\gamma)}. \tag{2.14}$$

In Figs. 5 and 6 the evolution of the Universe caused by the spinor field given by (2.12) and (2.14) is illustrated.

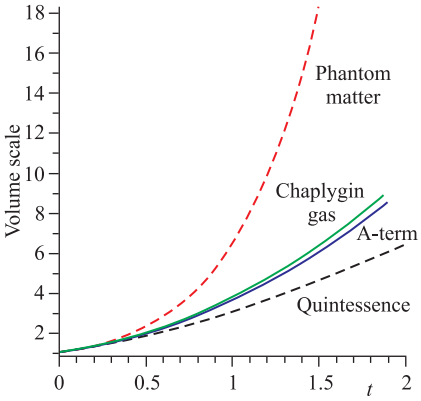

Fig. 5. Evolution of the Universe filled with dark energy

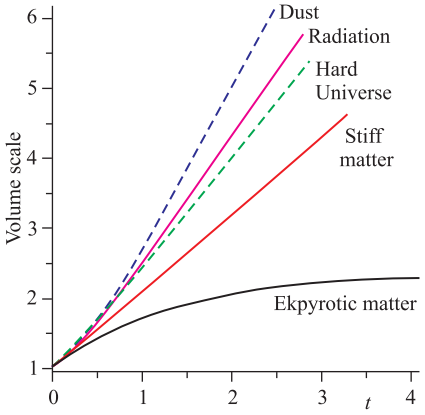

Fig. 6. Evolution of the Universe filled with perfect fluid

It should be noted that the specific behavior of spinor field in curve space–time with the exception of FRW model almost always gives rise to nontrivial nondiagonal components of the energy–momentum tensor. This nontriviality of nondiagonal components of the energy–momentum tensor imposes some severe restrictions either on the spinor field or on the metric functions. Within the BI space–time it is found that there exist two possibilities [151,152]. In one scenario, the initially anisotropic Universe evolves into an isotropic one asymptotically, but in this case the spinor field itself undergoes some severe restrictions. In the second scenario, the isotropization takes places almost at the beginning of the process.

3. COSMOLOGICAL MODELS

One of the principal goals of cosmological models is to describe the different phases of evolution of the Universe. The first epoch is that of rapid expansion of the Universe, also known as inflationary period. Most of the theories describe this phase by means of a scalar field related to the hypothetic inflaton. The next phase corresponds to the deceleration when the matter and radiation dominate over the scalar field. The present era is characterized by the accelerated mode of expansion where dark matter and dark energy play the dominating role. By this acceleration we understand the acceleration that we observe at present time.

Cosmological models, considered in literature, can be divided in a few groups [104].

3.1. Spatially Homogeneous and Isotropic Models. The simplest models of expanding Universe are the spatially homogeneous and isotropic ones. These are Friedmann–Lemiter–Robertson–Walker (FLRW) models and the Standard Model. These models were first studied by Friedmann [68], Robertson [122, 123], and

Walker [194]. Though the spatially homogeneous and isotropic FLRW models are widely used as a good approximation of present and early stages of evolution of the Universe, the large-scale distribution of matter in the observational Universe, mainly presented in the form of discrete structure, does not show the homogeneousness in higher order. Contrary to that, the cosmic microwave background radiation is significantly homogeneous. In the de Cartesian coordinates this distribution is given by

$$ds^2 = dt^2 - a^2(t)[dx^2 + dy^2 + dz^2], \tag{3.1}$$

where $a(t)$ is the scale factor. The most used version of this model is given by spherical coordinates and takes the form

$$ds^2 = dt^2 - R^2(t)\left[\frac{dr^2}{1-kr^2} + r^2(d\theta^2 + \sin^2(\theta)\, d\phi^2)\right], \tag{3.2}$$

where $R(t)$ is some unknown function of time, and k is some constant, taking the value $+1, 0, -1$. For $k = -1$ or $k = 0$ the space comes out to be infinity (open). For $k = 0$ the space is flat, while $k = +1$ space is finite (closed), though not limited.

3.2. Spatially Homogeneous and Anisotropic Models. Experimental studies of the isotropy of the cosmic microwave background radiation and reflection of the amount of helium formed in the initial stages of the evolution of the Universe, stimulated theoretical study of anisotropic cosmological models. At present stage of evolution, the Universe is spherically symmetric and the distribution of matter in it is generally isotropic and homogeneous. But in the early stages of evolution, the picture might not be as smooth as near the Big Bang singularity, the assumption of spherical symmetry, as well as that of isotropy could not be strictly valid. The anisotropy of the cosmic expansion, which is supposed to disappear with time, is a very important quantity. Recent experimental data as well as theoretical arguments support the existence of anisotropic expansion phase, which evolves into an isotropic one. This very fact forces one to study evolution of the Universe with the anisotropic background.

Cosmologists use the term to describe the uneven temperature distribution of the cosmic microwave background radiation. There is evidence for the so-called *Axis of Evil* in the early Universe that is at odds with the currently favored theory of rapid expansion after the Big Bang. Cosmic anisotropy has also been seen in the alignment of the galaxies' rotation axes and polarization angles of quasars.

In Fig. 3.2, the cosmic microwave temperature fluctuations from the 5-year WMAP data are seen over the full sky. The average temperature is 2.725 K, and the colors represent the tiny temperature fluctuations, as in a weather map. Red regions are warmer and blue regions are colder by about 0.0002 K.

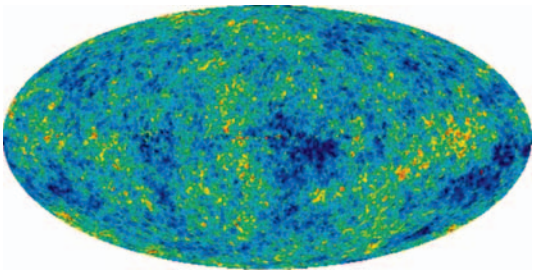

Fig. 7 (color online). The 5-year WMAP image of background cosmic radiation (2010) (Credit NASA/WMAP Science Team; http://www.gsfc.nasa.gov)

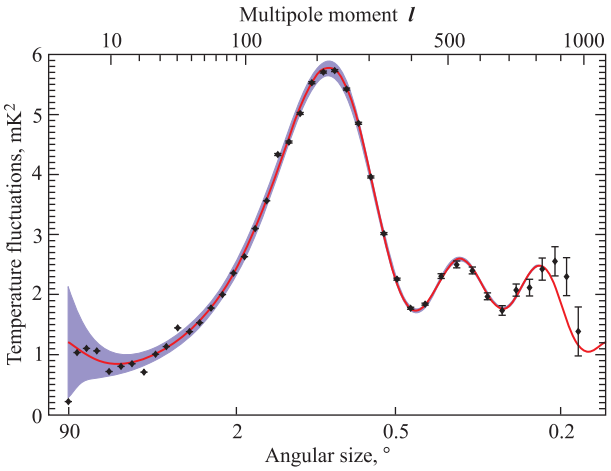

Fig. 8. The 5-year WMAP image of background cosmic radiation (2010) (Credit NASA/WMAP Science Team; http://www.gsfc.nasa.gov)

Figure 8 illustrates how much the temperature fluctuates on different angular sizes in the map of Fig. 3.2. Very large angles are on the left, and smaller angles are on the right. Note that there is the large first peak, illustrating a preferred spot size in the map. This means that there is a preferred length for the sound waves in the early Universe, just as a guitar string length produces a specific note. The second and third peaks are the harmonic overtones of the first peak. The third overtone is now clearly captured in the new 5-year WMAP data. It helps provide evidence for the proportion of neutrinos in the early Universe.

The first anisotropic model to study the realistic cosmological problems was used by Lemaitre [99]. The aim of his work was to clarify whether the Big Bang singularity, that appears in the FRW model, is simply the consequence of the pro-

posed symmetry. By the end of 1960s, three different paradigms of astrophysical studies defined the interest towards homogeneous but anisotropic models [188]: discussing the probability of a primordial magnetic field Zel'dovich [208] and Thorne [187] considered the anisotropic models; studying the factors that can affect the quantity of primordial helium in the Bing Bang cosmology, Hawking and Tayler [81] considered the anisotropic models; Kristian and Sachs [97], as well as Kantowski and Sachs [92], considered the anisotropic models in order to study the degree of isotropy of our Universe. Zel'dovich was the first to propose that the early isotropization process of cosmic expansion could occur as a result of quantum effect of particle creation near singularity [209]. This assumption was farther supported by different authors [84, 85, 103].

Here we give a short description of Bianchi models as well as a few others.

The first group of Bianchi models can be given by [129, 130]

$$ds^2 = dt^2 - a_1^2\,\mathrm{e}^{-2m_1 z}\,dx^2 - a_2^2\,\mathrm{e}^{2m_2 z}\,dy^2 - a_3^2\,dz^2, \tag{3.3}$$

with a_1, a_2, a_3 being the functions of time only. Here m, n are some arbitrary constants and the velocity of light is taken to be unity. The metric (3.3) is known as Bianchi type-VI model. A suitable choice of m_1, m_2 as well as of the metric functions a_1, a_2, a_3 in the BVI given by (3.3) evokes the following Bianchi-type Universes. Thus

• for $m_1 = m_2$, the BVI metric transforms to a Bianchi-type VI_0 (BVI_0) one, i.e., $m_1 = m_2$, BVI $\Longrightarrow$ $\mathrm{BVI}_0 \in$ open FRW with the line elements

$$ds^2 = dt^2 - a_1^2\,\mathrm{e}^{-2m_1 z}\,dx^2 - a_2^2\,\mathrm{e}^{2m_1 z}\,dy^2 - a_3^2\,dz^2; \tag{3.4}$$

• for $m_1 = -m_2$, the BVI metric transforms to a Bianchi-type V (BV) one, i.e., $m_1 = -m_2$, BVI $\Longrightarrow$ BV $\in$ open FRW with the line elements

$$ds^2 = dt^2 - a_1^2\,\mathrm{e}^{2m_1 z}\,dx^2 - a_2^2\,\mathrm{e}^{2m_1 z}\,dy^2 - a_3^2\,dz^2; \tag{3.5}$$

• for $m_2 = 0$, the BVI metric transforms to a Bianchi-type III (BIII) one, i.e., $m_2 = 0$, BVI $\Longrightarrow$ BIII with the line elements

$$ds^2 = dt^2 - a_1^2\,\mathrm{e}^{-2m_1 z}\,dx^2 - a_2^2\,dy^2 - a_3^2\,dz^2; \tag{3.6}$$

• for $m_1 = m_2 = 0$, the BVI metric transforms to a Bianchi-type I (BI) one, i.e., $m_1 = m_2 = 0$, BVI $\Longrightarrow$ BI with the line elements

$$ds^2 = dt^2 - a_1^2\,dx^2 - a_2^2\,dy^2 - a_3^2\,dz^2; \tag{3.7}$$

• for $m_1 = m_2 = 0$ and equal scale factor in all three directions, the BVI metric transforms to a Friedmann–Robertson–Walker (FRW) Universe, i.e., $m_1 = m_2 = 0$ and $a = b = c$, BVI $\Longrightarrow$ FRW with the line elements

$$ds^2 = dt^2 - a^2(dx^2 + dy^2 + dz^2). \tag{3.8}$$

The anisotropic nondiagonal Bianchi space–times take the form [147, 148]

$$ds^2 = dt^2 - a_1^2(t)\,dx_1^2 - \left[h^2(x_3)a_1^2(t) + f^2(x_3)a_2^2(t)\right]\,dx_2^2 - \\ - a_3^2(t)\,dx_3^2 + 2a_1^2(t)h(x_3)\,dx_1\,dx_2, \quad (3.9)$$

with a_1, a_2, a_3 being the functions of t; and h, f, functions of x_3 only. Defining

$$\delta = -\frac{1}{f}\frac{\partial^2 f}{\partial x_3^2} \quad (3.10)$$

from (3.9) we find BII, BVIII, and BIX models, respectively, as follows:

$$\delta = 0 \quad \text{corresponds to BII model,} \quad (3.11a)$$

$$\delta = -1 \quad \text{corresponds to BVIII model,} \quad (3.11b)$$

$$\delta = 1 \quad \text{corresponds to BIX model.} \quad (3.11c)$$

The Kantowski–Sachs models can be defined as [83]

$$ds^2 = -d\tau^2 - H(\tau)\,dr^2 - R^2(\tau)(d\theta^2 + \sin^2(\theta)\,d\phi^2), \quad (3.12)$$

where τ is cosmological time.

3.3. Isotropic but Spatially Inhomogeneous Models. These are the spherically symmetric models of Tolman–Bondi, which were first discussed by Lemaitre [99]. In general, the spherically symmetric metric takes the form

$$ds^2 = Y^2\left[\left(d\theta^2 + \sin^2(\theta)d\phi^2\right)\right] + \mathrm{e}^{2\lambda}dr^2 - \mathrm{e}^{2\nu}dt^2, \quad (3.13)$$

where $Y = Y(r,t)$, $\lambda = \lambda(r,t)$, and $\nu = \nu(r,t)$.

The Tolman–Bondi metric is given by [72]

$$ds^2 = -dt^2 + \frac{Y'^2}{1-kr^2}dr^2 + Y^2\left(d\theta^2 + \sin^2(\theta)\,d\phi^2\right), \quad (3.14)$$

where $Y = Y(r,\,t)$. Here stroke denotes differentiation with respect to r. The indices $k = 0,\,\pm 1$ correspond to flat, closed, and open geometry.

3.4. Models with Two Ignorable Coordinates. Models with two ignorable coordinates usually have two commuting Killing vectors. It might be plane-symmetric or cylindrically-symmetric models. The plane-symmetric models are given by [162–164, 183, 184]

$$ds^2 = e^{2\chi}dt^2 - \mathrm{e}^{2\alpha}\,dx^2 - \mathrm{e}^{2\beta}(dy^2 + dz^2), \quad (3.15)$$

where the velocity of light c is taken to be unity, and χ, α, β are the functions of x and t.

The cylindrically-symmetric models take the form [29, 126, 176]

$$ds^2 = \mathrm{e}^{2\gamma}dt^2 - \mathrm{e}^{2\alpha}dx^2 - \mathrm{e}^{2\beta}dy^2 - \mathrm{e}^{2\mu}dz^2, \tag{3.16}$$

where the metric functions depend on x only. Sometimes, it is convenient to use the harmonic coordinates, satisfying the coordinate condition

$$\alpha = \gamma + \beta + \mu. \tag{3.17}$$

In the sections to follow, we consider the dark energy models within the scope of different Bianchi models as well as FRW one. In doing so, we only consider the cases, when the energy–momentum tensor has only nontrivial diagonal elements, i.e.,

$$T_\alpha^\beta = \mathrm{diag}\,[T_0^0,\, T_1^1,\, T_2^2,\, T_3^3]. \tag{3.18}$$

4. BIANCHI TYPE-VI MODELS WITH A VARIABLE DECELERATION PARAMETER

A Bianchi type-VI model describes an anisotropic but homogeneous Universe. This model was studied by several authors [87, 129, 130, 165, 178, 195, 207], specially due to the existence of magnetic fields in galaxies, which was proved by a number of astrophysical observations. A spinor description of dark energy within the scope of a BVI model was given in [146].

Bianchi type-VI model is given by [129, 130]

$$ds^2 = dt^2 - a_1^2\,\mathrm{e}^{-2m_1 z}\,dx^2 - a_2^2\,\mathrm{e}^{2m_2 z}\,dy^2 - a_3^2\,dz^2, \tag{4.1}$$

with a_1, a_2, a_3 being the functions of time only. Here m, n are some arbitrary constants and the velocity of light is taken to be unity. The metric (4.1) is known as Bianchi type-VI model. A suitable choice of m, n as well as of the metric functions a_1, a_2, a_3 in the BVI given by (4.1) evokes Bianchi-type VI_0, V, III, I and FRW Universes.

The Einstein field equations for the metric (4.1) on account of (3.18) have the form [129]

$$\frac{\ddot a_2}{a_2} + \frac{\ddot a_3}{a_3} + \frac{\dot a_2}{a_2}\frac{\dot a_3}{a_3} - \frac{m_2^2}{a_3^2} = \kappa T_1^1, \tag{4.2a}$$

$$\frac{\ddot a_3}{a_3} + \frac{\ddot a_1}{a_1} + \frac{\dot a_3}{a_3}\frac{\dot a_1}{a_1} - \frac{m_1^2}{a_3^2} = \kappa T_2^2, \tag{4.2b}$$

$$\frac{\ddot a_1}{a_1} + \frac{\ddot a_2}{a_2} + \frac{\dot a_1}{a_1}\frac{\dot a_2}{a_2} + \frac{m_1 m_2}{a_3^2} = \kappa T_3^3, \tag{4.2c}$$

$$\frac{\dot a_1}{a_1}\frac{\dot a_2}{a_2} + \frac{\dot a_2}{a_2}\frac{\dot a_3}{a_3} + \frac{\dot a_3}{a_3}\frac{\dot a_1}{a_1} - \frac{m_1^2 - m_1 m_2 + m_2^2}{a_3^2} = \kappa T_0^0, \tag{4.2d}$$

$$m_1\frac{\dot a_1}{a_1} - m_2\frac{\dot a_2}{a_2} - (m_1 - m_2)\frac{\dot a_3}{a_3} = 0. \tag{4.2e}$$

We define the spatial volume of the model (4.1) as

$$V = a_1 a_2 a_3, \tag{4.3}$$

and the average scale factor as

$$a = V^{1/3} = (a_1 a_2 a_3)^{1/3}. \tag{4.4}$$

Let us now find expansion and shear for BVI metric. The expansion is given by

$$\vartheta = u^{\mu}_{;\mu} = u^{\mu}_{\mu} + \Gamma^{\mu}_{\mu\alpha} u^{\alpha}, \tag{4.5}$$

and the shear is given by

$$\sigma^2 = \frac{1}{2}\sigma_{\mu\nu}\sigma^{\mu\nu}, \tag{4.6}$$

with

$$\sigma_{\mu\nu} = \frac{1}{2}\left[u_{\mu;\alpha}P^{\alpha}_{\nu} + u_{\nu;\alpha}P^{\alpha}_{\mu}\right] - \frac{1}{3}\vartheta P_{\mu\nu}, \tag{4.7}$$

where the projection vector P is

$$P^2 = P, \quad P_{\mu\nu} = g_{\mu\nu} - u_{\mu}u_{\nu}, \quad P^{\mu}_{\nu} = \delta^{\mu}_{\nu} - u^{\mu}u_{\nu}. \tag{4.8}$$

In comoving system we have $u^{\mu} = (1, 0, 0, 0)$. In this case one finds

$$\vartheta = \frac{\dot{a}_1}{a_1} + \frac{\dot{a}_2}{a_2} + \frac{\dot{a}_3}{a_3} = \frac{\dot{V}}{V} \tag{4.9}$$

and

$$\sigma^1_1 = -\frac{1}{3}\left(-2\frac{\dot{a}_1}{a_1} + \frac{\dot{a}_2}{a_2} + \frac{\dot{a}_3}{a_3}\right) = \frac{\dot{a}_1}{a_1} - \frac{1}{3}\vartheta, \tag{4.10}$$

$$\sigma^2_2 = -\frac{1}{3}\left(-2\frac{\dot{a}_2}{a_2} + \frac{\dot{a}_3}{a_3} + \frac{\dot{a}_1}{a_1}\right) = \frac{\dot{a}_2}{a_2} - \frac{1}{3}\vartheta, \tag{4.11}$$

$$\sigma^3_3 = -\frac{1}{3}\left(-2\frac{\dot{a}_3}{a_3} + \frac{\dot{a}_1}{a_1} + \frac{\dot{a}_2}{a_2}\right) = \frac{\dot{a}_3}{a_3} - \frac{1}{3}\vartheta. \tag{4.12}$$

One then finds

$$\sigma^2 = \frac{1}{2}\left[\sum_{i=1}^{3}\left(\frac{\dot{a}_i}{a_i}\right)^2 - \frac{1}{3}\vartheta^2\right] = \frac{1}{2}\left[\sum_{i=1}^{3} H_i^2 - \frac{1}{3}\vartheta^2\right]. \tag{4.13}$$

As one sees, neither the expansion nor the components of shear tensor depend on m or n, hence the Bianchi cosmological models of type VI, VI_0, V, III, and I have the same expansion and shear tensor.

The Hubble constant of the model is defined by

$$H = \frac{\dot{a}}{a} = \frac{1}{3}\left(\frac{\dot{a}_1}{a_1} + \frac{\dot{a}_2}{a_2} + \frac{\dot{a}_3}{a_3}\right) = \frac{1}{3}\frac{\dot{V}}{V}. \tag{4.14}$$

The deceleration parameter q and the average anisotropy parameter A_m are defined by

$$q = -\frac{a\ddot{a}}{\dot{a}^2} = 2 - 3\frac{V\ddot{V}}{\dot{V}^2}, \tag{4.15}$$

$$A_m = \frac{1}{3}\sum_{i=1}^{3}\left(\frac{H_i}{H} - 1\right)^2, \tag{4.16}$$

where H_i are the directional Hubble constants:

$$H_1 = \frac{\dot{a}_1}{a_1}, \quad H_2 = \frac{\dot{a}_2}{a_2}, \quad H_3 = \frac{\dot{a}_3}{a_3}. \tag{4.17}$$

Note that, none of the above-defined quantities depends on m or n, hence it will be valid not only for BVI, but also for BVI_0, BV, BIII, and BI.

4.1. Solution to the Field Equations. From (4.2e) immediately follows

$$\left(\frac{a_1}{a_3}\right)^{m_1} = k_1\left(\frac{a_2}{a_3}\right)^{m_2}, \quad k_1 = \text{const}. \tag{4.18}$$

We also impose to use the proportionality condition, widely used in literature, demanding that the expansion is proportion to a component of the shear tensor, namely:

$$\vartheta = N_3\sigma_3^3. \tag{4.19}$$

The motivation behind assuming this condition is explained with reference to Thorne [188], the observations of the velocity-red-shift relation for extragalactic sources suggest that Hubble expansion of the Universe is isotropic today within $\approx 30\%$ [92, 97]. To put more precisely, red-shift studies place the limit

$$\frac{\sigma}{H} \leqslant 0.3 \tag{4.20}$$

on the ratio of shear σ to Hubble constant H in the neighborhood of our Galaxy today. Collins et al. (1980) have pointed out that for spatially homogeneous metric, the normal congruence to the homogeneous expansion satisfies that the condition σ/θ is constant.

On account of (4.9) and (4.12) we find

$$a_3 = N_0 V^{\frac{1}{3}+\frac{1}{N_3}}, \quad N_0 = \text{const}. \tag{4.21}$$

In view of (4.3) and (4.21) from (4.18) we find [149]

$$a_1 = k_1^{\frac{1}{m_1+m_2}} N_0^{\frac{m_1-2m_2}{m_1+m_2}} V^{\frac{1}{3}+\frac{m_1-2m_2}{3N_3(m_1+m_2)}}, \tag{4.22}$$

$$a_2 = k_1^{-\frac{1}{m_1+m_2}} N_0^{\frac{m_2-2m_1}{m_1+m_2}} V^{\frac{1}{3}+\frac{m_2-2m_1}{3N_3(m_1+m_2)}}. \tag{4.23}$$

Thus, we have derived metric functions in terms of V. In order to find the equation for V, we take the following steps. Subtractions of (4.2a) from (4.2b), (4.2c) from (4.2c), and (4.2c) from (4.2a) on account of (4.22), (4.23) and (4.21) give

$$\frac{\ddot{V}}{V} - \frac{N_3(m_1+m_2)^2}{3N_0^2V^{2/3+2/N_3}} = \kappa\frac{T_2^2 - T_1^1}{X_{12}}, \tag{4.24a}$$

$$\frac{\ddot{V}}{V} - \frac{N_3(m_1+m_2)^2}{3N_0^2V^{2/3+2/N_3}} = \kappa\frac{T_3^3 - T_2^2}{X_{23}}, \tag{4.24b}$$

$$\frac{\ddot{V}}{V} - \frac{N_3(m_1+m_2)^2}{3N_0^2V^{2/3+2/N_3}} = \kappa\frac{T_1^1 - T_3^3}{X_{31}}, \tag{4.24c}$$

where $X_{12} = 3(m_1 - m_2)/N_3(m_1 + m_2)$, $X_{23} = -3m_1/N_3(m_1 + m_2)$, and $X_{31} = 3n_2/N_3(m_1 + m_2)$. From (4.24) immediately follows

$$\frac{T_2^2 - T_1^1}{X_{12}} = \frac{T_3^3 - T_2^2}{X_{23}} = \frac{T_1^1 - T_3^3}{X_{31}}. \tag{4.25}$$

After a little manipulation, it could be established that

$$T_1^1 = T_2^2 = T_3^3 \equiv -p. \tag{4.26}$$

Thus we conclude that under the proportionality condition, the energy-momentum distribution of the model should be strictly isotropic. Let us now go back to the equation for V that now reads

$$\ddot{V} - A_0V^{(N_3-6)/3N_3} = 0, \qquad A_0 = \frac{N_3(m_1+m_2)^2}{3N_0^2}, \tag{4.27}$$

which allows the solution in quadrature

$$\int \frac{dV}{\sqrt{A_1V^{(4N_3-6)/3N_3} + C_0}} = t + t_0, \qquad A_1 = \frac{3N_3A_0}{(2N_3-3)}, \quad t_0 = \text{const}. \tag{4.28}$$

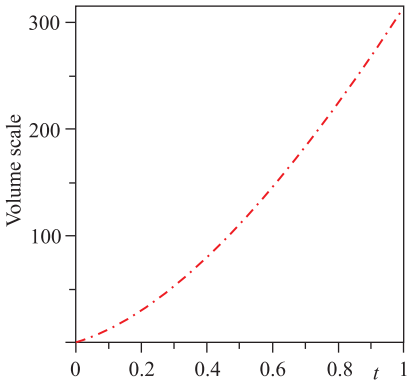

Fig. 9. Evolution of the Universe given by a BVI cosmological model

Thus we have the solution to the corresponding equation in quadrature. The system was further studied numerically. In doing so, we have used the following values for the problem parameters: $\kappa = 1$, $N_0 = 0.01$, $C_0 = -1$, $N_3 = 3$, $m_1 = 0.1$, $m_2 = 0.3$, $V(0) = 1.0E-6$ and $\dot{V}(0) = 0$.

Figure 9 shows the evolution of the Universe. As one sees, it is an expanding one.

4.2. Physical Aspects of Dark Energy Model. Let us now find the expressions for physical quantities.

Inserting (4.28) into (4.14) and (4.15) one finds the expression for expansion ϑ, Hubble parameter H:

$$\vartheta = 3H = \sqrt{A_1 V^{-(2N_3+6)/3N_3} + C_0/V^2}, \tag{4.29}$$

and deceleration parameter

$$q = 2 - \frac{3A_0 V^{-(2N_3+6)/3N_3}}{A_1 V^{-(2N_3+6)/3N_3} + C_0/V^2}. \tag{4.30}$$

The anisotropy parameter A_m has the expression

$$A_m = \frac{54(m_1^2 - m_1 m_2 + m_2^2)}{N_3^2 (m_1 + m_2)^2}. \tag{4.31}$$

The directional Hubble parameters are

$$\begin{gathered} H_1 = \left[\frac{1}{3} - \frac{2m_2 - m_1}{N_3(m_1 + m_2)}\right]\frac{\dot V}{V}, \\ H_2 = \left[\frac{1}{3} - \frac{2m_1 - m_2}{N_3(m_1 + m_2)}\right]\frac{\dot V}{V}, \quad H_3 = \left[\frac{1}{3} + \frac{1}{N_3}\right]\frac{\dot V}{V}. \end{gathered} \tag{4.32}$$

Figures 10 and 11 show the behavior of the Hubble parameter and deceleration parameter, respectively. It should be noted that we have confined to that interval of time, which shows the most interesting behavior of the physical quantities in question.

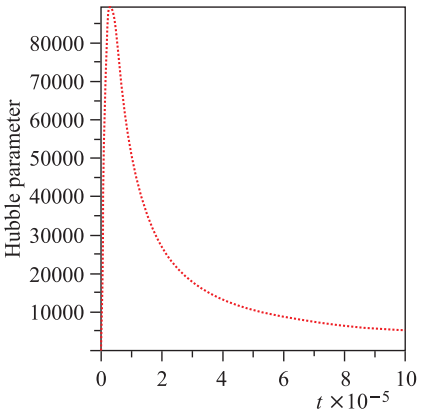

Fig. 10. Evolution of the Hubble parameter

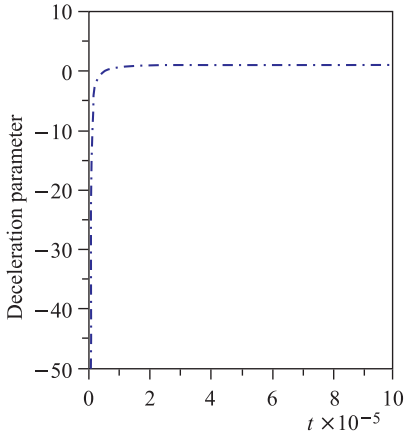

Fig. 11. Evolution of the deceleration parameter

From (4.2d) we find the expression for energy density

$$\varepsilon = T_0^0 = \frac{1}{\kappa}\left[X_1 V^{-2} - X_2 V^{-(2N_3+6)/3N_3}\right], \tag{4.33}$$

where

$$X_1 = \left[\frac{1}{3} - 3\frac{m_1^2 - m_1 m_2 + m_2^2}{N_3^2(m_1+m_2)^2}\right]C_0, \quad X_2 = \frac{m_1^2 - m_1 m_2 + m_2^2}{N_0^2} - \frac{X_1 A_1}{C_0}.$$

Further we obtain

$$\omega = \frac{p}{\varepsilon} = -\frac{X_1 - X_4 V^{(4N_3-6)/3N_3}}{X_1 - X_2 V^{(4N_3-6)/3N_3}}, \tag{4.34}$$

where

$$X_4 = \frac{2N_3 - 3}{3N_3}A_0 + \frac{m_1 m_2}{N_0^2} - \frac{X_1 A_1}{C_0}.$$

Figures 12 and 13 show the behavior of the energy density and EoS parameter, respectively. As we see, energy density is a decreasing function of time, while the EoS parameter changes its sign.

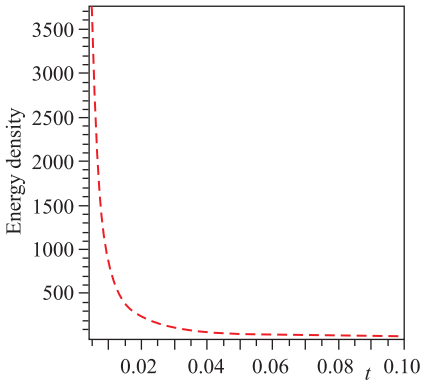

Fig. 12. Evolution of the energy density

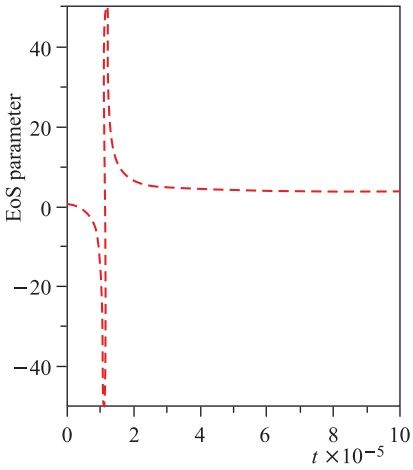

Fig. 13. Evolution of the EoS parameter

From equation (4.34), it is observed that the equation of state parameter ω is time-dependent, it can be a function of red-shift z or scale factor a as well. The red-shift dependence of ω can be linear-like

$$\omega(z) = \omega_0 + \omega' z, \tag{4.35}$$

with $\omega' = \left.\frac{d\omega}{dz}\right|_{z=0}$ (see [86, 198] or nonlinear as [38, 100]

$$\omega(z) = \omega_0 + \frac{\omega_1 z}{1+z}. \tag{4.36}$$

So, as far as the scale factor dependence of ω is concerned, the parameterization

$$\omega(a) = \omega_0 + \omega_a(1-a), \tag{4.37}$$

where ω_0 is the present value ($a = 1$) and ω_a is the measure of the time variation ω', is widely used in the literature [102].

So, if the present work is compared with experimental results obtained in [82, 93,94,186], then one can conclude that the limit of ω provided by equation (4.34) may accommodate with the acceptable range of EoS parameter. Also it is observed that for $V = V_c$, ω vanishes, where V_c is a critical volume given by

$$V_c = \left(\frac{X_1}{X_4}\right)^{3N_3/(4N_3-6)}. \tag{4.38}$$

Thus, for this particular volume, our model represents a dusty Universe. We also note that the earlier real matter at $V \leqslant V_c$, where $\omega \geqslant 0$, later on at $V > V_c$, where $\omega < 0$, is converted to the dark energy dominated phase of Universe.

For the value of ω to be consistent with observation [93], we have the following general condition:

$$V_1 < V < V_2, \tag{4.39}$$

where

$$V_1 = \left(\frac{X_1 + 1.67X_1}{X_4 + 1.67X_2}\right)^{3N_3/(4N_3-6)} \tag{4.40}$$

and

$$V_2 = \left(\frac{X_1 + 0.62X_1}{X_4 + 0.62X_2}\right)^{3N_3/(4N_3-6)}. \tag{4.41}$$

For this constraint, we obtain $-1.67 < \omega < -0.62$, which is in good agreement with the limit obtained from observational results coming from SNe Ia data [93].

For the value of ω to be consistent with observation [186], we have the following general condition:

$$V_3 < V < V_4, \tag{4.42}$$

where

$$V_3 = \left(\frac{X_1 + 1.33X_1}{X_4 + 1.33X_2}\right)^{3N_3/(4N_3-6)}, \tag{4.43}$$

and

$$V_4 = \left(\frac{X_1 + 0.79X_1}{X_4 + 0.79X_2}\right)^{3N_3/(4N_3-6)}. \tag{4.44}$$

For this constraint, we obtain $-1.33 < \omega < -0.79$, which is in good agreement with the limit obtained from observational results coming from SNe Ia data [186].

For the value of ω to be consistent with observation [82, 94], we have the following general condition:

$$V_5 < V < V_6, \tag{4.45}$$

where

$$V_5 = \left(\frac{X_1 + 1.44X_1}{X_4 + 1.44X_2}\right)^{3N_3/(4N_3-6)} \tag{4.46}$$

and

$$V_6 = \left(\frac{X_1 + 0.92X_1}{X_4 + 0.92X_2}\right)^{3N_3/(4N_3-6)}. \tag{4.47}$$

For this constraint, we obtain $-1.44 < \omega < -0.92$, which is in good agreement with the limit obtained from observational results coming from SNe Ia data [82, 94].

We also observed that if

$$V_0 = \left(\frac{2X_1}{X_4 + X_2}\right)^{3N_3/(4N_3-6)}, \tag{4.48}$$

then for $V = V_0$ we have $\omega = -1$, i.e., we have Universe with cosmological constant. If $V < V_0$, then we have $\omega > -1$ that corresponds to quintessence, while for $V > V_0$ we have $\omega < -1$, i.e., Universe with phantom matter [33].

From (4.33) we found that the energy density is a decreasing function of time and $\varepsilon \geqslant 0$ when

$$V \leqslant \left(\frac{X_1}{X_2}\right)^{3N_3/(4N_3-6)}. \tag{4.49}$$

In absence of any curvature, matter energy density Ω_m and dark energy density Ω_Λ are related by the equation

$$\Omega_m + \Omega_\Lambda = \frac{\varepsilon}{3H^2} + \frac{\Lambda}{3H^2} = 1. \tag{4.50}$$

Inserting (4.29) and (4.33) into (4.50) we find the cosmological constant as

$$\Lambda = \left[3C_0^2 - \left(\frac{X_1}{\kappa}\right)\right] V^{-2} + \left[3A_1 - \frac{X_2}{\kappa}\right] V^{-2(N_3+3)/3N_3}. \tag{4.51}$$

As we see, the cosmological function is a decreasing function of time and it is always positive when

$$V \geqslant \left(\frac{X_1/\kappa - 3C_0}{3A_1 - X_2/\kappa}\right)^{3N_3/(4N_3-6)}. \tag{4.52}$$

Recent cosmological observations suggest the existence of a positive cosmological constant Λ with the magnitude $\Lambda(G\hbar/c^3) \approx 10^{-123}$. These observations on magnitude and red-shift of type Ia supernova suggest that our Universe may be an accelerating one with induced cosmological density through the cosmological Λ-term. Thus, the nature of Λ in our derived DE model is supported by recent observations. Figure 14 shows the evolution of the cosmological constant. As is seen, it is a decreasing function of time.

For the stability of corresponding solutions, we should check that our models are physically acceptable. For this, the velocity of sound is less than that of light, i.e.,

$$0 \leqslant v_s = \frac{dp}{d\varepsilon} < 1. \tag{4.53}$$

In this case, we find

$$v_s = \frac{dp}{d\varepsilon} = -\frac{X_1 - [(N_3+3)X_4/3N_3]V^{(4N_3-6)/3N_3}}{X_1 - [(N_3+3)X_2/3N_3]V^{(4N_3-6)/3N_3}}. \tag{4.54}$$

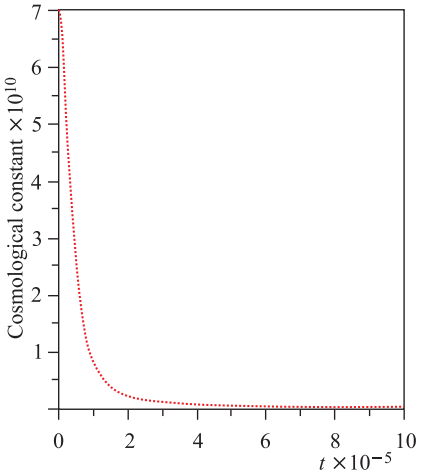

Fig. 14. Evolution of the cosmological constant

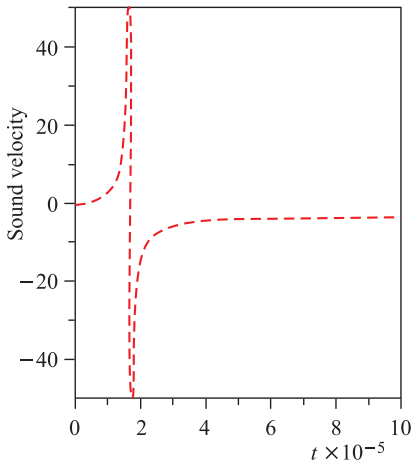

Fig. 15. Speed of sound with respect to cosmic time

Figure 15 shows the behavior of the velocity of sound v_s in time. As one sees, there are regions, where the solution is stable. Choosing the problem parameters, such as m_1, m_2, N_3 we can obtain the stable solutions.

5. BIANCHI TYPE-VI$_0$ MODELS WITH A VARIABLE EoS

A Bianchi type-VI$_0$ space–time, describes an anisotropic space–time and generates particular interest among physicists. Weaver [196], Ibáñez et al. [87], Socorro and Medina [178], and Bali et al. [8] have studied B-VI$_0$ space–time in connection with massive strings. Recently, Belinchon [14] studied several cosmological models with B-VI$_0$ & III symmetries under the self-similar approach. Given the growing interest of cosmologists, here we study the evolution of the Universe within the framework of a B-VI$_0$ cosmological model. It should be noted that unlike B-I space–time in the case considered, the two of the three metric functions are rigidly connected to each other. A spinor description of dark energy within the scope of a BVI$_0$ model was given in [146].

Let us now consider the Bianchi type-VI$_0$ space–time given by (3.4). We generalize the EoS parameter in the following way [4]:

$$\begin{aligned} T_\alpha^\beta &= \operatorname{diag}[\varepsilon,\, -p_x,\, -p_y,\, -p_z], \\ &= \operatorname{diag}[1,\, -\omega_x,\, -\omega_y,\, -\omega_z]\varepsilon, \\ &= \operatorname{diag}[1,\, -(\omega+\delta),\, -(\omega+\gamma),\, -\omega]\varepsilon. \end{aligned} \tag{5.1}$$

It should be noted that cosmological evolution of matter sources with small anisotropic pressures was studied in [9, 10].

Setting $m_1 = m_2$, we find the Einstein system of equations for BVI$_0$. In this case, as well as in those for BV and BIII, we have only one parameter m_1 instead of two, i.e., m_1 and m_2. For simplicity, we set $m_1 = m$. The Einstein field equations then read

$$\frac{\ddot{a}_2}{a_2} + \frac{\ddot{a}_3}{a_3} + \frac{\dot{a}_2}{a_2}\frac{\dot{a}_3}{a_3} - \frac{m^2}{a_3^2} = -\kappa(\omega+\delta)\varepsilon, \tag{5.2a}$$

$$\frac{\ddot{a}_3}{a_3} + \frac{\ddot{a}_1}{a_1} + \frac{\dot{a}_3}{a_3}\frac{\dot{a}_1}{a_1} - \frac{m^2}{a_3^2} = -\kappa(\omega+\gamma)\varepsilon, \tag{5.2b}$$

$$\frac{\ddot{a}_1}{a_1} + \frac{\ddot{a}_2}{a_2} + \frac{\dot{a}_1}{a_1}\frac{\dot{a}_2}{a_2} + \frac{m^2}{a_3^2} = -\kappa\omega\varepsilon, \tag{5.2c}$$

$$\frac{\dot{a}_1}{a_1}\frac{\dot{a}_2}{a_2} + \frac{\dot{a}_2}{a_2}\frac{\dot{a}_3}{a_3} + \frac{\dot{a}_3}{a_3}\frac{\dot{a}_1}{a_1} - \frac{m^2}{a_3^2} = \kappa\varepsilon, \tag{5.2d}$$

$$\frac{\dot{a}_1}{a_1} - \frac{\dot{a}_2}{a_2} = 0. \tag{5.2e}$$

5.1. Solution to the Field Equations. From (5.2e) immediately follows

$$a_1 = \ell a_2. \tag{5.3}$$

Moreover, in view of (5.2e) from (5.2a) and (5.2b), one concludes that

$$\delta = \gamma, \tag{5.4}$$

i.e., in case of a Bianchi type-VI_0 given by (3.4), the nondiagonal component of the Einstein field equation leads to

$$T_1^1 = T_2^2, \tag{5.5}$$

allowing an anisotropic distribution of matter.

The system (5.2) now reduces to

$$\frac{\ddot{a}_2}{a_2} + \frac{\ddot{a}_3}{a_3} + \frac{\dot{a}_2}{a_2}\frac{\dot{a}_3}{a_3} - \frac{m^2}{a_3^2} = -\kappa(\omega+\gamma)\varepsilon, \tag{5.6a}$$

$$2\frac{\ddot{a}_2}{a_2} + \frac{\dot{a}_2^2}{a_2^2} + \frac{m^2}{a_3^2} = -\kappa\omega\varepsilon, \tag{5.6b}$$

$$\frac{\dot{a}_2^2}{a_2^2} + 2\frac{\dot{a}_2}{a_2}\frac{\dot{a}_3}{a_3} - \frac{m^2}{a_3^2} = \kappa\varepsilon. \tag{5.6c}$$

Thus we now have three linearly independent equations with five unknowns, namely a_2, a_3, ω, ε, and γ. Two additional constraints relating these parameters are required to obtain explicit solutions of the system.

Firstly, we apply the law of variation for Hubble parameter given by [20] which yields a constant value of deceleration parameter. Here, the law reads as

$$H = Da^{-n} = DV^{-n/3}, \tag{5.7}$$

where $D > 0$ and $n \geqslant 0$ are constants. Such a type of relations have firstly been considered by [20, 21] for solving FRW models. Latter on, many authors have used this law to study FRW and Bianchi-type models. In view of (4.14) and (5.7), we find

$$\frac{\dot{V}}{V} = 3DV^{-n/3}, \tag{5.8}$$

with the solution

$$V = (nDt + C_1)^{3/n}, \quad n \neq 0, \quad C_1 = \text{const}. \tag{5.9}$$

The value of deceleration parameter is found to be

$$q = n - 1, \tag{5.10}$$

which is a constant. The sign of q indicates whether the model inflates or not. The positive sign of q, i.e., $(n > 1)$, corresponds to «standard» decelerating model, whereas the negative sign of q, i.e., $0 \leqslant n < 1$ indicates inflation. It is remarkable to mention here that though the current observations of SNe Ia and CMBR favour accelerating models ($q < 0$), but both do not altogether rule out the decelerating ones, which are also consistent with these observations [191].

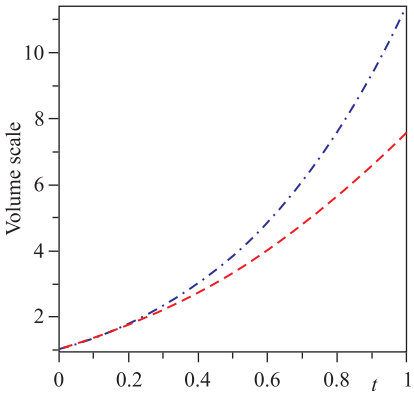

Fig. 16. Evolution of the Universe in power-law expansion. The dashed line corresponds to $q > 0$, while the dash-dotted line corresponds to $q < 0$

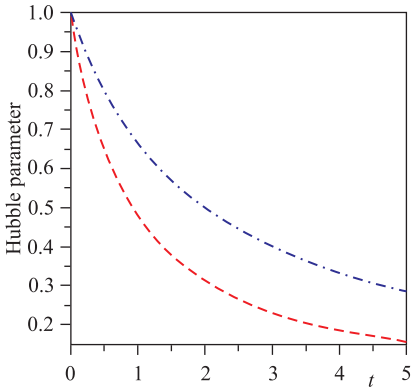

Fig. 17. Evolution of the Hubble parameter in power-law expansion. The dashed line corresponds to $q > 0$, while the dash-dotted line corresponds to $q < 0$

Figures 16 and 17 show the evolution of the Universe and the Hubble parameter for a positive and negative DP, respectively.

Secondly, we assume that the component $\sigma^3{}_3$ of the shear tensor $\sigma^j{}_i$ is proportional to the expansion scalar (ϑ) given by (4.19). In this case we come to the same conclusion as for BVI. Hence we find

$$a_1 = \sqrt{\frac{\ell}{N_0}}(nDt + C_1)^{(2N_3-3)/2nN_3}, \tag{5.11a}$$

$$a_2 = \sqrt{\frac{1}{\ell N_0}}(nDt + C_1)^{(2N_3-3)/2nN_3}, \tag{5.11b}$$

$$a_3 = N_0(nDt + C_1)^{(N_3+3)/nN_3}. \tag{5.11c}$$

5.2. Physical Aspects of Dark Energy Model. The directional Hubble parameters in this case have the form

$$\begin{aligned} H_1 = H_2 &= \frac{(2N_3 - 3)D}{2N_3(nDt + C_1)} = \left(1 - \frac{3}{2N_3}\right) H, \\ H_3 &= \frac{(N_3 + 3)D}{N_3(nDt + C_1)} = \left(1 + \frac{3}{N_3}\right) H. \end{aligned} \tag{5.12}$$

The expressions for the Hubble parameter H, scalar of expansion ϑ, shear scalar σ, and the average anisotropy parameter A_m for the model (5.11) are given by

$$\vartheta = 3H = \frac{3D}{nDt + C_1}, \tag{5.13}$$

$$\sigma^2 = \frac{3}{2}\left(\frac{3D}{N_3}\right)^2 \frac{1}{(nDt + C_1)^2}, \tag{5.14}$$

$$A_m = \frac{9}{2N_3^2}. \tag{5.15}$$

From (5.6c) we find

$$\varepsilon = \left(\frac{X_1}{\kappa}\right)(nDt + C_1)^{-2} - \left(\frac{m^2}{\kappa N_0^2}\right)(nDt + C_1)^{-2(N_3+3)/nN_3}, \tag{5.16}$$

where $X_1 = 3D^2(4N_3^2 - 9)/4N_3^2$. The EoS parameter ω can be found from (5.6b) and (5.6c) as

$$\omega = \frac{X_2(nDt + C_1)^{-2} - (m^2/N_0^2)(nDt + C_1)^{-2(N_3+3)/nN_3}}{X_1(nDt + C_1)^{-2} - (m^2/N_0^2)(nDt + C_1)^{-2(N_3+3)/nN_3}}, \tag{5.17}$$

where $X_2 = D^2(2N_3 - 3)[4nN_3 - 3(2N_3 - 3)]/4N_3^2$. The skewness parameters, δ or γ, i.e., deviations of ω along x-axis and y-axis, are found to be

$$\delta = \gamma = -\frac{X_3(nDt + C_1)^{-2} - 2(m^2/N_0^2)(nDt + C_1)^{-2(N_3+3)/nN_3}}{X_1(nDt + C_1)^{-2} - (m^2/N_0^2)(nDt + C_1)^{-2(N_3+3)/nN_3}}, \tag{5.18}$$

where $X_3 = 9D^2(n - 6)/2N_3$.

Figures 18 and 19 show the evolution of the energy density and the EoS parameter for a positive and negative DP, respectively. As was expected in the

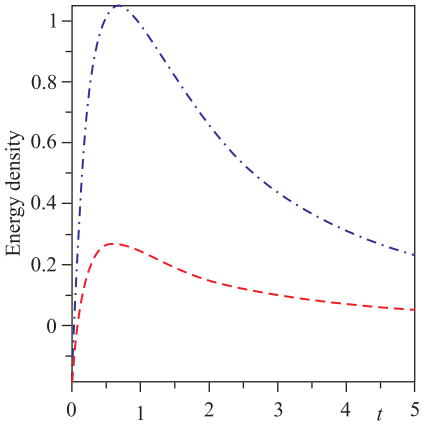

Fig. 18. Evolution of the energy density in power-law expansion. The dashed line corresponds to $q > 0$, while the dash-dotted line corresponds to $q < 0$

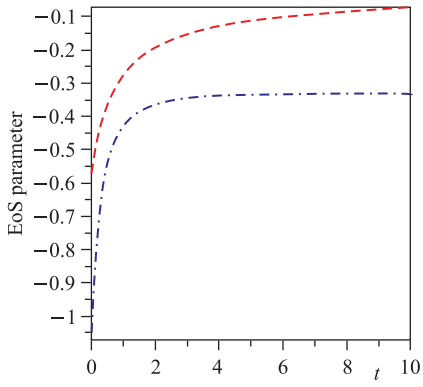

Fig. 19. Evolution of the EoS parameter in power-law expansion. The dashed line corresponds to $q > 0$, while the dash-dotted line corresponds to $q < 0$

case of a negative DP, the expansion of the Universe is rather rapid. In this section, we set the following values for the parameters: $D = 1$, $C_1 = 1$, $N_3 = 6$, $m = 1$, $N_0 = 1$, $\kappa = 1$, $n = 1.1$ (for $q > 0$) and $n = 0.5$ (for $q < 0$).

So, if the present work is compared with experimental results obtained in [82, 93,94,186], then one can conclude that the limit of ω provided by equation (5.17) may accommodated with the acceptable range of EoS parameter. Also it is observed that at $t = t_c$, ω vanishes, where t_c is a critical time given by

$$t_c = \frac{1}{nD}\left[\left(\frac{X_2 N_0^2}{m^2}\right)^{nN_3/2(n-N_3-3)} - C_1\right]. \tag{5.19}$$

Thus, for this particular time, our model represents a dusty Universe. We also note that the earlier real matter at $t \leqslant t_c$, where $\omega \geqslant 0$, later on at $t > t_c$, where $\omega < 0$, converted to the dark energy dominated phase of Universe.

For the value of ω to be consistent with observation [93], we have the following general condition:

$$t_1 < t < t_2, \tag{5.20}$$

where

$$t_1 = \frac{1}{nD}\left[\left(\frac{N_0^2(X_2 + 1.67X_1)}{2.67m^2}\right)^{nN_3/2(n-N_3-3)} - C_1\right] \tag{5.21}$$

and

$$t_2 = \frac{1}{nD}\left[\left(\frac{N_0^2(X_2 + 0.62X_1)}{1.62m^2}\right)^{nN_3/2(n-N_3-3)} - C_1\right]. \tag{5.22}$$

For this constraint, we obtain $-1.67 < \omega < -0.62$, which is in good agreement with the limit obtained from observational results coming from SNe Ia data [93].

For the value of ω to be consistent with observation [186], we have the following general condition:

$$t_3 < t < t_4, \tag{5.23}$$

where

$$t_3 = \frac{1}{nD}\left[\left(\frac{N_0^2(X_2 + 1.33X_1)}{2.33m^2}\right)^{nN_3/2(n-N_3-3)} - C_1\right] \tag{5.24}$$

and

$$t_4 = \frac{1}{nD}\left[\left(\frac{N_0^2(X_2 + 0.79X_1)}{1.79m^2}\right)^{nN_3/2(n-N_3-3)} - C_1\right]. \tag{5.25}$$

For this constraint, we obtain $-1.33 < \omega < -0.79$, which is in good agreement with the limit obtained from observational results coming from SNe Ia data [186].

For the value of ω to be consistent with observation [82, 94], we have the following general condition:

$$t_5 < t < t_6, \tag{5.26}$$

where

$$t_5 = \frac{1}{nD}\left[\left(\frac{N_0^2(X_2 + 1.44X_1)}{2.44m^2}\right)^{nN_3/2(n-N_3-3)} - C_1\right] \tag{5.27}$$

and

$$t_6 = \frac{1}{nD}\left[\left(\frac{N_0^2(X_2 + 0.92X_1)}{1.92m^2}\right)^{nN_3/2(n-N_3-3)} - C_1\right]. \tag{5.28}$$

For this constraint, we obtain $-1.44 < \omega < -0.92$, which is in good agreement with the limit obtained from observational results coming from SNe Ia data [82, 94].

We also observed that if

$$t_0 = \frac{1}{nD}\left[\left(\frac{N_0^2(X_2 + X_1)}{2m^2}\right)^{nN_3/2(n-N_3-3)} - C_1\right], \tag{5.29}$$

then for $t = t_0$ we have $\omega = -1$, i.e., we have Universe with cosmological constant. If $t < t_0$, then we have $\omega > -1$ that corresponds to quintessence, while for $t > t_0$ we have $\omega > -1$, i.e., Universe with phantom matter [33].

From (5.16) we found that the energy density is a decreasing function of time and $\varepsilon \geqslant 0$ when

$$t \leqslant \frac{1}{nD}\left[\left(\frac{N_0^2 X_1}{m^2}\right)^{nN_3/2(n-N_3-3)} - C_1\right]. \tag{5.30}$$

Inserting (5.13) and (5.16) into (4.50) we find the cosmological constant as

$$\Lambda = \left[3D^2 - \left(\frac{X_1}{\kappa}\right)\right](nDt+C_1)^{-2} + \left(\frac{m^2}{\kappa N_0^2}\right)(nDt+C_1)^{-2(N_3+3)/nN_3}. \tag{5.31}$$

As we see, the cosmological function is a decreasing function of time and it is always positive when

$$t \geqslant \frac{1}{nD}\left[\left(\frac{m^2}{N_0^2(X_1 - 3\kappa D^2)}\right)^{nN_3/2(N_3+3-n)} - C_1\right]. \tag{5.32}$$

Recent cosmological observations suggest the existence of a positive cosmological constant Λ with the magnitude $\Lambda(G\hbar/c^3) \approx 10^{-123}$. These observations on magnitude and red-shift of type Ia supernova suggest that our Universe may

be an accelerating one with induced cosmological density through the cosmological Λ-term. Thus, the nature of Λ in our derived DE model is supported by recent observations.

The velocity of sound in this case is found to be

$$v_s = \frac{dp}{d\varepsilon} = \frac{X_2 - [m^2(N_3+3)/nN_0^2N_3](nDt+C_1)^{2(n-N_3-3)/nN_3}}{X_1 - [m^2(N_3+3)/nN_0^2N_3](nDt+C_1)^{2(n-N_3-3)/nN_3}}. \quad (5.33)$$

Figures 20 and 21 show the evolution of the cosmological constant and the sound velocity for a positive and negative DP, respectively.

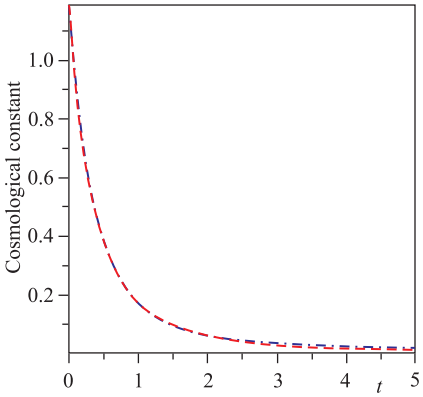

Fig. 20. Evolution of the cosmological constant in power-law expansion. The dashed line corresponds to $q > 0$, while the dash-dotted line corresponds to $q < 0$

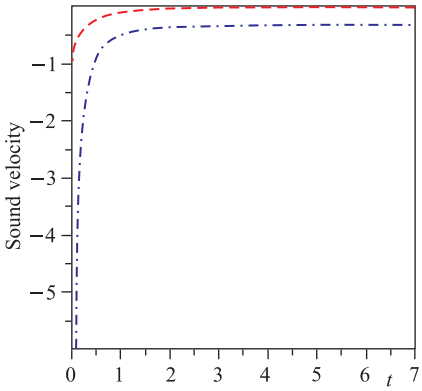

Fig. 21. Evolution of the sound velocity in power-law expansion. The dashed line corresponds to $q > 0$, while the dash-dotted line corresponds to $q < 0$

As one sees, cosmological constant remains the same for both positive and negative DP. As far as sound velocity is concerned, in both cases the system becomes stable at the later stage of the evolution.

6. BIANCHI TYPE-V SPACE–TIME WITH VARIABLE EoS PARAMETER

Let us now consider the case with Bianchi type-V space–time. Some dark energy model within the scope of a BV cosmology was studied in [204]. Bianchi type-V space–time with variable EoS parameter was studied in [150]. A spinor description of dark energy within the scope of a BV model was given in [146]. Bianchi type-V cosmological models in Brans–Dicke theory were studied in [36, 39].

Einstein field equations for the metric (3.5) on account of (3.18) have the form [150]

$$\frac{\ddot{a}_2}{a_2}+\frac{\ddot{a}_3}{a_3}+\frac{\dot{a}_2}{a_2}\frac{\dot{a}_3}{a_3}-\frac{m^2}{a_3^2}=\kappa T_1^1, \tag{6.1a}$$

$$\frac{\ddot{a}_3}{a_3}+\frac{\ddot{a}_1}{a_1}+\frac{\dot{a}_3}{a_3}\frac{\dot{a}_1}{a_1}-\frac{m^2}{a_3^2}=\kappa T_2^2, \tag{6.1b}$$

$$\frac{\ddot{a}_1}{a_1}+\frac{\ddot{a}_2}{a_2}+\frac{\dot{a}_1}{a_1}\frac{\dot{a}_2}{a_2}-\frac{m^2}{a_3^2}=\kappa T_3^3, \tag{6.1c}$$

$$\frac{\dot{a}_1}{a_1}\frac{\dot{a}_2}{a_2}+\frac{\dot{a}_2}{a_2}\frac{\dot{a}_3}{a_3}+\frac{\dot{a}_3}{a_3}\frac{\dot{a}_1}{a_1}-3\frac{m^2}{a_3^2}=\kappa T_0^0, \tag{6.1d}$$

$$\frac{\dot{a}_1}{a_1}+\frac{\dot{a}_2}{a_2}-2\frac{\dot{a}_3}{a_3}=0. \tag{6.1e}$$

As we have already mentioned, the physically observable variables in this case coincide with those of Bianchi type-VI model.

6.1. Solution to the Field Equations. From (6.1e) immediately follows

$$a_1a_2=k_1a_3^2, \quad k_1=\text{const}. \tag{6.2}$$

We also impose to use the proportionality condition, widely used in literature, demanding that the expansion is proportion to a component of the shear tensor, namely:

$$\vartheta=N_1\sigma_1^1. \tag{6.3}$$

On account of (4.9) and (4.12) we find

$$a_1=N_0V^{\frac{1}{3}+\frac{1}{N_1}}, \quad N_0=\text{const}. \tag{6.4}$$

In view of (4.3) and (4.21) from (4.18) we find

$$a_2=\frac{k_1^{1/3}}{N_0}V^{\frac{1}{3}-\frac{1}{N_1}}, \tag{6.5}$$

$$a_3=\frac{1}{k_1^{1/3}}V^{\frac{1}{3}}. \tag{6.6}$$

Thus, we have derived metric functions in terms of V. In order to find the equation for V, we take the following steps. Subtractions of (6.1a) from (6.1b), (6.1b) from (6.1c), and (6.1c) from (6.1a) on account of (6.4), (6.5) and (6.6) give

$$\frac{\ddot{V}}{V}=\frac{\kappa N_1}{2}[T_2^2-T_1^1], \tag{6.7a}$$

$$\frac{\ddot{V}}{V}=-\kappa N_1[T_3^3-T_2^2], \tag{6.7b}$$

$$\frac{\ddot{V}}{V}=-\kappa N_1[T_1^1-T_3^3]. \tag{6.7c}$$

From (4.24) immediately follows [150]

$$\frac{1}{2}[T_2^2 - T_1^1] == [T_3^3 - T_2^2] == [T_1^1 - T_3^3]. \tag{6.8}$$

After a little manipulation, it could be established that

$$T_1^1 + T_2^2 = 2T_3^3. \tag{6.9}$$

Hence, the energy–momentum tensor can be taken as

$$\begin{aligned} T_\alpha^\beta &= \mathrm{diag}\,[\varepsilon,\, -p_x,\, -p_y,\, -p_z], \\ &= \mathrm{diag}\,[1,\, -\omega_x,\, -\omega_y,\, -\omega_z]\varepsilon, \\ &= \mathrm{diag}\,[1,\, -(\omega+\delta),\, -(\omega-\delta),\, -\omega]\varepsilon. \end{aligned} \tag{6.10}$$

Thus we conclude that under the proportionality condition, the energy–momentum distribution of the model should obey (6.8), and the matter distribution in this case may be anisotropic.

As one sees, in order to find V we have to impose some additional condition. Let us apply the law of variation for Hubble parameter given by (5.7) which yields a constant value of deceleration parameter. In this case we find the expression for V given by

$$V = (nDt + C_1)^{3/n}, \quad n \neq 0, \quad C_1 = \mathrm{const}. \tag{6.11}$$

In view of (6.11) for the metric functions, we find

$$a_1 = N_0(nDt + C_1)^{(N_1+3)/nN_1}, \tag{6.12a}$$

$$a_2 = \frac{k_1^{1/3}}{N_0}(nDt + C_1)^{(N_1-3)/nN_1}, \tag{6.12b}$$

$$a_3 = \frac{1}{k_1^{1/3}}(nDt + C_1)^{1/n}. \tag{6.12c}$$

The Universe in this case is an expanding one and coincides with that illustrated in Fig. 16.

6.2. Physical Aspects of Dark Energy Model. The DP in this case is a constant and has the form given by (5.10). Directional Hubble parameters in this case read

$$\begin{gathered} H_1 = \left(\frac{1}{3} + \frac{1}{N_1}\right)\frac{3D}{nDt + C_1}, \\ H_2 = \left(\frac{1}{3} - \frac{1}{N_1}\right)\frac{3D}{nDt + C_1}, \quad H_3 = \frac{D}{nDt + C_1}. \end{gathered} \tag{6.13}$$

In this case the expression for expansion ϑ and Hubble parameter H read

$$\vartheta = 3H = \frac{3D}{nDt + C_1}. \tag{6.14}$$

The evolution of the Hubble parameter in this case is similar to that given in Fig. 17. As one sees, it is a decreasing function of time.

The value of deceleration parameter is found to be

$$q = n - 1, \tag{6.15}$$

and the anisotropy parameter A_m has the expression

$$A_m = \frac{6}{N_1^2}. \tag{6.16}$$

For energy density in this case we have

$$\varepsilon = \frac{X_1}{(nDt + C_1)^2} - \frac{3m^2C_1^2}{(nDt + C_1)^{2/n}}, \tag{6.17}$$

where $X_1 = 3D^2(N_1^2 - 3)/N_1^2)$. The EoS parameter in this case has the form

$$\omega = \frac{X_2/(nDt + C_1)^2 + m^2C_1^2/(nDt + C_1)^{2/n}}{X_1/(nDt + C_1)^2 - 3m^2C_1^2/(nDt + C_1)^{2/n}}, \tag{6.18}$$

where $X_2 = X_1 - 2D^2(3 - n)$. From Eq. (6.18), it is observed that the equation of state parameter ω is time-dependent.

The corresponding expressions were investigated numerically for the following values of parameters: $D = 1$, $C_1 = 0.1$, $N_1 = 2$, $m = 3$, $\kappa = 1$, $n = 2$ (for $q > 0$) and $n = 0.4$ (for $q < 0$).

Figure 22 shows the evolution of energy density for a positive and negative DP, respectively. As one sees, for a positive DP, energy density is a decreasing function of time, and beginning from some moment of time it may be negative as well. Where as for a negative DP, it is an increasing function of time, which is a negative one at the initial stage of evolution.

Figure 23 shows the evolution of the EoS parameter. As one sees, it is a time varying function and changes its sign in the course of evolution.

Let us now compare our results with the experimental results obtained in [82, 93, 94, 186]. It enables us to conclude that the limit of ω provided by Eq. (6.18) may accommodated with the acceptable range of EoS parameter. Also it is observed that at $t = t_c$, ω vanishes, where t_c is a critical time given by

$$t_c = \frac{1}{nD}\left[\left(\frac{X_2}{m^2C_1^2}\right)^{n/2(n-1)} - C_1\right]. \tag{6.19}$$

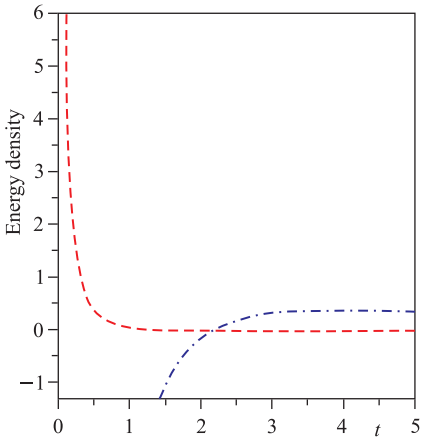

Fig. 22. Evolution of energy density. The dashed line corresponds to $q > 0$, while the dash-dotted line corresponds to $q < 0$

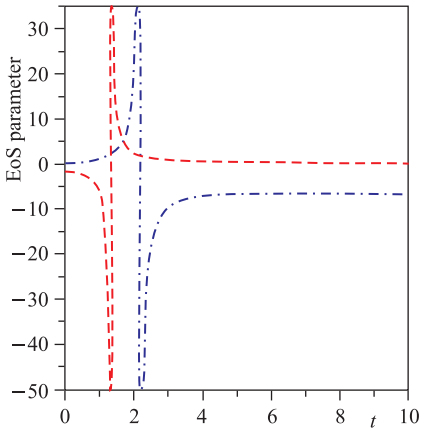

Fig. 23. Evolution of the EoS parameter. The dashed line corresponds to $q > 0$, while the dash-dotted line corresponds to $q < 0$

Thus, for this particular time, our model represents a dusty Universe. We also note that the earlier real matter at $t \leqslant t_c$, where $\omega \geqslant 0$, later on at $t > t_c$, where $\omega < 0$, is converted to the dark energy dominated phase of Universe.

For the value of ω to be consistent with observation [93], we have the following general condition:

$$t_1 < t < t_2, \tag{6.20}$$

where

$$t_1 = \frac{1}{nD}\left[\left(\frac{X_2 + 1.67X_1}{-4.01m^2C_1^2}\right)^{n/2(n-1)} - C_1\right] \tag{6.21}$$

and

$$t_1 = \frac{1}{nD}\left[\left(\frac{X_2 + 0.62X_1}{-0.86m^2C_1^2}\right)^{n/2(n-1)} - C_1\right]. \tag{6.22}$$

For this constraint, we obtain $-1.67 < \omega < -0.62$, which is in good agreement with the limit obtained from observational results coming from SNe Ia data [93].

For the value of ω to be consistent with observation [186], we have the following general condition:

$$t_3 < t < t_4, \tag{6.23}$$

where

$$t_1 = \frac{1}{nD}\left[\left(\frac{X_2 + 1.33X_1}{-2.99m^2C_1^2}\right)^{n/2(n-1)} - C_1\right] \tag{6.24}$$

and

$$t_1 = \frac{1}{nD}\left[\left(\frac{X_2 + 0.79X_1}{-1.37m^2C_1^2}\right)^{n/2(n-1)} - C_1\right]. \tag{6.25}$$

For this constraint, we obtain $-1.33 < \omega < -0.79$, which is in good agreement with the limit obtained from observational results coming from SNe Ia data [186].

For the value of ω to be consistent with observation [82, 94], we have the following general condition:

$$t_5 < t < t_6, \tag{6.26}$$

where

$$t_1 = \frac{1}{nD}\left[\left(\frac{X_2 + 1.44X_1}{-3.32m^2C_1^2}\right)^{n/2(n-1)} - C_1\right] \tag{6.27}$$

and

$$t_1 = \frac{1}{nD}\left[\left(\frac{X_2 + 0.92X_1}{-1.76m^2C_1^2}\right)^{n/2(n-1)} - C_1\right]. \tag{6.28}$$

For this constraint, we obtain $-1.44 < \omega < -0.92$, which is in good agreement with the limit obtained from observational results coming from SNe Ia data [82, 94].

We also observed that if

$$t_1 = \frac{1}{nD}\left[\left(\frac{X_2 + X_1}{-2m^2C_1^2}\right)^{n/2(n-1)} - C_1\right], \tag{6.29}$$

then for $t = t_0$ we have $\omega = -1$, i.e., we have Universe with cosmological constant. If $t < t_0$, then we have $\omega > -1$ that corresponds to quintessence, while for $t > t_0$ we have $\omega > -1$, i.e., Universe with phantom matter [33].

From (6.17) we found that the energy density is a decreasing function of time and $\varepsilon \geqslant 0$ when

$$t \geqslant \frac{1}{nD}\left[\left(-\frac{X_1}{m^2C_1^2}\right)^{n/2(n-1)} - C_1\right]. \tag{6.30}$$

Inserting (5.13) and (6.17) into (4.50) we find the cosmological constant as

$$\Lambda = \frac{3D^2 - X_1}{(nDt + C_1)^2} + \frac{3m^2C_1^2}{(nDt + C_1)^{2/n}}. \tag{6.31}$$

As we see, the cosmological function is a decreasing function of time and it is always positive when

$$t \geqslant \frac{1}{nD}\left[\left(\frac{X_1 - 3D^2}{3m^2C_1^2}\right)^{n/2(n-1)} - C_1\right]. \tag{6.32}$$

Figure 24 shows the evolution of the cosmological constant. As one sees, it is a time varying function and decreases with time.

Recent cosmological observations suggest the existence of a positive cosmological constant Λ with the magnitude $\Lambda(G\hbar/c^3) \approx 10^{-123}$. These observations on magnitude and red-shift of type Ia supernova suggest that our Universe may be an accelerating one with induced cosmological density through the cosmological Λ-term. Thus, the nature of Λ in our derived DE model is supported by recent observations.

The velocity of sound in this case is found to be

$$v_s = \frac{dp}{d\varepsilon} = \frac{nX_2 + m^2C_1^2(nDt + C_1)^{2-2/n}}{nX_1 - 3m^2C_1^2(nDt + C_1)^{2-2/n}}. \tag{6.33}$$

Figure 25 shows the behavior of v_s in time.

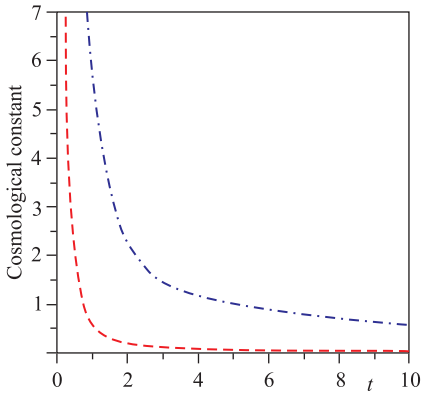

Fig. 24. Evolution of the Λ-term. The dashed line corresponds to $q > 0$, while the dash-dotted line corresponds to $q < 0$

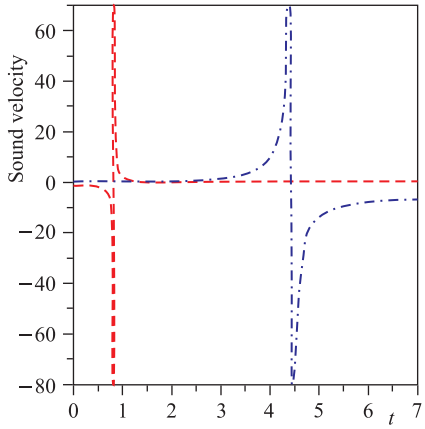

Fig. 25. Speed of sound with respect to cosmic time. The dashed line corresponds to $q > 0$, while the dash-dotted line corresponds to $q < 0$

As one sees, there are regions, where the solution is stable. Figure 25 shows that the solution becomes unstable during the transition from deceleration to acceleration phase of evolution. Choosing the problem parameters, such as n, D, we can obtain the stable solutions before or after the transition.

7. BIANCHI TYPE-III SPACE–TIME WITH VARIABLE EoS PARAMETER

Spatially homogeneous and anisotropic cosmological models play a significant role in the description of large scale behavior of Universe and such models have been widely studied in the framework of General Relativity in the search

for a realistic picture of the Universe in its early stages. Yadav et al. [205], Pradhan et al. [116, 117] have recently studied homogeneous and anisotropic Bianchi type-III space–time in the context of massive strings. Recently, Yadav [206] has obtained Bianchi type-III anisotropic DE models with constant deceleration parameter. In this paper, we have investigated a new anisotropic Bianchi type-III DE model with variable ω without assuming constant deceleration parameter. A spinor description of dark energy within the scope of a BIII model was given in [146].

Let us now consider the Bianchi type-III space–time given by (3.6). We consider the case when the energy–momentum tensor is given by (5.1). Einstein system of equations in this case reads

$$\frac{\ddot{a}_2}{a_2}+\frac{\ddot{a}_3}{a_3}+\frac{\dot{a}_2}{a_2}\frac{\dot{a}_3}{a_3}=-\kappa(\omega+\delta)\varepsilon, \tag{7.1a}$$

$$\frac{\ddot{a}_3}{a_3}+\frac{\ddot{a}_1}{a_1}+\frac{\dot{a}_3}{a_3}\frac{\dot{a}_1}{a_1}-\frac{m^2}{a_3^2}=-\kappa(\omega+\gamma)\varepsilon, \tag{7.1b}$$

$$\frac{\ddot{a}_1}{a_1}+\frac{\ddot{a}_2}{a_2}+\frac{\dot{a}_1}{a_1}\frac{\dot{a}_2}{a_2}=-\kappa\omega\varepsilon, \tag{7.1c}$$

$$\frac{\dot{a}_1}{a_1}\frac{\dot{a}_2}{a_2}+\frac{\dot{a}_2}{a_2}\frac{\dot{a}_3}{a_3}+\frac{\dot{a}_3}{a_3}\frac{\dot{a}_1}{a_1}-\frac{m^2}{a_3^2}=\kappa\varepsilon, \tag{7.1d}$$

$$\frac{\dot{a}_1}{a_1}-\frac{\dot{a}_3}{a_3}=0. \tag{7.1e}$$

As we have already mentioned, the physically observable variables in this case coincide with those of Bianchi type-VI model.

7.1. Solution to the Field Equations. In view of (7.1e) from (7.1a) and (7.1c) immediately follows

$$\delta=0. \tag{7.2}$$

Moreover, from (7.1e) we find

$$a_1=\ell a_3, \tag{7.3}$$

i.e., in case of a Bianchi type-III given by (3.6), the nondiagonal component of the Einstein field equation leads to

$$T_1^1=T_3^3, \tag{7.4}$$

allowing an anisotropic distribution of matter.

Hence we have the following system of equations:

$$2\frac{\ddot{a}_3}{a_3}+\frac{\dot{a}_3^2}{a_3^2}-\frac{m^2}{a_3^2}=-\kappa(\omega+\gamma)\varepsilon, \tag{7.5a}$$

$$\frac{\ddot{a}_3}{a_3}+\frac{\ddot{a}_2}{a_2}+\frac{\dot{a}_2}{a_2}\frac{\dot{a}_3}{a_3}=-\kappa\omega\varepsilon, \tag{7.5b}$$

$$2\frac{\dot{a}_2}{a_2}\frac{\dot{a}_3}{a_3}+\frac{\dot{a}_3^2}{a_3^2}-\frac{m^2}{a_3^2}=\kappa\varepsilon. \tag{7.5c}$$

Thus, we now have three linearly independent equations with five unknowns, namely a_2, a_3, ω, ε, and γ. Two additional constraints relating these parameters are required to obtain explicit solutions of the system.

Let us first consider the proportionality condition demanding

$$\vartheta = N_3\sigma_2^2, \tag{7.6}$$

which together with (4.3) and (7.3) immediately gives

$$a_1 = \sqrt{\frac{\ell}{N_0}}V^{(2N_3-3)/6N_3}, \tag{7.7a}$$

$$a_2 = N_0V^{(N_3+3)/3N_3}, \tag{7.7b}$$

$$a_3 = \sqrt{\frac{1}{\ell N_0}}V^{(2N_3-3)/6N_3}. \tag{7.7c}$$

As in the previous case, we apply the law of variation for Hubble parameter given by (5.7) which yields a constant value of deceleration parameter. Then for V we find the expression (5.9):

$$V = (nDt + C_1)^{3/n}, \quad n \neq 0, \quad C_1 = \text{const}. \tag{7.8}$$

Numerical study of the corresponding expression shows that it coincides with that of Fig. 16.

Inserting (7.8) into (7.7) one finds

$$a_1 = \sqrt{\frac{\ell}{N_0}}(nDt + C_1)^{(2N_3-3)/2nN_3}, \tag{7.9a}$$

$$a_2 = N_0(nDt + C_1)^{(N_3+3)/nN_3}, \tag{7.9b}$$

$$a_3 = \sqrt{\frac{1}{\ell N_0}}(nDt + C_1)^{(2N_3-3)/2nN_3}. \tag{7.9c}$$

7.2. Physical Aspects of Dark Energy Model. The directional Hubble parameters in this case have the form

$$\begin{aligned} H_1 = H_3 &= \frac{(2N_3-3)D}{2N_3(nDt+C_1)} = \left(1 - \frac{3}{2N_3}\right)H, \\ H_2 &= \frac{(N_3+3)D}{N_3(nDt+C_1)} = \left(1 + \frac{3}{N_3}\right)H. \end{aligned} \tag{7.10}$$

The expressions for the Hubble parameter H, scalar of expansion ϑ, shear scalar σ, and the average anisotropy parameter A_m for the model coincide with

those for Bianchi type-VI$_0$. In particular, the graphical view of the Hubble parameter coincides with Fig. 17. Energy density ε is given by

$$\varepsilon = \left(\frac{X_1}{\kappa}\right)(nDt + C_1)^{-2} - \left(\frac{m^2 \ell N_0}{\kappa}\right)(nDt + C_1)^{-(2N_3-3)/nN_3}, \quad (7.11)$$

with $X_1 = 3D^2(4N_3^2 - 9)/4N_3^2$. The EoS parameter ω is given by

$$\omega = \frac{X_2(nDt + C_1)^{-2}}{X_1(nDt + C_1)^{-2} - (m^2 \ell N_0)(nDt + C_1)^{-(2N_3-3)/nN_3}}, \quad (7.12)$$

where $X_2 = D^2[(4N_3 + 3)2N_3 n - (12N_3^2 + 18N_3 + 27)]/4N_3^2$. The skewness parameter γ, i.e., deviation of ω along y-axis, has the form

$$\gamma = -\frac{X_3(nDt + C_1)^{-2} - (m^2 \ell N_0)(nDt + C_1)^{-(2N_3-3)/nN_3}}{X_1(nDt + C_1)^{-2} - (m^2 \ell N_0)(nDt + C_1)^{-(2N_3-3)/nN_3}}, \quad (7.13)$$

where $X_3 = 9D^2(3 - n)/2N_3^2$.

As in the case of Bianchi type-VI$_0$ space–time, here too the EoS parameter ω is a function of time. We also observe that unlike the Bianchi type-VI$_0$ case, here the EoS parameter becomes zero, only when $X_2 = 0$. For $X_2 > 0$ we have matter dominated Universe, whereas, for $X_2 < 0$ we have dark energy dominated Universe.

Figure 26 shows the evolution of energy density for a positive and negative DP, respectively. As one sees, for both cases, it is a decreasing function of time. Here we use the following set of problem parameters: $D = 1$, $C_1 = 1$, $N_3 = 6$, $m = 1$, $n = 1.1$ (for $q > 0$) and $n = 0.5$ (for $q < 0$.).

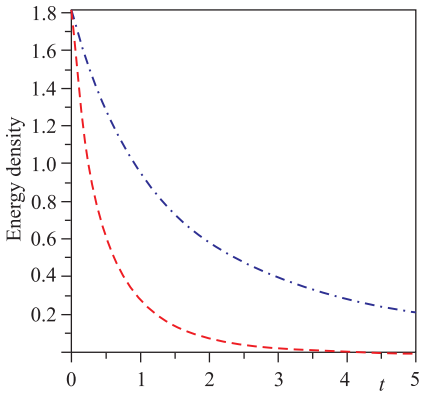

Fig. 26. Evolution of energy density. The dashed line corresponds to $q > 0$, while the dash-dotted line corresponds to $q < 0$

Figures 27 and 28 show the evolution of the EoS parameter for a positive and negative DP, respectively. As one sees, it is a time-varying function and changes its sign in the course of evolution.

For the value of ω to be consistent with observation [93], we have the following general condition:

$$t_1 < t < t_2, \quad (7.14)$$

where

$$t_1 = \frac{1}{nD}\left[\left(\frac{X_2 + 1.67X_1}{1.67m^2 \ell N_0}\right)^{nN_3/(2(n-1)N_3+3)} - C_1\right] \quad (7.15)$$

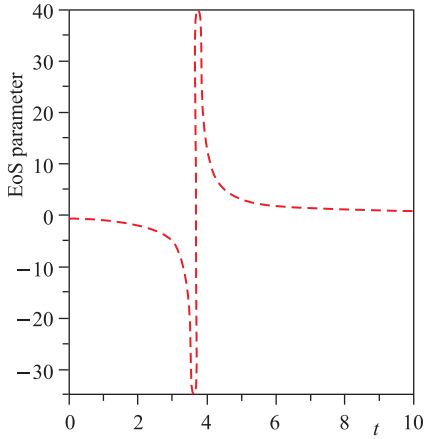

Fig. 27. Evolution of the EoS parameter for a positive DP

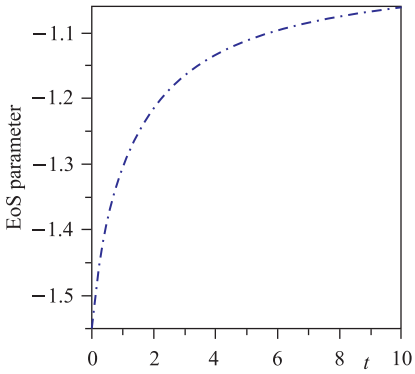

Fig. 28. Evolution of the EoS parameter for a negative DP

and

$$t_1 = \frac{1}{nD}\left[\left(\frac{N_0^2(X_2+0.62X_1)}{0.62m^2}\right)^{nN_3/(2(n-1)N_3+3)} - C_1\right]. \tag{7.16}$$

For this constraint, we obtain $-1.67 < \omega < -0.62$, which is in good agreement with the limit obtained from observational results coming from SNe Ia data [93].

For the value of ω to be consistent with observation [186], we have the following general condition:

$$t_3 < t < t_4, \tag{7.17}$$

where

$$t_3 = \frac{1}{nD}\left[\left(\frac{N_0^2(X_2+1.33X_1)}{1.33m^2}\right)^{nN_3/(2(n-1)N_3+3)} - C_1\right] \tag{7.18}$$

and

$$t_4 = \frac{1}{nD}\left[\left(\frac{N_0^2(X_2+0.79X_1)}{0.79m^2}\right)^{nN_3/(2(n-1)N_3+3)} - C_1\right]. \tag{7.19}$$

For this constraint, we obtain $-1.33 < \omega < -0.79$, which is in good agreement with the limit obtained from observational results coming from SNe Ia data [186].

For the value of ω to be consistent with observation [82, 94], we have the following general condition:

$$t_5 < t < t_6, \tag{7.20}$$

where

$$t_5 = \frac{1}{nD}\left[\left(\frac{N_0^2(X_2 + 1.44X_1)}{1.44m^2}\right)^{nN_3/(2(n-1)N_3+3)} - C_1\right] \tag{7.21}$$

and

$$t_6 = \frac{1}{nD}\left[\left(\frac{N_0^2(X_2 + 0.92X_1)}{0.92m^2}\right)^{nN_3/(2(n-1)N_3+3)} - C_1\right]. \tag{7.22}$$

For this constraint, we obtain $-1.44 < \omega < -0.92$, which is in good agreement with the limit obtained from observational results coming from SNe Ia data [82, 94].

We also observed that if

$$t_0 = \frac{1}{nD}\left[\left(\frac{N_0^2(X_2 + X_1)}{m^2}\right)^{nN_3/(2(n-1)N_3+3)} - C_1\right], \tag{7.23}$$

then for $t = t_0$ we have $\omega = -1$, i.e., we have Universe with cosmological constant. If $t < t_0$, then we have $\omega > -1$ that corresponds to quintessence, while for $t > t_0$ we have $\omega > -1$, i.e., Universe with phantom matter [33].

The energy density in this case remains positive if

$$t \leqslant \frac{1}{nD}\left[\left(\frac{X_1}{m^2\ell N_0}\right)^{nN_3/(2N_3(n-1)+3)} - C_1\right]. \tag{7.24}$$

The cosmological term in this case takes the form

$$\Lambda = \left[3D^2 - \left(\frac{X_1}{\kappa}\right)\right](nDt + C_1)^{-2} + \left(\frac{m^2\ell N_0}{\kappa}\right)(nDt + C_1)^{-(2N_3-3)/nN_3}. \tag{7.25}$$

As we see, the cosmological function is a decreasing function of time and it is always positive when

$$t \geqslant \frac{1}{nD}\left[\left(\frac{X_1 - 3\kappa D^2}{m^2\ell N_0}\right)^{nN_3/(2N_3(n-1)+3)} - C_1\right]. \tag{7.26}$$

Figure 29 shows the evolution of the cosmological constant. As one sees, it is decreasing function of time.

In this case, for the energy density and cosmological constant to be non-negative we find the expressions analogical to (4.49) and (4.52).

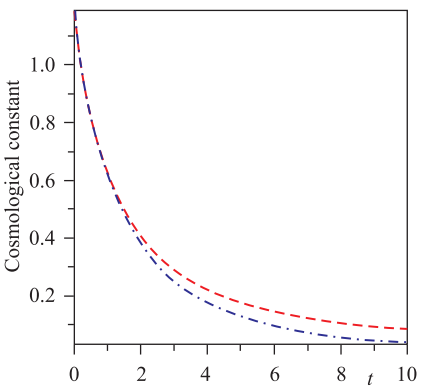

Fig. 29. Evolution of Λ-term. The dashed line corresponds to $q > 0$, while the dash-dotted line corresponds to $q < 0$

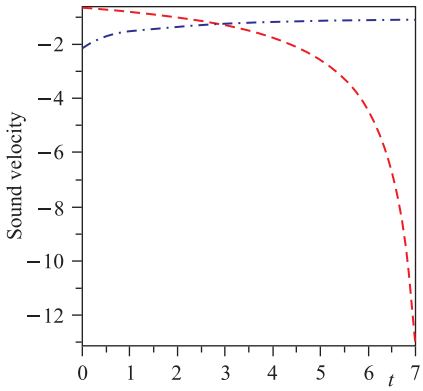

Fig. 30. Evolution of the velocity of sound. The dashed line corresponds to $q > 0$, while the dash-dotted line corresponds to $q < 0$

The velocity of sound in this case is found to be

$$v_s = \frac{dp}{d\varepsilon} = \frac{2nN_3X_2}{2nN_3X_1 - m^2\ell N_0(2N_3 - 3)(nDt + C_1)^{(2(n-1)N_3+3)/nN_3}}. \quad (7.27)$$

Figure 30 shows the evolution of the velocity of sound. As one sees, for a positive DP, the system is stable at the initial stage, while becomes instable later on. On the contrary, for a negative DP, it is instable initially, but becomes stable in the course of evolution of the Universe.

8. BIANCHI TYPE-I COSMOLOGICAL MODELS

Let us now consider the Bianchi type-I cosmological model.

A Bianchi type-I (BI) Universe, being the straightforward generalization of the flat Friedmann–Robertson–Walker (FRW) Universe, is one of the simplest models of an anisotropic Universe that describes a homogeneous and spatially flat Universe. Unlike the RW Universe, which has the same scale factor for each of the three spatial directions, a BI Universe has a different scale factor in each direction, thereby introducing an anisotropy to the system. It moreover has the agreeable property that near the singularity it behaves like a Kasner Universe, even in the presence of matter, and consequently falls within the general analysis of the singularity given by Belinskii et al. [13]. Also in a Universe filled with matter for $p = \zeta\varepsilon$, $\zeta < 1$, it has been shown that any initial anisotropy in a BI Universe quickly dies away, and a BI Universe eventually evolves into a

FRW Universe [89]. Since the present-day Universe is surprisingly isotropic, this feature of the BI Universe makes it a prime candidate for studying the possible effects of an anisotropy in the early Universe on present-day observations. In light of the importance mentioned above, several authors have studied BI Universe from different aspects.

The Einstein field equations in this case take the form:

$$\frac{\ddot{a}_2}{a_2}+\frac{\ddot{a}_3}{a_3}+\frac{\dot{a}_2}{a_2}\frac{\dot{a}_3}{a_3}=\kappa T_1^1, \tag{8.1a}$$

$$\frac{\ddot{a}_3}{a_3}+\frac{\ddot{a}_1}{a_1}+\frac{\dot{a}_3}{a_3}\frac{\dot{a}_1}{a_1}=\kappa T_2^2, \tag{8.1b}$$

$$\frac{\ddot{a}_1}{a_1}+\frac{\ddot{a}_2}{a_2}+\frac{\dot{a}_1}{a_1}\frac{\dot{a}_2}{a_2}=\kappa T_3^3, \tag{8.1c}$$

$$\frac{\dot{a}_1}{a_1}\frac{\dot{a}_2}{a_2}+\frac{\dot{a}_2}{a_2}\frac{\dot{a}_3}{a_3}+\frac{\dot{a}_3}{a_3}\frac{\dot{a}_1}{a_1}=\kappa T_0^0. \tag{8.1d}$$

We consider two different cases.

8.1. Model with Constant Deceleration Parameter. First, we consider the case with constant deceleration parameter [114]. To begin with we consider the energy–momentum tensor given by (5.1). In this case, the Einstein system Eqs. (8.1a)–(8.1d) take the form

$$\frac{\ddot{a}_2}{a_2}+\frac{\ddot{a}_3}{a_3}+\frac{\dot{a}_2}{a_2}\frac{\dot{a}_3}{a_3}=-\kappa(\omega+\delta)\varepsilon, \tag{8.2a}$$

$$\frac{\ddot{a}_3}{a_3}+\frac{\ddot{a}_1}{a_1}+\frac{\dot{a}_3}{a_3}\frac{\dot{a}_1}{a_1}=-\kappa(\omega+\gamma)\varepsilon, \tag{8.2b}$$

$$\frac{\ddot{a}_1}{a_1}+\frac{\ddot{a}_2}{a_2}+\frac{\dot{a}_1}{a_1}\frac{\dot{a}_2}{a_2}=-\kappa\omega\varepsilon, \tag{8.2c}$$

$$\frac{\dot{a}_1}{a_1}\frac{\dot{a}_2}{a_2}+\frac{\dot{a}_2}{a_2}\frac{\dot{a}_3}{a_3}+\frac{\dot{a}_3}{a_3}\frac{\dot{a}_1}{a_1}=\kappa\varepsilon. \tag{8.2d}$$

As one sees, we have four equations for seven unknowns, namely a_1, a_2, a_3, ε, ω, δ, and γ. So we need three additional constraints.

8.1.1. Solution to the Equations. As we have already mentioned, we will consider the case with deceleration parameter. On account of (4.14), the definition of the deceleration parameter (4.15) can be rewritten as

$$q=-\frac{\dot{H}}{H^2}-1. \tag{8.3}$$

Now, taking into account that as per assumption q is a constant, from (8.3) we immediately find

$$H=\frac{1}{(1+q)t+C_1},\quad C_1=\text{const}. \tag{8.4}$$

Further calculation gives

$$a = [(1+q)t + C_1]^{1/(1+q)}, \tag{8.5}$$

and

$$V = [(1+q)t + C_1]^{3/(1+q)}. \tag{8.6}$$

Secondly, we assume the proportionality condition given by (4.19), from which immediately follows (4.21).

And finally we assume that $\delta = \gamma$. Then subtraction of (8.2a) from (8.2b) leads to

$$\frac{a_1}{a_2} = D_1 \exp\left(X_1 \int \frac{dt}{V}\right), \quad D_1 = \text{const}, \quad X_1 = \text{const}. \tag{8.7}$$

On account of (4.3), (4.21), (8.7) and (8.6) we finally find

$$a_1 = \sqrt{\frac{D_1}{N_0}}[(1+q)t + C_1]^{(2N_3-3)/2N_3(1+q)} \times \\ \times \exp\left\{\frac{X_1}{2(q-2)}[(1+q)t + C_1]^{(q-2)/(q+1)}\right\}, \tag{8.8a}$$

$$a_2 = \sqrt{\frac{1}{D_1 N_0}}[(1+q)t + C_1]^{(2N_3-3)/2N_3(1+q)} \times \\ \times \exp\left\{\frac{-X_1}{2(q-2)}[(1+q)t + C_1]^{(q-2)/(q+1)}\right\}, \tag{8.8b}$$

$$a_3 = N_0[(1+q)t + C_1]^{(N_3+3)/N_3(1+q)}. \tag{8.8c}$$

8.1.2. Physical Aspects of the Model. The directional Hubble parameters take the form

$$H_1 = \left[1 - \frac{3}{2N_3}\right] H + \frac{X_1}{2}, \quad H_2 = \left[1 - \frac{3}{2N_3}\right] H - \frac{X_1}{2}, \\ H_3 = \left[1 + \frac{3}{N_3}\right] H. \tag{8.9}$$

From (8.2d) in this case we find the energy density as

$$\varepsilon = \left(\frac{X_2}{\kappa}\right)[(1+q)t + C_1]^{-2} - X_1^2/4\kappa, \tag{8.10}$$

where $X_2 = (12N_3^2 - 27)/4N_3^2$. As we can see, the energy density is a decreasing function of time, if $(1+q)t + C_1 \neq 0$. In this case the model behaves like the one filled with fluid or dark energy with $q < -1$. But since q may be negative as well,

in that case there is a possibility, when at some moment of time $(1+q)t+C_1 = 0$. In this case we have the model with phantom matter, which gives rise to a Big Rip-type solution, when the energy density becomes infinity at a finite moment of time [132–134, 155–158].

In Fig. 31, we have shown the evolution of energy density and EoS parameter for a positive DP. As expected, the energy density is decreasing function of time and it is qualitative the same as in the case of Bianchi type-VI_0 or III models.

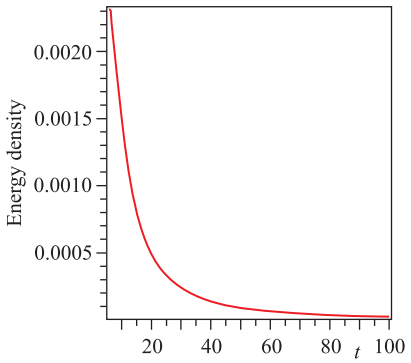

Fig. 31. Evolution of energy density ε versus t in power-law expansion for $q > 0$

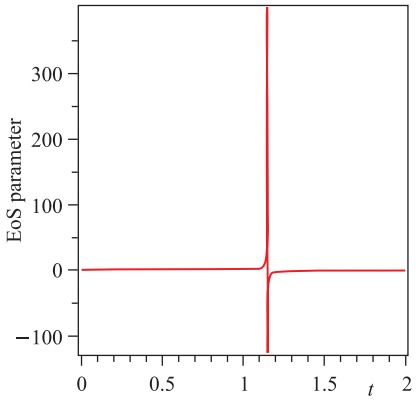

Fig. 32. Evolution of EoS parameter for $q > 0$

The variation of EoS parameter (ω) with cosmic time (t) is clearly shown in Fig. 32, as a representative case with appropriate choice of constants of integration and other physical parameters using reasonably well-known situations. From Fig. 32, we conclude that in early stage of evolution of the Universe, the EoS parameter was positive (i.e., the Universe was matter-dominated) and at late time it is evolving with negative value (i.e., at the present time). The earlier real matter later on was converted to the dark energy dominated phase of the Universe.

From (8.2c) we find the EoS parameter

$$\omega = \frac{X_3[(1+q)t + C_1]^{-2} - X_1^2/4}{X_2[(1+q)t + C_1]^{-2} - X_1^2/4}, \tag{8.11}$$

where we define $X_3 = [(2q-1)4N_3^2 + (2-q)126N_3 - 27]/4N_3^2$. From (8.2a) we find the skewness parameter

$$\gamma = -\frac{X_4[(1+q)t + C_1]^{-2}}{X_2[(1+q)t + C_1]^{-2} - X_1^2/4}, \tag{8.12}$$

where we define $X_4 = 9[4+q]/2N_3$.

Analyzing as in the previous case, we find that the EoS parameter is a function of t and can be presented as a function of red-shift as well. So, if the present work is compared with experimental results obtained in [82,93,94,186], then one can conclude that the limit of ω provided by equation (8.11) may accommodated with the acceptable range of EoS parameter. Also it is observed that at $t = t_c$, ω vanishes, where t_c is a critical time given by

$$t_c = \frac{1}{1+q}\left[\frac{2}{X_1}\sqrt{X_3} - C_1\right]. \tag{8.13}$$

Thus, for this particular time, our model represents a dusty Universe. We also note that the earlier real matter at $t \leqslant t_c$, where $\omega \geqslant 0$, later on at $t > t_c$, where $\omega < 0$, is converted to the dark energy dominated phase of Universe.

For the value of ω to be consistent with observation [93], we have the following general condition:

$$t_1 < t < t_2, \tag{8.14}$$

where

$$t_1 = \frac{1}{1+q}\left[\frac{2}{X_1}\sqrt{\frac{X_3 + 1.67X_2}{2.67}} - C_1\right] \tag{8.15}$$

and

$$t_2 = \frac{1}{1+q}\left[\frac{2}{X_1}\sqrt{\frac{X_3 + 0.62X_2}{1.62}} - C_1\right]. \tag{8.16}$$

For this constraint, we obtain $-1.67 < \omega < -0.62$, which is in good agreement with the limit obtained from observational results coming from SNe Ia data [93].

For the value of ω to be consistent with observation (Tegmark et al., 2004), we have the following general condition:

$$t_3 < t < t_4, \tag{8.17}$$

where

$$t_3 = \frac{1}{1+q}\left[\frac{2}{X_1}\sqrt{\frac{X_3 + 1.33X_2}{2.33}} - C_1\right] \tag{8.18}$$

and

$$t_4 = \frac{1}{1+q}\left[\frac{2}{X_1}\sqrt{\frac{X_3 + 0.79X_2}{1.79}} - C_1\right]. \tag{8.19}$$

For this constraint, we obtain $-1.33 < \omega < -0.79$, which is in good agreement with the limit obtained from observational results coming from SNe Ia data [186].

For the value of ω to be consistent with observation [82, 94], we have the following general condition:

$$t_5 < t < t_6, \tag{8.20}$$

where

$$t_5 = \frac{1}{1+q}\left[\frac{2}{X_1}\sqrt{\frac{X_3 + 1.44X_2}{2.44}} - C_1\right] \tag{8.21}$$

and

$$t_6 = \frac{1}{1+q}\left[\frac{2}{X_1}\sqrt{\frac{X_3 + 0.92X_2}{1.92}} - C_1\right]. \tag{8.22}$$

For this constraint, we obtain $-1.44 < \omega < -0.92$, which is in good agreement with the limit obtained from observational results coming from SNe Ia data [82, 94].

We also observed that if

$$t_0 = \frac{1}{1+q}\left[\frac{2}{X_1}\sqrt{\frac{X_3 + X_2}{2}} - C_1\right], \tag{8.23}$$

then for $t = t_0$ we have $\omega = -1$, i.e., we have Universe with cosmological constant. If $t < t_0$, then we have $\omega > -1$ that corresponds to quintessence, while for $t > t_0$ we have $\omega > -1$, i.e., Universe with phantom matter [33].

In this case, from (8.10) we find that the energy density ε is a decreasing function of time and $\varepsilon \geqslant 0$ when

$$t \leqslant \frac{1}{1+q}\left(\frac{\sqrt{X_2}}{2X_1} - C_1\right). \tag{8.24}$$

For the cosmological constant from (4.50) we find the cosmological constant as

$$\Lambda = \left[3 - \left(\frac{X_2}{\kappa}\right)\right] \times \times \left[(1+q)t + C_1\right]^{-2} + \frac{X_1^2}{4\kappa}. \tag{8.25}$$

As we see, the cosmological function is a decreasing function of time and it is always positive when

$$t \geqslant \frac{1}{1+q}\left[\frac{X_1}{2\sqrt{X_2 - 3\kappa}} - C_1\right]. \tag{8.26}$$

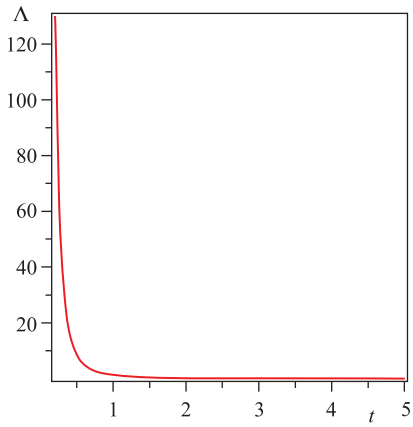

Fig. 33. Evolution of cosmological constant with respect to cosmic time

In Fig. 33, evolution of the cosmological constant is illustrated.

8.2. LRS BI Model with Dominance Dark Energy. Let us now consider a LRS Bianchi type-I model filled with a binary mixture of perfect fluid and dark energy. The energy–momentum tensor in this case is given by $T_j^i = T_j^{(m)i} + T_j^{(\mathrm{de})i}$, where

$$T_j^{(m)i} = \mathrm{diag}\,[-\rho^{(m)}, p^{(m)}, p^{(m)}, p^{(m)}] = \\ = \mathrm{diag}\,[-1, \omega^{(m)}, \omega^{(m)}, \omega^{(m)}]\rho^{(m)} \quad (8.27)$$

and

$$T_j^{(\mathrm{de})i} = \mathrm{diag}\,[-\rho^{(\mathrm{de})}, p^{(\mathrm{de})}, p^{(\mathrm{de})}, p^{(\mathrm{de})}] = \\ = \mathrm{diag}\,[-1, \omega^{(\mathrm{de})}, \omega^{(\mathrm{de})}, \omega^{(\mathrm{de})}]\rho^{(\mathrm{de})}, \quad (8.28)$$

where $\rho^{(m)}$ and $p^{(m)}$ are, respectively, the energy density and pressure of the perfect fluid component or ordinary baryonic matter, while $\omega^{(m)}$ is its EoS parameter. Similarly, $\rho^{(\mathrm{de})}$ and $p^{(\mathrm{de})}$ are, respectively, the energy density and pressure of the DE component, while $\omega^{(\mathrm{de})}$ is the corresponding EoS parameter.

The Einstein system of equations for LRS BI model on account of $a_2 = a_3$ then reads

$$2\frac{\ddot{a}_2}{a_2} + \frac{\dot{a}_2^2}{a_2^2} = -\kappa(\omega^{(m)}\rho^{(m)} + \omega^{(\mathrm{de})}\rho^{(\mathrm{de})}), \quad (8.29a)$$

$$\frac{\ddot{a}_1}{a_1} + \frac{\ddot{a}_2}{a_2} + \frac{\dot{a}_1}{a_1}\frac{\dot{a}_2}{a_2} = -\kappa(\omega^{(m)}\rho^{(m)} + \omega^{(\mathrm{de})}\rho^{(\mathrm{de})}), \quad (8.29b)$$

$$2\frac{\dot{a}_1}{a_1}\frac{\dot{a}_2}{a_2} + \frac{\dot{a}_2^2}{a_2^2} = \kappa(\rho^{(m)} + \rho^{(\mathrm{de})}). \quad (8.29c)$$

Following Akarsu and Kilinc [1], we assume the EoS parameter of the perfect fluid to be a constant

$$\omega^{(m)} = \frac{p^{(m)}}{\rho^{(m)}} = \mathrm{const}, \quad (8.30)$$

whereas the EoS of the dark energy

$$\omega^{(\mathrm{de})} = \frac{p^{(\mathrm{de})}}{\rho^{(\mathrm{de})}} \quad (8.31)$$

is considerd to be a function of time, since the current cosmological data from SNIa, CMB and large scale structures mildly favor dynamically evolving DE crossing the phantom divide-line (PDL) [201].

8.2.1. Solution to the Equation. In order to solve the field equations completely, firstly we assume that the perfect fluid and DE components interact minimally. Therefore, the energy momentum tensors of the two sources may be conserved separately.

The Bianchi identity $G^{ij}_{;j} = 0$, in this case, leads to the two separate equations for perfect fluid

$$\dot{\rho}^{(m)} + 3(1 + \omega^{(m)})\rho^{(m)} H = 0 \tag{8.32}$$

and dark energy

$$\dot{\rho}^{(\mathrm{de})} + 3(1 + \omega^{(\mathrm{de})})\rho^{(\mathrm{de})} H = 0. \tag{8.33}$$

We constrain the system of equations with proportionality relation between shear (σ) and expansion (θ). This condition leads to the following relation between the metric potentials:

$$a_1 = a_2^n, \tag{8.34}$$

where n is a positive constant. For anisotropic model $n \neq 1$.

In view of (8.34), from (8.29a) and (8.29b), we find

$$\frac{\ddot{a_2}}{a_2} + (n+1)\frac{\dot{a_2}^2}{a_2^2} = 0, \tag{8.35}$$

with the solution

$$a_2 = (k_1 t + k_0)^{\frac{1}{n+2}}\ , \tag{8.36}$$

where k_0 and k_1 are the constants of integration.

From equations (8.34) and (8.36), we obtain

$$a_1 = (k_1 t + k_0)^{\frac{n}{n+2}}. \tag{8.37}$$

The mean Hubble parameter (H), expansion scalar (ϑ), and shear scalar (σ) are given by

$$\vartheta = 3H = \frac{k_1}{(k_1 t + k_0)}, \tag{8.38}$$

$$\sigma^2 = \frac{(n-1)^2}{3(n+2)^2}\vartheta^2. \tag{8.39}$$

The rate of expansion in the direction of x, y, and z are given by

$$H_1 = \frac{\dot{a_1}}{a_1} = \frac{3n}{(n+2)}H, \quad H_2 = H_3 = \frac{\dot{a_2}}{a_2} = \frac{3}{(n+2)}H. \tag{8.40}$$

The spatial volume (V), mean anisotropy parameter (A_m), and DP (q) are found to be

$$V = a_1 a_2^2 = (k_1 t + k_0), \tag{8.41}$$

$$A_m = \frac{2(n-1)^2}{(n+2)^2}, \tag{8.42}$$

$$q = \frac{d}{dt}\left(\frac{1}{H}\right) - 1 = 2. \tag{8.43}$$

It is important to note here that the proportionality relation between shear and expansion leads to the positive deceleration parameter (q) with isotropic distribution of DE in LRS Bianchi-I space–time. Since we are looking for a model explaining an expanding Universe with acceleration, so, we assume the anisotropic distribution of DE to ensure the present acceleration of Universe. So we write equations (8.29a), (8.29b), and (8.33) as

$$2\frac{\ddot{a}_2}{a_2}+\frac{\dot{a}_2^2}{a_2^2}=-\kappa[\omega^{(m)}\rho^{(m)}+(\omega^{(\mathrm{de})}+\delta)\rho^{(\mathrm{de})}], \tag{8.44}$$

$$\frac{\ddot{a}_1}{a_1}+\frac{\ddot{a}_2}{a_2}+\frac{\dot{a}_1}{a_1}\frac{\dot{a}_2}{a_2}=-\kappa[\omega^{(m)}\rho^{(m)}+(\omega^{(\mathrm{de})}+\gamma)\rho^{(\mathrm{de})}], \tag{8.45}$$

$$\dot{\rho}^{(\mathrm{de})}+3\rho^{(\mathrm{de})}(1+\omega^{(\mathrm{de})})H+\rho^{(\mathrm{de})}(\delta H_1+2\gamma H_2)=0. \tag{8.46}$$

The third term of Eq. (8.46) arises due to the deviation from $\omega^{(\mathrm{de})}$, while the first and second terms of Eq. (8.46) are deviation free part of $T_j^{(\mathrm{de})i}$. According to Eq. (8.46), the behavior of $\rho^{(\mathrm{de})}$ is controlled by the deviation free part of EoS parameter of DE, but deviation will affect $\rho^{(\mathrm{de})}$ indirectly, since, as can be seen later, they affect the value of EoS parameter. But we are looking for physically viable models of Universe consistent with observations. Hence we constrained $\delta(t)$ and $\gamma(t)$ by assuming the special dynamics which is consistent with (8.46). The dynamics of skewness parameter on x-axis (δ) and y-axis or z-axis (γ) is given by

$$\delta=-\frac{2mHH_2}{\rho^{(\mathrm{de})}}\,, \tag{8.47}$$

$$\gamma=\frac{mHH_1}{\rho^{(\mathrm{de})}}\,, \tag{8.48}$$

where m is the dimensionless constant that parameterizes the amplitude of the deviation from $\omega^{(\mathrm{de})}$ and can be given as real values.

Subtraction of (8.44) from (8.45) gives

$$\frac{\ddot{a}_2}{a_2}-\frac{\ddot{a}_1}{a_1}+\frac{\dot{a}_2^2}{a_2^2}-\frac{\dot{a}_1}{a_1}\frac{\dot{a}_2}{a_2}=(\gamma-\delta)\rho^{(\mathrm{de})}. \tag{8.49}$$

Using Eqs. (8.34), (8.47), and (8.48), from (8.49), we obtain

$$\frac{\ddot{a_2}}{a_2}+\left[\frac{3(n^2-1)+m(n+2)^2}{3(n-1)}\right]\frac{\dot{a_2}^2}{a_2^2}=0. \tag{8.50}$$

The general solution of Eq. (8.50) has the form

$$a_2=(k_1t+k_0)^{\frac{3(n-1)}{n_1}}, \tag{8.51}$$

where $n_1 = 3N_1 + m(n+2)^2$ with $N_1 = (n-1)(n+2)$. For a_1 in this case we find

$$a_1 = (k_1 t + k_0)^{\frac{3n(n-1)}{n_1}}. \tag{8.52}$$

It is important to note here that we obtain power law solution by assuming proportionality relation between shear scalar (σ) and expansion (θ) which seems to describe the dynamics of Universe from Big Bang to the present epoch, while a series of works [1, 4, 98, 202–204] have obtained the power law solution by assuming special law of variation of the Hubble parameter. So, we represent the new features of power law expansion. In this paper, we show how $\sigma \propto \theta$ model with LRS BI metric behaves in the presence of perfect fluid and anisotropic DE components.

In view of the assumption $\omega^{(m)} = \text{const}$, Eq. (8.32) can be integrated to obtain

$$\rho^{(m)} = \rho_0 a^{-3(\omega^{(m)}+1)}, \tag{8.53}$$

where ρ_0 is the positive constant of integration.

Average Hubble parameter (H), expansion scalar (ϑ) in this case is expressed as

$$\vartheta = 3H = \frac{3N_1}{n_1}\frac{k_1}{(k_1 t + k_0)}. \tag{8.54}$$

The shear scalar (σ), directional Hubble parameters $(H_1,\ H_2$ or $H_3)$, and the anisotropy parameter (A_m) have the same form as in the previous case, i.e., given by the expressions (8.39), (8.40), and (8.42), respectively. The spatial volume (V), average scale factor (a) and DP (q) of the model are found to be

$$V = (k_1 t + k_0)^{(3N_1/n_1)}, \tag{8.55}$$

$$a = (k_1 t + k_0)^{(N_1/n_1)}, \tag{8.56}$$

$$q = \frac{n_1}{N_1} - 1 = 2 + \frac{m}{N_1}(n+2)^2. \tag{8.57}$$

As one sees, the DP q is a constant. The sign of q indicates whether the model inflates or not. A positive sign of q, i.e., $n_1/N_1 > 1$, corresponds to standard decelerating model whereas negative sign of q, i.e., $0 < n_1/N_1 < 1$, indicates acceleration. The recent observations SN Ia, reveal that the present Universe is accelerating and the value of DP lies somewhere in the range $-1 < q < 0$. It follows that in the derived model, one can choose the value of DP consistent with observations.

From (8.53) we then find the energy density of perfect fluid

$$\rho^{(m)} = \rho_0 (k_1 t + k_0)^{-3(\omega^{(m)}+1)N_1/n_1}, \tag{8.58}$$

on account of (8.58) from (8.29c) we obtain the dark energy density

$$\rho^{(\mathrm{de})} = \frac{9(2n+1)(n-1)^2k_1^2}{n_1^2(k_1t+k_0)^2} - \frac{\rho_0}{(k_1t+k_0)^{3(\omega^m+1)N_1/n_1}}. \tag{8.59}$$

In Fig. 34, we plot the energy density of matter and that of dark energy with respect to cosmic time. We see that they both are positive, hence the weak and null energy conditions are satisfied for the model in question.

Now from (8.47) and (8.48) skewness parameters are obtained as

$$\delta(t) = -\frac{6m(n-1)N_1k_1^2}{9(2n+1)(n-1)^2k_1^2 - \rho_0 n_1^2(k_1t+k_0)^{2-3(\omega^{(m)}+1)N_1/n_1}}, \tag{8.60}$$

$$\gamma(t) = \frac{3mn(n-1)N_1k_1^2}{9(2n+1)(n-1)^2k_1^2 - \rho_0 n_1^2(k_1t+k_0)^{2-3(\omega^{(m)}+1)N_1/n_1}}. \tag{8.61}$$

The EoS parameter of DE is given by

$$\omega^{(\mathrm{de})} = \\ = -\frac{\dfrac{\omega^{(m)}\rho_0}{(k_1t+k_0)^{3(\omega^{(m)}+1)N_1/n_1}} + \dfrac{3(n-1)^2k_1^2(6-2m(n+2)-n_1/(n-1))}{n_1^2(k_1t+k_0)^2}}{\dfrac{9(2n+1)(n-1)^2k_1^2}{n_1^2(k_1t+k_0)^2} - \dfrac{\rho_0}{(k_1t+k_0)^{3(\omega^m+1)N_1/n_1}}}. \tag{8.62}$$

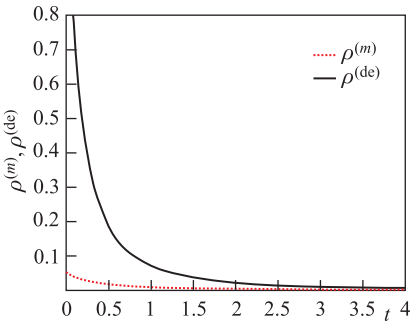

Fig. 34. Evolution of matter and dark energy density with respect to cosmic time

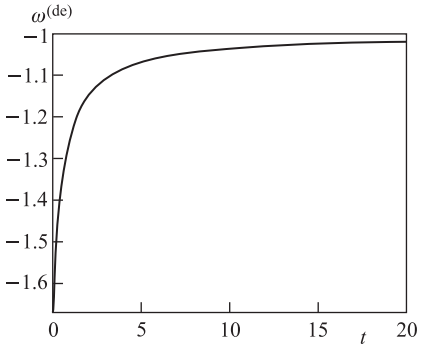

Fig. 35. Evolution of EoS parameter with respect to cosmic time

In Fig. 35, we have plotted the evolution of the EoS parameter with respect to cosmic time.

It is observed that at $t = -k_0/k_1$, the spatial volume vanishes while all other parameters diverge. Thus the derived model starts expanding with the Big Bang

singularity at $t = -k_0/k_1$ which can be shifted to $t = 0$ by choosing $k_0 = 0$. This singularity is of point type because the directional scale factors $A(t)$ and $B(t)$ vanish at initial moment. We observe that $\rho^{(m)}$ as well as $\rho^{(\mathrm{de})}$ remains positive during the cosmic evolution. Therefore, the weak energy condition (WEC) as well as null energy condition (NEC) are obeyed in the derived model. Further $\rho^{(m)}$ and $\rho^{(\mathrm{de})}$ decrease with time and approach a small positive values at the present epoch. The parameters H, σ, and θ start off with extremely large values and continue to decrease with expansion of Universe. As is seen from Fig. 35, the dark energy density $\omega^{(\mathrm{de})}$ evolves with negative value, and its range is in nice agreement with large scale structure data [94].

The density parameters of perfect fluid and DE are as follows:

$$\Omega^{(m)} = \frac{\rho_0 n_1^2}{3N_1^2 k_1^2}(k_1 t + k_0)^{2-3(\omega^{(m)}+1)N_1/n_1}, \tag{8.63}$$

$$\Omega^{(\mathrm{de})} = \frac{3(2n+1)}{(n+2)^2} - \frac{\rho_0 n_1^2}{3N_1^2 k_1^2}(k_1 t + k_0)^{2-3(\omega^{(m)}+1)N_1/n_1}. \tag{8.64}$$

After adding Eqs. (8.63) and (8.64), the overall density parameter (Ω) is obtained as

$$\Omega = \Omega^{(m)} + \Omega^{(\mathrm{de})} = \frac{3(2n+1)}{2(n-1)^2} A_m. \tag{8.65}$$

This shows that the overall density parameter (Ω) depends on the anisotropy parameter (A_m). The behavior of density parameters in the evolution of Universe with appropriate choice of constants of integration and other physical parameters gives reasonably well-known situations. We observe that initially the ordinary matter density dominates the Universe. But later on, the DE density dominates the evolution which is probably responsible for the accelerated expansion of the present-day Universe.

8.2.2. The Statefinder and Distance Modulus Curves. Sahni et al. [169] proposed a cosmological diagnostic pair $\{r, s\}$ called state finder, which is defined as

$$r = \frac{\dddot{a}}{aH^3} = \left(2\frac{n_1}{N_1} + 1\right)\left(\frac{n_1}{N_1} - 1\right), \tag{8.66}$$

$$s = \frac{r-1}{3\left(q - \frac{1}{2}\right)} = \frac{\left(2\frac{n_1}{N_1} + 1\right)\left(\frac{2n_1}{N_1} - 1\right) - 1}{3\left(\frac{n_1}{N_1} - \frac{3}{2}\right)}. \tag{8.67}$$

The dynamics of state finder $\{r, s\}$ depends on constants n and n_1. It follows that in derived model, one can choose the pair of state finders which can successfully differentiate between a wide variety of DE models including cosmological

constant, quintessence, phantom, quintom, the Chaplygin gas, braneworld models and interacting DE models. For example, if we put $n_1 = 0$, the state-finder pair will be $\{1, 0\}$ which yields the ΛCDM (cosmological constant cold dark matter) model. The state-finder diagnosis for holographic DE model in nonflat Universe has been analyzed by Setare et al. [173].

The distance modulus is given by

$$\mu = 5 \log d_L + 25, \tag{8.68}$$

where the luminosity distance d_L is defined as

$$d_L = r_1(1 + z)a_0, \tag{8.69}$$

where z and a_0 represent red-shift parameter and present scale factor, respectively. Let us now assume that $T = k_1 t + k_0$. Thus equation (8.56) may be rewritten as

$$a = T^{n_2}, \tag{8.70}$$

where $n_2 = N_1/n_1$.

For determination of r_1, we assume that a photon is emitted by a source with co-ordinates $r = r_1$ and $T = T_1$ and is received at a time T_0 by an observer located at $r = 0$. Then we determine r_1 from

$$r_1 = \int_{T_1}^{T_0} \frac{dT}{a}. \tag{8.71}$$

Solving Eqs. (8.68)–(8.71), one can easily obtain the expression for distance modulus (μ) in terms of red-shift parameter (z) as

$$\mu = 5 \log \left[\frac{n_2 k_1}{H_0(1 - n_2)(1 + z)^{\frac{1-2n_2}{n_2}}} \left((1 + z)^{\frac{1-n_2}{n_2}} - 1 \right) \right] + 25. \tag{8.72}$$

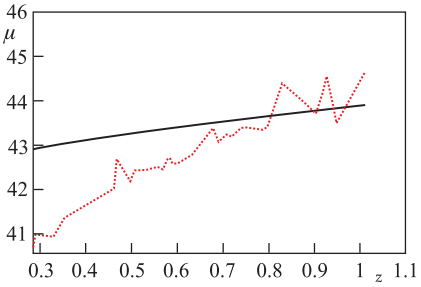

Fig. 36. Evolution of EoS parameter with respect to cosmic time

The comparison between the derived model and SNLS type Ia supernovae data can be seen in Fig. 36. The dotted line represents the observed distance modulus by SNLS type Ia supernovae data, whereas the solid line represents the analyzed distance modulus μ of the derived model.

It is observed that the derived model is the best fit with high red-shift values.

9. INTERACTING TWO-FLUID SCENARIO IN FRW MODEL

FRW model is the most studied cosmological model. It is the simplest model of an expanding Universe. As was mentioned earlier, this isotropic and homogeneous cosmological model was first suggested by A. A. Friedmann [68,69]. Since that time it was widely believed that our Universe was a static one, his finding was overlooked as a mere mathematical exercise. But when in 1929 Hubble experimentally proved that our Universe is indeed expanding, the search for an expanding Universe became an ultimate task. The model proposed by Friedmann enjoyed a wide range of popularity after the independent papers by Robertson [122, 123] and Walker [194].

In this section, we study the evolution of the dark energy parameter within the scope of a FRW model, given by (3.2). For convenience, we will rewrite the metric in the following form:

$$ds^2 = -dt^2 + a^2(t)\left[\frac{dr^2}{1-kr^2} + r^2\left(d\theta^2 + \sin^2(\theta)\, d\phi^2\right)\right], \tag{9.1}$$

where $a(t)$ is some unknown function of time, and k is some constant, taking the value $+1, 0, -1$. For $k = -1$ or $k = 0$ the space comes out to be infinity (open). For $k = 0$ the space is flat, while $k = +1$ space is finite (closed), though not limited.

Corresponding Einstein field equations we write in the form

$$p_{\rm tot} = -\left(2\frac{\ddot{a}}{a} + \frac{\dot{a}^2}{a^2} + \frac{k}{a^2}\right), \tag{9.2a}$$

$$\rho_{\rm tot} = 3\left(\frac{\dot{a}^2}{a^2} + \frac{k}{a^2}\right), \tag{9.2b}$$

where $p_{\rm tot} = p_m + p_D$ and $\rho_{\rm tot} = \rho_m + \rho_D$. Here p_m and ρ_m are pressure and energy density of barotropic fluid and p_D and ρ_D are pressure and energy density of dark fluid, respectively.

The Bianchi identity $G^{;j}_{ij} = 0$ leads to $T^{;j}_{ij} = 0$ which yields

$$\dot{\rho}_{\rm tot} + 3\frac{\dot{a}}{a}(\rho_{\rm tot} + p_{\rm tot}) = 0. \tag{9.3}$$

The EoS of the barotropic fluid and dark field are given by

$$\omega_m = \frac{p_m}{\rho_m} \tag{9.4}$$

and

$$\omega_D = \frac{p_D}{\rho_D}, \tag{9.5}$$

respectively. In the following sections, we deal with two cases, (i) noninteracting two-fluid model and (ii) interacting two-fluid model.

9.1. Noninteracting Two-Fluid Model. Let us first consider the case when the fluid and dark energy are minimally coupled. In this case, Eq. (9.3) can be written as two separate equations:

$$\dot{\rho}_m + 3\frac{\dot{a}}{a}(\rho_m + p_m) = 0 \tag{9.6}$$

and

$$\dot{\rho}_D + 3\frac{\dot{a}}{a}(\rho_D + p_D) = 0. \tag{9.7}$$

Assuming the perfect fluid EoS parameter ω_m is constant, Eq. (9.6) can be immediately integrated to obtain

$$\rho_m = \rho_0 a^{-3(1+\omega_m)}, \tag{9.8}$$

where ρ_0 is a constant of integration. Inserting (9.8) into (9.2b) and (9.2a), we first obtain the ρ_D and p_D in terms of scale factor $a(t)$

$$\rho_D = 3\left(\frac{\dot{a}^2}{a^2} + \frac{k}{a^2}\right) - \rho_0 a^{-3(1+\omega_m)} \tag{9.9}$$

and

$$p_D = -\left(2\frac{\ddot{a}}{a} + \frac{\dot{a}^2}{a^2} + \frac{k}{a^2}\right) - \rho_0\omega_m a^{-3(1+\omega_m)}. \tag{9.10}$$

In what follows, we consider three different *ansätze* for the scale factor those give rise to a time-dependent deceleration parameter (DP):

$$q = -\frac{a\ddot{a}}{\dot{a}^2} = \frac{d}{dt}\left(\frac{1}{H}\right) - 1, \tag{9.11}$$

where H is the Hubble parameter defined as

$$H = -\frac{\dot{a}}{a}. \tag{9.12}$$

The motivation to use such *ansatz* is dictated by the fact that our Universe has recently entered into a phase of accelerated mode of expansion from the decelerating one. It means the DP has changed its sign, i.e., DP should be a function of time. Moreover, the transition of red-shift from deceleration to acceleration is about 0.5. Hence only a time variable DP, not constant one, can adequately draw the realistic picture of the evolution of the Universe. In what follows, we consider a new time parameter τ:

$$\tau = \frac{t}{t_1}, \tag{9.13}$$

where t_1 is a constant of unit time [t]. But for simplicity, we use the notation t instead of τ. As a result, $a(t)$ is still a unitless function. For simplicity, here and further we write a as a function of t with t now being unitless.

9.1.1. Ansatz I. First, we consider the case when the scale factor is given by [115]

$$a(t) = (t - t_0)^n, \tag{9.14}$$

where n is a positive constant. Under this assumption for ρ_D and p_D we obtain

$$\rho_D = \frac{3n^2}{(t-t_0)^2} + \frac{3k}{(t-t_0)^{2n}} - \rho_0 (t-t_0)^{-3n(1+\omega_m)} \tag{9.15}$$

and

$$p_D = -\left[\frac{n(3n-2)}{(t-t_0)^2} + \frac{k}{(t-t_0)^{2n}} + \rho_0 \omega_m (t-t_0)^{-3n(1+\omega_m)}\right], \tag{9.16}$$

respectively. Inserting (9.15) and (9.16) into (9.5), we find the EoS parameter of dark energy as

$$\omega_D = -\left[\frac{\dfrac{n(3n-2)}{(t-t_0)^2} + \dfrac{k}{(t-t_0)^{2n}} + \rho_0 \omega_m (t-t_0)^{-3n(1+\omega_m)}}{\dfrac{3n^2}{(t-t_0)^2} + \dfrac{3k}{(t-t_0)^{2n}} - \rho_0 (t-t_0)^{-3n(1+\omega_m)}}\right]. \tag{9.17}$$

It is observed that though for open, closed and flat Universe the EoS parameter is an increasing function of time, the rapidity of its growth at the early stage depends on the type of the Universe, while later on, it tends to the same constant value independent to it.

The expressions for the matter-energy density Ω_m and dark-energy density Ω_D are given by

$$\Omega_m = \frac{\rho_m}{3H^2} = \frac{\rho_0}{3n^2}(t-t_0)^{-3n(1+\omega_m)+2} \tag{9.18}$$

and

$$\Omega_D = \frac{\rho_D}{3H^2} = 1 + \frac{k}{n^2(t-t_0)^{2(n-1)}} - \frac{\rho_0}{3n^2}(t-t_0)^{-3n(1+\omega_m)+2}, \tag{9.19}$$

respectively. From (9.18) and (9.19) one obtains

$$\Omega = \Omega_m + \Omega_D = 1 + \frac{k}{n^2(t-t_0)^{2(n-1)}}. \tag{9.20}$$

From the right-hand side of Eq. (9.20) it is clear that in flat Universe ($k = 0$), $\Omega = 1$, in open Universe ($k = -1$), $\Omega < 1$ and in closed Universe ($k = +1$), $\Omega > 1$. But at late time, we see for all flat, open and closed Universes $\Omega \to 1$. This result is also compatible with the observational results. Since our model

predicts a flat Universe for large times and the present-day Universe is very close to flat, so the derived model is also compatible with the observational results.

In view of (9.2b) and (9.2a) from (9.11) we derive

$$q = \frac{1}{6H^2}[\rho_m(1+3\omega_m) + \rho_D(1+3\omega_D)]. \tag{9.21}$$

On the other hand, inserting (9.14) into (9.11), we find

$$q = \frac{1-n}{n}. \tag{9.22}$$

From (9.22) we observe that $q > 0$ for $0 < n < 1$ and $q < 0$ for $n > 1$.

In the Universe, nearly 70% of the energy is in the form of dark energy. Baryonic matter amounts to only 3–4%, while the rest of the matter (27% is believed to be in the form of a nonluminous component of nonbaryonic nature with a dust-like equation of state ($w = 0$)) is known as cold dark matter (CDM). In this case, if the dark energy is composed just by a cosmological constant, then this scenario is called Λ-CDM model. A convenient method to describe models close to Λ CDM is based on the cosmic jerk parameter j, the dimensionless third derivative of the scale factor with respect to the cosmic time [26, 40, 192, 193]. A deceleration-to-acceleration transition occurs for models with a positive value of j_0 and negative q_0. Flat Λ-CDM models have a constant jerk $j = 1$. The jerk parameter in cosmology is defined as the dimensionless third derivative of the scale factor with respect to cosmic time

$$j(t) = \frac{1}{H^3}\frac{\dddot{a}}{a}, \tag{9.23}$$

and in terms of the scale factor with respect to cosmic time

$$j(t) = \frac{(a^2H^2)''}{2H^2}, \tag{9.24}$$

where the «dots» and «primes» denote derivatives with respect to cosmic time and scale factor, respectively. The jerk parameter appears in the fourth term of a Taylor expansion of the scale factor around a_0:

$$\frac{a(t)}{a_0} = 1 + H_0(t-t_0) - \frac{1}{2}q_0H_0^2(t-t_0)^2 + \frac{1}{6}j_0H_0^3(t-t_0)^3 + O\left[(t-t_0)^4\right], \tag{9.25}$$

where the subscript 0 shows the present value. One can rewrite Eq. (9.23) as

$$j(t) = q + 2q^2 - \frac{\dot{q}}{H}. \tag{9.26}$$

In view of (9.14), from (9.22) and (9.26) we obtain

$$j(t) = \frac{(n-1)(n-2)}{n^2}. \tag{9.27}$$

This value overlaps with the value $j \simeq 2.16$ obtained from the combination of three kinematical data sets: the gold sample of type Ia supernovae [121], the SNIa data from the SNLS project [7], and the X-ray galaxy cluster distance measurements [118] for $n \simeq 0.55$.

9.1.2. Ansatz II. First, we consider the case when the scale factor is given by [5]

$$a(t) = \sqrt{te^t}. \tag{9.28}$$

Under this assumption ρ_D and p_D take the form

$$\rho_D = 3\left(\frac{n+t}{2t}\right)^2 + \frac{3k}{t^n e^t} - \rho_0 (t^n e^t)^{-\frac{3}{2}(1+\omega_m)} \tag{9.29}$$

and

$$p_D = -\left[3\left(\frac{n+t}{2t}\right)^2 - \frac{n}{t^2} + \frac{k}{t^n e^t} + \rho_0 \omega_m (t^n e^t)^{-\frac{3}{2}(1+\omega_m)}\right], \tag{9.30}$$

respectively. The EoS parameter for dark energy now reads

$$\omega_D = -\frac{3\left(\frac{n+t}{2t}\right)^2 - \frac{n}{t^2} + \frac{k}{t^n e^t} + \rho_0 \omega_m (t^n e^t)^{-\frac{3}{2}(1+\omega_m)}}{\left(\frac{n+t}{2t}\right)^2 + \frac{k}{t^n e^t} - \rho_0 (t^n e^t)^{-\frac{3}{2}(1+\omega_m)}}. \tag{9.31}$$

The behavior of EoS parameter qualitatively remains the same as in the previous case.

The expressions for the matter-energy density Ω_m and dark-energy density Ω_D are given by

$$\Omega_m = \frac{\rho_m}{3H^2} = \frac{4\rho_0 t^2}{3(t+n)^2} (t^n e^t)^{-\frac{3}{2}(1+\omega_m)} \tag{9.32}$$

and

$$\Omega_D = 1 + \frac{4k}{t^{n-2} e^t (n+t)^2} - \frac{4\rho_0 t^2}{3(t+n)^2} (t^n e^t)^{-\frac{3}{2}(1+\omega_m)}, \tag{9.33}$$

respectively. From (9.32) and (9.33) we find

$$\Omega = \Omega_m + \Omega_D = 1 + \frac{4k}{t^{n-2} e^t (n+t)^2}. \tag{9.34}$$

From the right-hand side of Eq. (9.34) it is clear that in flat Universe ($k = 0$), $\Omega = 1$, in open Universe ($k = -1$), $\Omega < 1$ and in closed Universe ($k = +1$), $\Omega > 1$. But at late time, we see for all flat, open and closed Universes $\Omega \to 1$. This result is also compatible with the observational results. Since our model predicts a flat Universe for large times and the present-day Universe is very close to flat, so the derived model is also compatible with the observational results.

For the deceleration parameter in this case we find

$$q = \frac{2}{(t+1)^2} - 1, \tag{9.35}$$

which is a function of time. From (9.22) we observe that $q > 0$ for $t < 0.41$ and $q < 0$ for $t > 0.41$.

The jerk in this case is a time varying function:

$$j(t) = 1 - \frac{6n}{(n+t)^2} + \frac{8n}{(n+t)^3}. \tag{9.36}$$

This value overlaps with the value $j \simeq 2.16$ obtained from the combination of three kinematical data sets: the gold sample of type Ia supernovae [121], the SNIa data from the SNLS project [7], and the X-ray galaxy cluster distance measurements [118] for

$$t = A - \frac{50n}{A} - n, \tag{9.37}$$

where

$$A = 0.03 \left(84100n + 1450\sqrt{1450n^3 + 3364n^2}\right)^{1/3}.$$

9.1.3. Ansatz III. Finally, we consider the case where the metric function is given by [153]

$$a(t) = \sqrt{t^n e^t}. \tag{9.38}$$

This *ansatz* generalizes the one proposed in [5].

Using this scale factor we find ρ_D and p_D as

$$\rho_D = 3\left(\frac{n+t}{2t}\right)^2 + \frac{3k}{t^n e^t} - \rho_0 (t^n e^t)^{-\frac{3}{2}(1+\omega_m)} \tag{9.39}$$

and

$$p_D = -\left[3\left(\frac{n+t}{2t}\right)^2 - \frac{n}{t^2} + \frac{k}{t^n e^t} - \rho_0 \omega_m (t^n e^t)^{-\frac{3}{2}(1+\omega_m)}\right], \tag{9.40}$$

respectively. The EoS parameter for dark energy now reads

$$\omega_D = -\frac{3\left(\frac{n+t}{2t}\right)^2 - \frac{n}{t^2} + \frac{k}{t^n e^t} - \rho_0 \omega_m (t^n e^t)^{-\frac{3}{2}(1+\omega_m)}}{\left(\frac{n+t}{2t}\right)^2 + \frac{k}{t^n e^t} - \rho_0 (t^n e^t)^{-\frac{3}{2}(1+\omega_m)}}. \tag{9.41}$$

Its behavior is qualitatively the same as in the previous cases.

The behavior of EoS in term of cosmic time t is shown in Fig. 37. It is observed that though for open, closed and flat Universes the EoS parameter is an increasing function of time, the rapidity of its growth at the early stage depends on the type of the Universe, while later on, it tends to the same constant value independent of it.

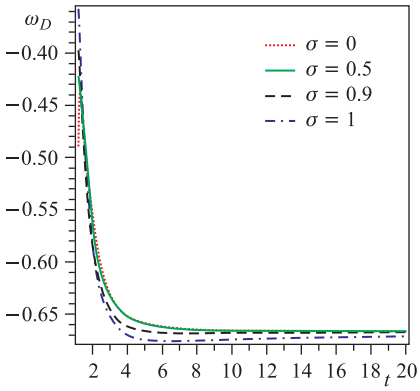

Fig. 37. Evolution of EoS parameter with respect to cosmic time

The expressions for the matter-energy density Ω_m and dark-energy density Ω_D are given by

$$\Omega_m = \frac{\rho_m}{3H^2} = \frac{4\rho_0 t^2}{3(t+n)^2}(t^n e^t)^{-\frac{3}{2}(1+\omega_m)} \tag{9.42}$$

and

$$\Omega_D = 1 + \frac{4k}{t^{n-2}e^t(n+t)^2} - \frac{4\rho_0 t^2}{3(t+n)^2}(t^n e^t)^{-\frac{3}{2}(1+\omega_m)}, \tag{9.43}$$

respectively. Equations (9.42) and (9.43) are reduced to

$$\Omega = \Omega_m + \Omega_D = 1 + \frac{4k}{t^{n-2}e^t(n+t)^2}. \tag{9.44}$$

From the right-hand side of Eq. (9.44) it is clear that in flat Universe ($k = 0$), $\Omega = 1$, in open Universe ($k = -1$), $\Omega < 1$ and in closed Universe ($k = +1$), $\Omega > 1$. But at late time, we see for all flat, open and closed Universes $\Omega \to 1$. This result is also compatible with the observational results. Since our model predicts a flat Universe for large times and the present-day Universe is very close to flat, so the derived model is also compatible with the observational results. The variation of density parameter Ω with respect to cosmic time is shown in Fig. 38.

The deceleration parameter (DP) in this case reads

$$q = \frac{2n}{(n+t)^2} - 1. \tag{9.45}$$

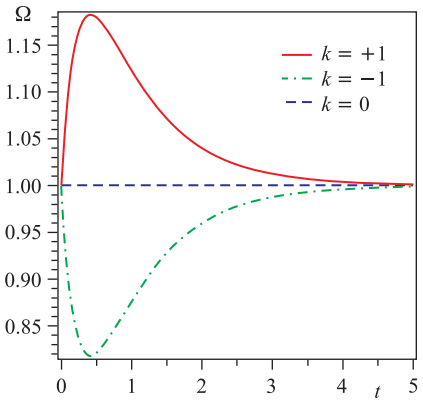

Fig. 38. Evolution of density parameter with respect to cosmic time

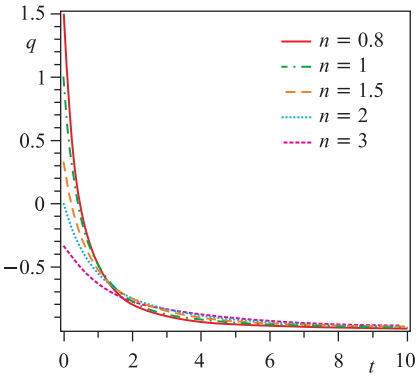

Fig. 39. Evolution of deceleration parameter with respect to cosmic time for different values of n

From Eq. (9.45), we observe that $q > 0$ for $t < \sqrt{2n} - n$ and $q < 0$ for $t > \sqrt{2n} - n$. It is observed that for $0 < n < 2$, our model is evolving from deceleration phase to acceleration phase. Also, recent observations of SNe Ia expose that the present Universe is accelerating and the value of DP lies to some place in the range $-1 < q < 0$. It follows that in our derived model, one can choose the value of DP consistent with the observation. Figure 39 depicts the deceleration parameter (q) versus time which gives the behavior of q from decelerating to accelerating phase for different values of n.

The jerk in this case takes the form

$$j(t) = 1 - \frac{6n}{(n+t)^2} + \frac{8n}{(n+t)^3}. \tag{9.46}$$

This value overlaps with the value $j \simeq 2.16$ obtained from the combination of three kinematical data sets: the gold sample of type Ia supernovae [121], the SNIa data from the SNLS project [7], and the X-ray galaxy cluster distance measurements [118] for

$$t = A - \frac{50n}{A} - n, \tag{9.47}$$

where

$$A = 0.03\left(84100n + 1450\sqrt{1450n^3 + 3364n^2}\right)^{1/3}.$$

9.2. Interacting Two-Fluid Scenario. Let us now consider the interaction between dark and barotropic fluids. For this purpose, we can write the continuity equations for dark fluid and barotropic fluids as

$$\dot{\rho}_m + 3\frac{\dot{a}}{a}(\rho_m + p_m) = Q, \tag{9.48}$$

and

$$\dot{\rho}_D + 3\frac{\dot{a}}{a}(\rho_D + p_D) = -Q. \tag{9.49}$$

The quantity Q expresses the interaction between the dark components. Since we are interested in an energy transfer from the dark energy to dark matter, we consider $Q > 0$. This assumption ensures that the second law of thermodynamics is fulfilled [111]. Here we emphasize that the continuity Eqs. (9.48) and (9.49) imply that the interaction term (Q) should be proportional to a quantity with units of inverse of time, i.e., $Q \propto 1/t$. Therefore, a first and natural candidate can be the Hubble factor H multiplied by the energy density. Following Amendola et al. [3] and Gou et al. [77], we consider

$$Q = 3H\sigma\rho_m, \tag{9.50}$$

where σ is a coupling constant. Using Eq. (9.50) in Eq.(9.48) and after integrating, we obtain

$$\rho_m = \rho_0 a^{-3(1+\omega_m-\sigma)}. \tag{9.51}$$

In view of (9.51), ρ_D and p_D can be expressed in term of scale factor $a(t)$:

$$\rho_D = 3\left(\frac{\dot{a}^2}{a^2} + \frac{k}{a^2}\right) - \rho_0 a^{-3(1+\omega_m-\sigma)} \tag{9.52}$$

and

$$p_D = -\left(2\frac{\ddot{a}}{a} + \frac{\dot{a}^2}{a^2} + \frac{k}{a^2}\right) - \rho_0(\omega_m - \sigma)a^{-3(1+\omega_m-\sigma)}, \tag{9.53}$$

respectively.

As in the case of noninteracting fluids, we again study the three cases.

9.2.1. Ansatz I. Inserting (9.14) into (9.49) and (9.53), we obtain

$$\rho_D = \frac{3n^2}{(t-t_0)^2} + \frac{3k}{(t-t_0)^{2n}} - \rho_0(t-t_0)^{-3n(1+\omega_m-\sigma)} \tag{9.54}$$

and

$$p_D = -\left[\frac{n(3n-2)}{(t-t_0)^2} + \frac{k}{(t-t_0)^{2n}} + \rho_0(\omega_m - \sigma)(t-t_0)^{-3n(1+\omega_m-\sigma)}\right], \tag{9.55}$$

respectively. Inserting (9.54) and (9.55) into (9.5), we can find the EoS parameter of dark field as

$$\omega_D = -\left[\frac{\dfrac{n(3n-2)}{(t-t_0)^2} + \dfrac{k}{(t-t_0)^{2n}} + \rho_0(\omega_m - \sigma)(t-t_0)^{-3n(1+\omega_m-\sigma)}}{\dfrac{3n^2}{(t-t_0)^2} + \dfrac{3k}{(t-t_0)^{2n}} - \rho_0(t-t_0)^{-3n(1+\omega_m-\sigma)}}\right]. \tag{9.56}$$

It is observed that, unlike the minimal coupling case, the EoS parameter is an increasing function of time though for open and flat Universes and a decreasing function of time for a closed one. At the later stage of evolution all the three tend to the same constant value independent of the type of the Universe.

The expressions for the matter-energy density Ω_m and dark-energy density Ω_D are given by

$$\Omega_m = \frac{\rho_m}{3H^2} = \frac{\rho_0}{3n^2}(t-t_0)^{-3n(1+\omega_m-\sigma)} \tag{9.57}$$

and

$$\Omega_D = \frac{\rho_D}{3H^2} = 1 + \frac{k}{n^2(t-t_0)^{2(n-1)}} - \frac{\rho_0}{3n^2}(t-t_0)^{-3n(1+\omega_m-\sigma)}, \tag{9.58}$$

respectively. From Eqs. (9.57) and (9.58), we obtain

$$\Omega = \Omega_m + \Omega_D = 1 + \frac{k}{n^2(t-t_0)^{2(n-1)}}, \tag{9.59}$$

which is the same as Eq. (9.59). Therefore, we observe that in the interacting case the density parameter has the same properties as in the noninteracting case. The expressions for deceleration parameter and jerk parameter are also the same as in the case of noninteracting case.

Studying the interaction between the dark energy and ordinary matter will open a possibility of detecting the dark energy. It should be pointed out that evidence was recently provided by the Abell Cluster A586 in support of the interaction between dark energy and dark matter [23, 49]. We observe that in noninteracting case both open and flat Universes can cross the phantom region, whereas in interacting case only open Universe can cross phantom region.

9.2.2. Ansatz II. Let us now study the interacting system of two-fluid scenario for the second assumption given by (9.28). In this case we obtain

$$\rho_D = 3\left(\frac{n+t}{2t}\right)^2 + \frac{3k}{t^n e^t} - \rho_0 (t^n e^t)^{-\frac{3}{2}(1+\omega_m-\sigma)} \tag{9.60}$$

and

$$p_D = -\left[3\left(\frac{n+t}{2t}\right)^2 - \frac{n}{t^2} + \frac{k}{t^n e^t} - \rho_0(\omega_m-\sigma)(t^n e^t)^{-\frac{3}{2}(1+\omega_m-\sigma)}\right], \tag{9.61}$$

respectively. The EoS parameter of dark field now reads

$$\omega_D = -\frac{3\left(\frac{n+t}{2t}\right)^2 - \frac{n}{t^2} + \frac{k}{t^n e^t} - \rho_0(\omega_m-\sigma)(t^n e^t)^{-\frac{3}{2}(1+\omega_m-\sigma)}}{3\left(\frac{n+t}{2t}\right)^2 + \frac{3k}{t^n e^t} - \rho_0 (t^n e^t)^{-\frac{3}{2}(1+\omega_m-\sigma)}}. \tag{9.62}$$

It is observed that, unlike the minimal coupling case, the EoS parameter is an increasing function of time for open and flat Universes and a decreasing function of time for a closed one. At the later stage of evolution all the three tend to the same constant value independent of the type of the Universe.

The expressions for the matter-energy density Ω_m and dark-energy density Ω_D are given by

$$\Omega_m = \frac{\rho_m}{3H^2} = \frac{4\rho_0 t^2}{3(t+n)^2}(t^n e^t)^{-\frac{3}{2}(1+\omega_m-\sigma)} \tag{9.63}$$

and

$$\Omega_D = 1 + \frac{4k}{t^{n-2}e^t(n+t)^2} - \frac{4\rho_0 t^2}{3(t+n)^2}(t^n e^t)^{-\frac{3}{2}(1+\omega_m-\sigma)}, \tag{9.64}$$

respectively. Hence, we obtain

$$\Omega = \Omega_m + \Omega_D = 1 + \frac{4k}{t^{n-2}e^t(n+t)^2}, \tag{9.65}$$

which is the same as Eq. (9.34). Therefore, we observe that in the interacting case the density parameter has the same properties as in the noninteracting case. The expressions for deceleration parameter and jerk parameter are also the same as in the case of noninteracting case.

9.2.3. Ansatz III. Finally we study the case when the scale factor is given by (9.38). In this case, for dark energy density and pressure of dark energy we obtain

$$\rho_D = 3\left(\frac{n+t}{2t}\right)^2 + \frac{3k}{t^n e^t} - \rho_0(t^n e^t)^{-\frac{3}{2}(1+\omega_m-\sigma)} \tag{9.66}$$

and

$$p_D = -\left[3\left(\frac{n+t}{2t}\right)^2 - \frac{n}{t^2} + \frac{k}{t^n e^t} - \rho_0(\omega_m-\sigma)(t^n e^t)^{-\frac{3}{2}(1+\omega_m-\sigma)}\right], \tag{9.67}$$

respectively. The EoS parameter of dark field in this case looks

$$\omega_D = -\frac{3\left(\frac{n+t}{2t}\right)^2 - \frac{n}{t^2} + \frac{k}{t^n e^t} - \rho_0(\omega_m-\sigma)(t^n e^t)^{-\frac{3}{2}(1+\omega_m-\sigma)}}{3\left(\frac{n+t}{2t}\right)^2 + \frac{3k}{t^n e^t} - \rho_0(t^n e^t)^{-\frac{3}{2}(1+\omega_m-\sigma)}}. \tag{9.68}$$

It is observed that, unlike the minimal coupling case, the EoS parameter is an increasing function of time for open and flat Universes and a decreasing function

of time for a closed one. At the later stage of evolution all the three tend to the same constant value independent of the type of the Universe.

The expressions for the matter-energy density Ω_m and dark-energy density Ω_D are given by

$$\Omega_m = \frac{\rho_m}{3H^2} = \frac{4\rho_0 t^2}{3(t+n)^2}(t^n e^t)^{-\frac{3}{2}(1+\omega_m-\sigma)} \tag{9.69}$$

and

$$\Omega_D = 1 + \frac{4k}{t^{n-2}e^t(n+t)^2} - \frac{4\rho_0 t^2}{3(t+n)^2}(t^n e^t)^{-\frac{3}{2}(1+\omega_m-\sigma)}, \tag{9.70}$$

respectively. The expression for $\Omega = \Omega_m + \Omega_D$ in this case coincides with that of noninteracting case, i.e.,

$$\Omega = \Omega_m + \Omega_D = 1 + \frac{4k}{t^{n-2}e^t(n+t)^2}. \tag{9.71}$$

9.3. Physical Acceptability and Stability of Solutions. For the stability of corresponding solutions in both noninteracting and interacting models, we should check that our models are physically acceptable. For this, firstly, it is required that the velocity of sound is less than that of light, i.e.,

$$0 \leqslant v_s = \frac{dp}{d\rho} < 1. \tag{9.72}$$

In view of (9.2b) and (9.2a) we find that

$$v_s = -\frac{1}{3} - \frac{2\dfrac{d}{dt}\left(\dfrac{\ddot{a}}{a}\right) - 3\rho_0\sigma(1+\omega_m-\sigma)a^{-3(1+\omega_m-\sigma)}\,\dfrac{\dot{a}}{a}}{3\dfrac{d}{dt}\left(\dfrac{\dot{a}^2}{a^2}\right) - \dfrac{6k}{a^2}\dfrac{\dot{a}}{a}}, \tag{9.73}$$

where we have taken into account the interaction. Setting $\sigma = 0$, we come to the noninteracting case. Being the *ansatz* III the most general one, we shall study the stability for that case only. In this case, we find for the interacting case

$$v_s = -\frac{1}{3} + \frac{2n(2-n-t) + 3\rho_0\sigma(1+\omega_m-\sigma)(n+t)\,t^2(t^n e^t)^{-3(1+\omega_m-\sigma)/2}}{3(n+t)[n+2kt^{2-n}e^{-t}]}. \tag{9.74}$$

As one sees, we can always choose n in such a way that the model satisfies the condition (9.72).

Figure 40 shows the sound speed with respect to cosmic time.

Secondly, let us study the energy conditions. The weak energy condition is given by

$$\rho \geqslant 0, \quad \rho + p \geqslant 0, \tag{9.75}$$

while the dominant energy condition has the form

$$\rho \geqslant |p|. \tag{9.76}$$

The strong energy condition reads

$$\rho + 3p \geqslant 0. \tag{9.77}$$

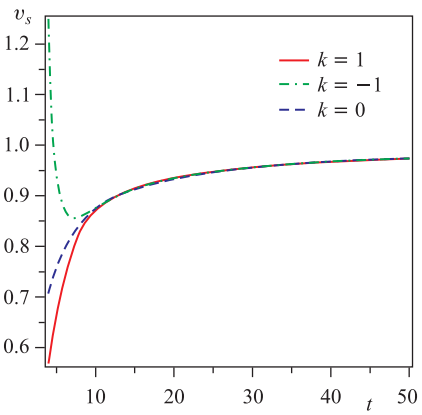

Fig. 40. Speed of sound with respect to cosmic time for different values of n

From the Eqs. (9.2b) and (9.2a) on account of interaction we find

$$\rho = 3\left[\left(\frac{\dot{a}}{a}\right)^2 + \frac{k}{a^2}\right], \tag{9.78}$$

$$\rho + p = 2\left[\left(\frac{\dot{a}}{a}\right)^2 + \frac{k}{a^2}\right] - 2\frac{\ddot{a}}{a} + \rho_0\sigma a^{-3(1+\omega-\sigma)}, \tag{9.79}$$

$$\rho + 3p = -6\frac{\ddot{a}}{a} + 3\rho_0\sigma a^{-3(1+\omega-\sigma)}. \tag{9.80}$$

For the *ansatz* (9.38) the foregoing equations give

$$\rho = 3\left[\left(\frac{n+t}{2t}\right)^2 + \frac{k}{t^n e^t}\right], \tag{9.81}$$

$$\rho + p = \left[\left(\frac{n+t}{2t}\right)^2 + 2\frac{k}{t^n e^t}\right] + \\ + \frac{n}{t^2} + \rho_0\sigma(t^n e^t)^{-3(1+\omega-\sigma)/2}, \tag{9.82}$$

$$\rho + 3p = 3\frac{n}{t^2} - \frac{3}{2}\frac{(n+t)^2}{t^2} + \\ + 3\rho_0\sigma(t^n e^t)^{-3(1+\omega-\sigma)/2}. \tag{9.83}$$

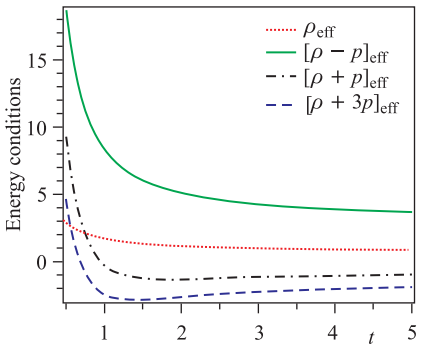

Fig. 41. Energy condition versus time for $k = 0$

As we see from Figs. 41–43, the weak and dominant energy conditions (9.75) and (9.76) for $k = 0$ and $k = 1$, i.e., for flat and closed models are satisfied. But

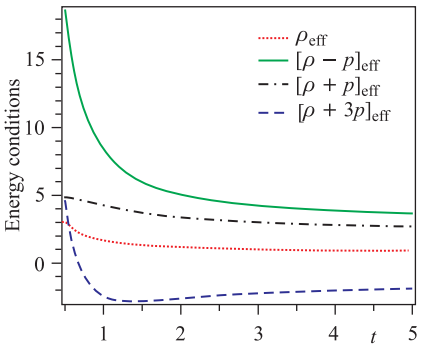

Fig. 42. Energy condition versus time for $k = +1$

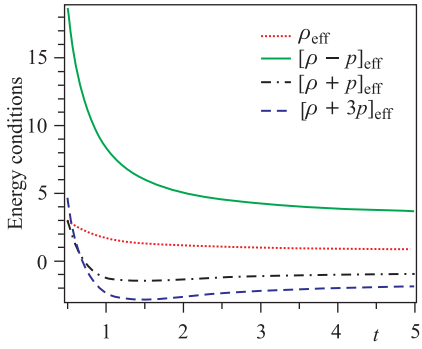

Fig. 43. Energy condition versus time for $k = -1$

for $k = -1$, i.e., for open model, this condition does not hold for the later stage of evolution. The strong energy condition holds only at the early stage of the evolution.

Based on the above discussion, we conclude that the corresponding solutions are physically acceptable.

CONCLUDING REMARKS ON THE RESULTS

In this review, we have studied the evolution of the Universe filled with dark energy with or without perfect fluid. In doing so, we considered a number of cosmological models, namely Bianchi type I, III, VI_0, VI, and FRW ones. For the anisotropic cosmological models we have used proportionality condition as an additional constraint.

In case of a BVI model, we found the exact solutions to the field equations in quadrature. It was found that if the proportionality condition is used, this together with the nondiagonal Einstein equation leads to the isotropic distribution of energy–momentum tensor, i.e., $T_1^1 = T_2^2 = T_3^3$. This fact allows one to solve the equation for volume scale V exactly. The behavior of EoS parameter ω is thoroughly studied.

A new anisotropic BVI_0 DE model with variable EoS parameter ω has been investigated by using the law of variation for the Hubble parameter proposed by Berman [20] which yields a constant value of deceleration parameter. In this case, it is found that two of the principal momenta are equal, i.e., $T_1^1 = T_2^2$. It is observed that, in early stage, the EoS parameter ω is positive, i.e., the Universe was matter-dominated in early stage but in late time, the Universe is evolving with negative values, i.e., the present epoch. DE model presents the dynamics of

EoS parameter ω whose range is in good agreement with the acceptable range by the recent observations [82, 93, 94, 186].

An anisotropic Bianchi type-V model is studied. It is found that under the proportionality condition the components of the energy–momentum tensor obey $T_1^1 + T_2^2 = 2T_3^3$. As a result like BVI_0 space–time, we need extra assumption to solve the equation for V, which is taken to the variation law of Hubble parameter. The model is thoroughly studied and the results are compared with observational data.

An anisotropic Bianchi type-III DE model with variable EoS parameter ω has been investigated, which is new and different from the other author's solutions. In the derived DE model of the Universe, the cosmological term is a decreasing function of time and it approaches a small positive value at late time (i.e., the present epoch). The value of cosmological «constant» for the model is found to be small and positive, which is supported by the recent observations.

A new anisotropic B-I DE model with variable EoS parameter ω has been investigated, which is different from the other author's solutions. The proposed law of variation for the Hubble parameter yields a constant value of deceleration parameter.

A spatially homogeneous and anisotropic locally rotationally symmetric Bianchi-I space–time filled with perfect fluid and anisotropic DE possessing dynamical energy density are studied. Studying the interaction between the ordinary matter and DE will open up the possibility of detecting DE. It should be pointed out that evidence was recently provided by Abell-Cluster A586 in support of interaction between DE and dark matter.

In the derived model, the EoS parameter of DE $(\omega^{(\mathrm{de})})$ is obtained as time varying and it is evolving with negative sign which may be attributed to the current accelerated expansion of Universe. Also note that the isotropic distribution of DE is not possible in LRS Bianchi type-I space–time because the isotropic distribution of DE leads to the positive value of DP which cannot explain the current accelerated expansion of Universe while for anisotropic distribution of DE, DP evolves with negative sign. The distance modulus curve of derived model is in good agreement with SNLS-type Ia supernovae for high red-shift value which in turn implies that the derived model is physically realistic.

A system of two fluids within the scope of a spatially flat and isotropic FRW model is studied. The role of two fluids either minimally or directly coupled in the evolution of the dark energy parameter has been investigated. In doing so, we have used three different *ansätze* regarding scale factor, that gives rise to a variable decelerating parameter. It is observed that in noninteracting case both open and flat Universes can cross the phantom region whereas in interacting case only open Universe can cross phantom region. The stability and acceptability of the solution obtained are also investigated.

Acknowledgements. This work is supported in part by a joint Romanian–LIT, JINR, Dubna Research Project, theme No. 05-6-1060-2005/2013. The author is thankful to Prof. A. Pradhan, Dr. H. Amirhashchi, Dr. A. K. Yadav, and V. Rikhvitsky for their support.

REFERENCES

1. *Akarsu O., Kilinc C. B.* LRS Bianchi Type-I Models with Anisotropic Dark Energy and Constant Deceleration Parameter // Gen. Rel. Grav. 2010. V. 42. P. 119.
2. *Amendola L. et al.* WMAP and the Generalized Chaplygin Gas // J. Cosmol. Astropart. Phys. 2003. V. 0307. P. 005.
3. *Amendola L., Camargo Campos G., Rosenfeld R.* Consequences of Dark Matter–Dark Energy Interaction on Cosmological Parameters Derived from Type Ia Supernova Data // Phys. Rev. D. 2007. V. 75. P. 083506.
4. *Amirhashchi H., Pradhan A., Saha B.* Variable Equation of State for Bianchi Type-VI_0 Dark Energy Models // Astrophys. Space Sci. 2011. V. 333. P. 295–303.
5. *Amirhashchi H., Pradhan A., Saha B.* An Interacting Two-Fluid Scenario for Dark Energy in an FRW Universe // Chin. Phys. Lett. 2011. V. 3. P. 039801.
6. *Armendáriz-Picón C., Greene P. B.* Spinors, Inflation, and Nonsingular Cyclic Cosmologies // Gen. Rel. Grav. 2003. V. 35, No. 9. P. 1637–1658.
7. *Astier P. et al.* The Supernova Legacy Survey: Measurement of Ω_M, Ω_Λ, and w from the First Year Data Set // Astron. Astrophys. 2006. V. 447. P. 31.
8. *Bali R., Pradhan A., Amirhashchi H.* Bianchi Type-VI 0 Magnetized Barotropic Bulk Viscous Fluid Massive String Universe in General Relativity // Intern. J. Theor. Phys. 2008. V. 47. P. 2594–2604.
9. *Barrow J. D.* Cosmological Limits on Slightly Skew Stress // Phys. Rev. D. 1997. V. 55. P. 7451.
10. *Barrow J. D., Maartens R.* Anisotropic Stresses in Inhomogeneous Universe // Phys. Rev. D. 1999. V. 59. P. 043502.
11. *Bean R., Dore O.* Are Chaplygin Gases Serious Contenders to the Dark Energy Throne? // Phys. Rev. D. 2003. V. 68. P. 023515.
12. *Beca L. M. et al.* The Role of Baryons in Unified Dark Matter Models // Phys. Rev. D. 2003. V. 67. P. 101301.
13. *Belinskii V. A., Khalatnikov I. M., Lifshitz E. M.* Oscillatory Approach to a Singular Point in the Relativistic Cosmology // Adv. Phys. 1970. V. 19. P. 525-573.
14. *Belinchon J. A.* Bianchi VI_0 and III Models: Self-Similar Approach // Class. Quant. Grav. 2009. V. 26. P. 175003.
15. *Benaoum H. B.* Accelerated Universe from Modified Chaplygin Gas and Tachyonic Fluid. hep-th/0205140.

16. *Bennett C. L. et al.* First Year Wilkinson Microwave Anisotropy Probe (WMAP) Observations: Preliminary Maps and Basic Results // Astrophys. J. Suppl. Ser. 2003. V. 148. P. 1.

17. *Bento M. C., Bertolami O., Sen A. A.* Generalized Chaplygin Gas, Accelerated Expansion and Dark Energy–Matter Unification // Phys. Rev. D. 2002. V. 66. P. 043507.

18. *Bento M. C., Bertolami O., Sen A. A.* Generalized Chaplygin Gas and CMBR Constraints // Phys. Rev. D. 2003. V. 67. P. 063003.

19. *Bento M. C., Bertolami O., Sen A. A.* WMAP Constraints on the Generalized Chaplygin Gas Model // Phys. Lett. B. 2003. V. 575. P. 172–180.

20. *Berman M. S.* A Special Law of Variation for Hubble Parameter // Nuovo Cim. B. 1983. V. 74. P. 182–186.

21. *Berman M. S., Gomide F. M.* Cosmological Models with Constant Deceleration Parameter // Gen. Rel. Grav. 1988. V. 20. P. 191–198.

22. *Bertolami O.* Challenges to the Generalized Chaplygin Gas Cosmology. astro-ph/0403310.

23. *Bertolami O., Gil Pedro F., Le Delliou M.* Dark Energy–Dark Matter Interaction and Putative Violation of the Equivalence Principle from the Abell Cluster A586 // Phys. Lett. B. 2007. V. 654. P. 165–169.

24. *Biesiada M., Godlowski W., Szydlowski M.* Generalized Chaplygin Gas Models Tested with SNIa // Astrophys. J. 2005. V. 622. P. 28–38; astro-ph/0403305.

25. *Bilic N., Tupper G. B., Viollier R. D.* Unification of Dark Matter and Dark Energy: The Inhomogeneous Chaplygin Gas // Phys. Lett. B. 2002. V. 353. P. 17–21.

26. *Blandford R. D. et al.* Cosmokinetics. arXiv:astro-ph/0408279. 2004.

27. *Bordemann M., Hoppe J.* The Dynamics of Relativistic Membranes I: Reduction to 2-Dimensional Fluid Dynamics // Phys. Lett. B. 1993. V. 317. P. 315–320.

28. *Brans C., Dicke R. H.* Mach's Principle and a Relativistic Theory of Gravitation // Phys. Rev. 1961. V. 124. P. 925–935.

29. *Bronnikov K. A.* Static Cyllindrically-Symmetric Einstein–Maxwell Fields // Problem of Theory of Gravity and Elementary Particles. M.: Atomizdat, 1979. Iss. 10. P. 37–50.

30. *Cai Y. et al.* Bouncing Universe with Quintom Matter // JHEP. 2007. V. 0710. P. 071.

31. *Cai Y., Wang J.* Dark Energy Model with Spinor Matter and Its Quintom Scenario // Class. Quant. Grav. 2008. V. 25. P. 165014.

32. *Caldwell R. R., Dave R., Steinhardt P. J.* Cosmological Imprint of an Energy Component with General Equation of State // Phys. Rev. Lett. 1998. V. 80, No. 8. P. 1582–1585.

33. *Caldwell R. R.* A Phantom Menace? Cosmological Consequences of a Dark Energy Component with Super-Negative Equation of State // Phys. Lett. B. 2002. V. 545. P. 23–29.

34. *Cardenas R. et al.* Model of the Universe Including Dark Energy Accounted for by Both a Quintessence Field and a (Negative) Cosmological Constant // Phys. Rev. D. 2003. V. 67. P. 083501.

35. *Cardenas V. H.* Tachyonic Quintessential Inflation // Phys. Rev. D. 2006. V. 73. P. 103512.

36. *Cervantes-Cota J. L.* Bianchi V Inflation in the Brans–Dicke Theory? arxiv: gr-qc/9912047v1. 1999.

37. *Chaplygin S. A.* On Gas Jet // Scientific Notes of the Department of Physico-Mathematical Science of Moscow University. 1904. Iss. 21. P. 1–112.

38. *Chevallier M., Polarski D.* Accelerating Universes with Dark Matter // Intern. J. Mod. Phys. D. 2001. V. 10. P. 213.

39. *Chauvet P., Cervantes-Cota J. L.* Isotropization of Bianchi Type Cosmological Solutions in Brans–Dicke Theory. arxiv: gr-qc/9502015v1. 1995.

40. *Chiba T., Nakamura T.* The Luminosity Distance, the Equation of State, and the Geometry of the Universe // Progress in Theor. Phys. 1998. V. 100. P. 1077–1082.

41. *Chimento L. P., Mollerach M. S.* Dirac Equation in Bianchi I Metrics // Phys. Lett. A. 1987. V. 121, No. 1. P. 7–10.

42. *Chimento L. P. et al.* Interacting Quintessence Solution to the Coincidence Problem // Phys. Rev. D. 2003. V. 67. P. 083513.

43. *Clocchiatti A. et al.* Hubble Space Telescope and Ground-Based Observations of Type Ia Supernovae at Redshift 0.5: Cosmological Implications // Astrophys. J. 2006. V. 642. P. 1–21.

44. *Colistete R. et al.* Dark Energy, Dark Matter and the Chaplygin Gas. gr-qc/0210079.

45. *Copeland E. J. et al.* What Is Needed of a Tachyon If It Is to Be the Dark Energy? // Phys. Rev. D. 2005. V. 71. P. 043003.

46. *Dabrowski M. P.* Phantom Dark Energy and Its Cosmological Consequences. gr-qc/0701057v1.

47. *Davydov E., Filippov A. T.* Dilaton-Scalar Models in Context of Generalized Affine Gravity Theories: Their Properties and Integrability. arXiv 1302.6969v1 [hep-th]. 2013.

48. *Dev A., Jain D., Alcaniz J. S.* Constraints on Chaplygin Quartessence from the CLASS Gravitational Lens Statistics and Supernova Data // Astron. Astrophys. 2004. V. 417. P. 847–852.

49. *Le Delliou M., Bertolami O., Gil Pedro F.* Dark Energy–Dark Matter Interaction from the Abell Cluster A586 and Violation of the Equivalence Principle // AIP Conf. Proc. 2007. V. 957. P. 421–424.

50. *Dicke H.* Dirac's Cosmology and Mach's Principle // Nature (London). 1961. V. 192, No. 4. P. 440–441.

51. *Diego J. M. et al.* Cosmological Constraints from the Cluster Contribution to the Power Spectrum of the Soft X-Ray Background. New Evidence for a Low σ_8 // Monthly Notice of Royal Astron. Soc. 2003. V. 344. P. 951–964.

52. *Eddington A. S.* // Proc. Roy. Soc. London. 1919. Ser. A. V. 99. P. 742.

53. *Eddington A. S.* Mathematical Theory of Relativity. Cambridge, 1923.

54. *Einstein A.* Kosmologische Betrachtungen zur allgemeinen Relativitätstheorie // Sitzungsber. Preuss. Acad. Wiss. 1917. V. 1. P. 142–152.

55. *Einstein A.* Spielen die Gravitationsfelder im Aufbau der materiellen Elementarteilchen eine wesentliche Rolle? // Sitzungsber. Preuss. Acad. Wiss. 1919. V. 1. P. 349–356.

56. *Einstein A.* Physikalisch-mathematische Klasse // Sitzungsber. Preuss. Acad. Wiss. 1923. V. 2. P. 32–38; 76–77; 137–140.

57. *Einstein A.* Appendix to the Book: Eddington A. S. Relativitäts Theorie in mathematischer Behandlung. Berlin: Springer, 1925.

58. *Fabris J. C., Goncalvez S. V., de Souza P. E.* Density Perturbations in an Universe Dominated by the Chaplygin Gas // Gen. Rel. Grav. 2002. V. 34. P. 53–63.

59. *Fabris J. C., Goncalvez S. V., de Souza P. E.* Mass Power Spectrum in a Universe Dominated by the Chaplygin Gas // Ibid. P. 2111–2126.

60. *Fay S.* Sufficient Conditions for Curvature Invariants to Avoid Divergences in Hyperextended Scalar–Tensor Theory for Bianchi Models // Class. Quant. Grav. 2000. V. 17. P. 2663–2673.

61. *Fay S.* Generalized Scalar–Tensor Theory in the Bianchi Type-I Model // Gen. Rel. Grav. 2000. V. 32. P. 187–202.

62. *Felder G. et al.* Cosmology with Negative Potentials // Phys. Rev. D. 2002. V. 66. P. 023507.

63. *Feng B., Wang X., Zhang X.* Dark Energy Constraints from the Cosmic Age and Supernova // Phys. Lett. B. 2005. V. 607. P. 35–41.

64. *Fierz M.* Zur Fermischen Theorie des β-Zerfalls // Zeit. Phys. A. Hadrons and Nuclei. 1937. V. 104. P. 553–565.

65. *Filippov A. T.* The Weyl–Eddington–Einstein Affine Gravity in the Context of Modern Cosmology // Theor. Math. Phys. 2010. V. 163, No. 3. P. 430–448.

66. *Filippov A. T.* Some Unusual Dimension Reductions of Gravity: Geometric Potentials, Separation of Variables, and Static–Cosmological Duality. arXiv 060527v2 [hep-th]. 2006.

67. *Filippov A. T.* Unified Description of Cosmological and Static Solutions in Affine Generalized Theories of Gravity: Vector–Scalar Duality and Its Applications. arXiv 1302.6372v2 [hep-th]. 2013.

68. *Friedmann A. A.* Uber die Krummung des Raumes // Z. Phys. 1922. V. 10. P. 377–386.

69. *Friedmann A. A.* Uber die Moglichkeit einer Welt mit konstanter negativer Krummung des Raumes // Z. Phys. 1924. V. 21. P. 326–332.

70. *Gannouji R. et al.* Scalar–Tensor Dark Energy Models. arXiv: astro-phys/0701650v1. 2007.

71. *Gannouji R. et al.* Scalar–Tensor Models of Normal and Phantom Dark Energy // J. Cosmol. Astropart. Phys. JCAP. 2006. V. 09. P. 016.

72. *Germani C., Tsagas C. G.* Magnetized Tolman–Bondi Collapse // Phys. Rev. D. 2006. V. 73. P. 064010.

73. *Gibbons G. W.* Pulse Propagation in Born–Infeld Theory, the World Volume Equivalence Principle and the Hagedorn-Like Equation of State of the Chaplygin Gas // Grav. Cosmol. 2002. V. 8. P. 2–6.

74. *Gonzalez T., Quiros I.* Exact Models with Non-Minimal Interaction between Dark Matter and (Either Phanton or Quintessence) Dark Energy. arXiv:gr-qc/0707.2089v1.

75. *Gorini V., Kamenshchik A., Moschella U.* Can the Chaplygin Gas Be a Plausible Model for Dark Energy? // Phys. Rev. D. 2003. V. 67. P. 063509.

76. *Gorini V. et al.* The Chaplygin Gas as a Model for Dark Energy. gr-qc/0403062.

77. *Guo Z. K., Ohta N., Tsujikawa S.* Probing the Coupling between Dark Components of the Universe // Phys. Rev. D. 2007. V. 76. P. 023508.

78. *Guth A.* Inflationary Universe: A Possible Solution to the Horizon and Flatness Problems // Phys. Rev. D. 1981. V. 23. P. 347–356.

79. *Hassaine M., Horvathy P. A.* Chaplygin Gas with Field-Dependent Poincare Symmetry // Lett. Math. Phys. 2001. V. 57. P. 33–40.

80. *Hassaine M.* Supersymmetric Chaplygin Gas // Phys. Lett. A. 2001. V. 290. P. 157–164.

81. *Hawking S. W., Taylor R. J.* Helium Production in Anisotropic Big Bang Universe // Nature. 1966. V. 299. P. 1278.

82. *Hinshaw G. et al.* Five-Year Wilkinson Microwave Anisotropy Probe (WMAP) Observations: Data Processing, Sky Maps, and Basic Results // Astrophys. J. Suppl. Ser. 2009. V.180. P. 225–245.

83. *Horvath Z., Kovacs Z.* Canonical Theory of the Kantowski–Sachs Cosmological Models // Astron. Deparment of Eotvos Univ. (PADEU). 2006. V. 17. P. 229–234.

84. *Hu B. L., Parker L.* Anisotropy Damping through Quantum Effects in the Early Universe // Phys. Rev. D. 1978. V. 17. P. 933–945.

85. *Hu B. L.* Gravitational Waves in a Bianchi Type-I Universe // Phys. Rev. D. 1978. V. 18, No. 4. P. 969–982.

86. *Huterer D., Turner M. S.* Probing Dark Energy: Methods and Strategies // Phys. Rev. D. 2001. V. 64. P. 123527.

87. *Ibáñez J., van der Hoogen R. J., Coley A. A.* Isotropization of Scalar Field Bianchi Models with an Exponential Potential // Phys. Rev. D. 1995. V. 51. P. 928–930.

88. *Jackiw R.* A Particle Field Theorist's Lectures on Supersymmetric, Non-Abelian Fluid Mechanics and *D*-Branes. physics/0010042.

89. *Jacobs K. C.* Spatially Homogeneous and Euclidean Cosmological Models with Shear // Astrophys. J. 1968. V. 153, No. 2. P. 661–678.

90. *Jordan P.* Zum Gegenwartigen Stand der Diracschen kosmologischen Hypothesen // Zeit. Phys. A. Hadrons and Nuclei. 1959. V. 157. P. 112–121.

91. *Kamenshchik A. Yu., Moschella U., Pasquier V.* An Alternative to Quintessence // Phys. Lett. B. 2001. V. 511, No. 2–4. P. 265–268.

92. *Kantowski R., Sachs R. K.* Some Spatially Homogeneous Anisotropic Relativistic Cosmological Models // J. Math. Phys. 1966. V. 7. P. 443–446.

93. *Knop R. K. et al.* New Constraints on Ω_M, Ω_N, and w from an Independent Set of Eleven High-Redshift Supernovae Observed with HST // Astrophys. J. 2003. V. 598. P. 102.

94. *Komatsu E. et al.* Five-Year Wilkinson Microwave Anisotropy Probe (WMAP) Observations: Cosmological Interpretation // Astrophys. J. Suppl. Ser. 2009. V. 180. P. 330–376.

95. *Krechet V. G., Fil'chenkov M. L., Shikin G. N.* Equivalence between the Descriptions of Cosmological Models Using a Spinor Field and a Perfect Fluid // Grav. Cosmol. 2008. V. 14, No. 3(55). P. 292–294.

96. *Kremer G. M.* Irreversible Processes in a Universe Modelled as a Mixture of a Chaplygin Gas and Radiation // Gen. Rel. Grav. 2003. V. 35. P. 1459–1466.

97. *Kristian J., Sachs R. K.* Observations in Cosmology // Astrophys. J. 1966. V. 143. P. 379–399.

98. *Kumar S., Yadav A. K.* Some Bianchi Type-V Models of Accelerating Universe with Dark Energy // Mod. Phys. Lett. A. 2011. V. 26. P. 647.

99. *Lemaitre G. H.* l'Univers en Expansion // Ann. Soc. Sci. Brux. A. 1933. V. 53. P. 51–85.

100. *Linder E. V.* Exploring the Expansion History of the Universe // Phys. Rev. Lett. 2003. V. 90. P. 91301.

101. *Linder E. V.* On Oscillating Dark Energy // Astropart. Phys. 2006. V. 25, No. 2. P. 167–171.

102. *Linder E. V.* The Dynamics of Quintessence, the Quintessence of Dynamics // Gen. Rel. Grav. 2008. V. 40. P. 329–356.

103. *Lukas V. N., Starobinskii A. A.* Isotropization of Cosmological Expansion Due to Particle Creation // J. Exp. Theor. Phys. 1974. V. 66. P. 1515–1527.

104. *MacCallum M. A. H.* Anisotropic and Inhomogeneous Cosmologies. gr-qc/9212914. 1992.

105. *Multamaki T., Manera M., Gaztanaga E.* Large Scale Structure and the Generalized Chaplygin Gas as Dark Energy // Phys. Rev. D. 2004. V. 69. P. 023004.

106. *Nojiri S., Odintsov S. D.* The Oscillating Dark Energy: Future Singularity and Coincidence Problem // Phys. Lett. B. 2006. V. 637, No. 3. P. 139–148.

107. *Ogawa N.* A Note on Classical Solution of Chaplygin Gas as D-Brane // Phys. Rev. D. 2000. V. 62. P. 085023.

108. *Olivares G., Atrio-Barandela F., Pavon D.* Observational Constraints on Interacting Quintessence Models // Phys. Rev. D. 2005. V. 71. P. 063523.

109. *Padmanabhan T.* Cosmological Constant — the Weight of the Vacuum // Phys. Rep. 2003. V. 380, No. 5-6. P. 235–320.

110. *Pavon D., Sen S., Zimdahl W.* CMB Constraints on Interacting Cosmological Models // J. Cosmol. Astropart. Phys. 2004. V. 0405. P. 009.

111. *Pavon D., Wang B.* Le Chtelier–Braun Principle in Cosmological Physics // Gen. Rel. Grav. 2009. V. 41. P. 1–5.

112. *Perlmutter S. et al.* Discovery of a Supernova Explosion at Half the Age of the Universe // Nature. 1998. V. 391. P. 51–54.

113. *Perlmutter S. et al. The Supernova Cosmology Project.* Measurements of Ω and Λ from 42 High-Redshift Supernovae // Astrophys. J. 1999. V. 517. P. 565–586.

114. *Pradhan A., Amirhashchi H., Saha B.* Bianchi Type-I Anisotropic Dark Energy Model with Constant Deceleration Parameter // Intern. J. Theor. Phys. 2011. V. 50. P. 2923–2938.

115. *Pradhan A., Amirhashchi H., Saha B.* An Interacting and Non-Interacting Two-Fluid Scenario for Dark Energy in FRW Universe with Constant Deceleration Parameter // Astroph. Space Sci. 2011. V. 333. P. 343–350.

116. *Pradhan A., Amirhashchi H., Zainuddin H.* Exact Solution of Perfect Fluid Massive String Cosmology in Bianchi Type III Space–Time with Decaying Vacuum Energy Density? // Ibid. V. 331. P. 679–687.

117. *Pradhan A., Lata S., Amirhashchi H.* Massive String Cosmology in Bianchi Type III Space–Time with Electromagnetic Field // Commun. Theor. Phys. 2010. V. 54. P. 950.

118. *Rapetti D. et al.* A Kinematical Approach to Dark Energy Studies // Monthly Notice of Roy. Astron. Soc. 2007. V. 375. P. 1510–1520.

119. *Ribas M. O., Devecchi F. P., Kremer G. M.* Fermions as Sources of Accelerated Regimes in Cosmology // Phys. Rev. D. 2005. V. 72. P. 123502.

120. *Riess A. G. et al.* Observational Evidence from Supernovae for an Accelerating Universe and a Cosmological Constant // Astron. J. 1998. V. 116. P. 1009–1038.

121. *Riess A. G. et al.* Type Ia Supernova Discoveries at $z > 1$ from the Hubble Space Telescope: Evidence for Past Deceleration and Constraints on Dark Energy Evolution // Astrophys. J. 2004. V. 607. P. 665–687.

122. *Robertson H. P.* Kinematics and World Structure // Astrophys. J. 1935. V. 82. P. 284.

123. *Robertson H. P.* Kinematics and World Structure II // Astrophys. J. 1936. V. 83. P. 187.

124. *Robertson H. P.* Kinematics and World Structure III // Ibid. P. 257.

125. *Rubano C., Scudellaro P., Piedipalumbo E.* Oscillating Dark Energy: A Possible Solution to the Problem of Eternal Acceleration // Phys. Rev. D. 2003. V. 68. P. 123501.

126. *Rybakov Yu. P., Saha B., Shikin G. N.* Solitons of Nonlinear Scalar Electrodynamics in General Relativity // Intern. J. Theor. Phys. 1997. V. 36, No. 6. P. 1475–1494.

127. *Saha B.* Dirac Spinor in Bianchi-I Universe with Time-Dependent Gravitational and Cosmological Constants // Mod. Phys. Lett. A. 2001. V. 16, No. 20. P. 1287–1296.

128. *Saha B.* Spinor Field in Bianchi Type-I Universe: Regular Solutions // Phys. Rev. D. 2001. V. 64. P. 123501.

129. *Saha B.* Nonlinear Spinor Field in Cosmology // Phys. Rev. D. 2004. V. 69. P. 124006.

130. *Saha B.* Spinor Field with Induced Nonlinearity in Bianchi VI Cosmology: Exact and Numerical Solutions // Grav. Cosmol. 2010. V. 16, No. 2. C. 160–167.

131. *Saha B.* Spinor Fields in Bianchi Type-I Universe // Phys. Part. Nucl. 2006. V. 37. Suppl. 1. P. S13–S44.

132. *Saha B.* Bianchi Type Universe with Viscous Fluid // Mod. Phys. Lett. A. 2005. V. 20, No. 28. P. 2127–2143.

133. *Saha B.* Nonlinear Spinor Field in Bianchi Type-I Universe Filled with Viscous Fluid: Some Special Solutions // Rom. Rep. Phys. 2005. V. 57, No. 1. P. 7–24.

134. *Saha B.* Nonlinear Spinor Field in Bianchi Type-I Universe Filled with Viscous Fluid: Numerical Solutions // Astrophys. Space Sci. 2007. V. 312. P. 3–11.

135. *Saha B.* Interacting Spinor and Scalar Fields in Bianchi Type-I Universe Filled with Viscous Fluid: Exact and Numerical Solutions // Grav. Cosmol. 2009. V. 25, No. 4. P. 353–361.

136. *Saha B.* Anisotropic Cosmological Models with Perfect Fluid and Dark Energy // Chin. J. Phys. 2005. V. 43, No. 6. P. 1035–1043.

137. *Saha B.* Anisotropic Cosmological Models with a Perfect Fluid and a Λ Term // Astroph. Space Sci. 2006. V. 302. P. 83–91.

138. *Saha B.* Anisotropic Cosmological Models with Perfect Fluid and Dark Energy Reexamined // Intern. J. Theor. Phys. 2006. V. 45, No. 5. P. 983–995.

139. *Saha B.* Spinor Field and Accelerated Regimes in Cosmology // Grav. Cosmol. 2006. V. 12, Nos. 2–3(46–47). P. 215–218.

140. *Saha B.* Nonlinear Spinor Field in Bianchi Type-I Cosmology: Inflation, Isotropization, and Late-Time Acceleration // Phys. Rev. D. 2006. V. 74. P. 124030.

141. *Saha B.* Nonlinear Spinor Field in Bianchi Type-I Cosmology: Accelerated Regimes // Rom. Rep. Phys. 2007. V. 59, No. 2. P. 649–660.

142. *Saha B.* Early Inflation, Isotropization and Late-Time Acceleration of a Bianchi Type-I Universe // Phys. Part. Nucl. 2009. V. 40. P. 656–673.

143. *Saha B.* Spinor Model of a Perfect Fluid // Central Eur. J. Phys. 2010. V. 8. P. 920–923.

144. *Saha B.* Spinor Model of a Perfect Fluid: Examples // Rom. Rep. Phys. 2010. V. 62. P. 209–216.

145. *Saha B.* Spinor Model of a Perfect Fluid and Their Applications in Bianchi Type-I and FRW Models // Astrophys. Space Sci. 2011. V. 331. P. 243–255.

146. *Saha B.* Nonlinear Spinor Fields and Its Role in Cosmology // Intern. J. Theor. Phys. 2012. V. 51. P. 1812–1837.

147. *Saha B.* Bianchi Type-II Cosmological Model: Some Remarks // Central Eur. J. Phys. 2011. V. 9. P. 939–941, DOI: 10.2474/s11534-011-0017-4.

148. *Saha B.* Some Remarks on Bianchi Type-II, VIII and IX Models // Grav. Cosmol. 2013. V. 19, No. 1. P. 65–69.

149. *Saha B.* Bianchi Type-VI Anisotropic Dark Energy Model with Varying EoS Parameter // Intern. J. Theor. Phys. 2013; (online first). arXiv: 1209.6029 [gr-qc]. 2012.

150. *Saha B.* Bianchi Type-V Dark Energy Model with Varying EoS Parameter // Intern. J. Theor. Phys. 2013. V. 52. P. 1314–1325.

151. *Saha B.* Some Problems of Modern Cosmology and Spinor Field // Bull. of PFUR. Ser. «Mathematics, Information Sciences, Physics». 2012. No. 4. P. 170–180.

152. *Saha B.* Nonlinear Spinor Fields in Bianchi Type-I Space–Time Reexamined. arXiv: 1302.1354 [gr-qc]. 2013.

153. *Saha B., Amirhashchi H., Pradhan A.* Two-Fluid Scenario for Dark Energy Models in an FRW Universe-Revisited // Astrophys. Space Sci. 2012. V. 342. P. 257–267.

154. *Saha B., Boyadjiev T.* Bianchi Type-I Cosmology with Scalar and Spinor Fields // Phys. Rev. D. 2004. V. 69. P. 124010.

155. *Saha B., Rikhvitsky V.* Bianchi Type-I Universe with Viscous Fluid and a Λ Term: A Qualitative Analysis // Physica D. 2006. V. 219. P. 168–176.

156. *Saha B., Rikhvitsky V.* Anisotropic Cosmological Models with Spinor Field and Viscous Fluid in Presence of a Λ Term: Qualitative Solutions // J. Phys. A: Math. and Theor. 2007. V. 40. P. 14011–14027.

157. *Saha B., Rikhvitsky V.* Anisotropic Cosmological Models with Spinor and Scalar Fields and Viscous Fluid in Presence of a Λ Term: Qualitative Solutions // J. Math. Phys. 2008. V. 49. P. 112502.

158. *Saha B., Rikhvitsky V. S.* Nonlinear Spinor Fields in Anisotropic Universe Filled with Viscous Fluid: Exact Solutions and Qualitative Analysis // Phys. Part. Nucl. 2009. V. 40. P. 612–655.

159. *Saha B., Shikin G. N.* Nonlinear Spinor Field in Bianchi Type-I Universe Filled with Perfect Fluid: Exact Self-Consistent Solutions // J. Math. Phys. 1997. V. 38, No. 10. P. 5305–5318.

160. *Saha B., Shikin G. N.* Interacting Spinor and Scalar Fields in Bianchi Type-I Universe Filled with Perfect Fluid: Exact Self-Consistent Solutions // Gen. Rel. Grav. 1997. V. 29, No. 9. P. 1099–1112.

161. *Saha B., Shikin G. N.* On the Role of Λ Term in the Evolution of Bianchi-I Cosmological Model with Nonlinear Spinor Field // PFU Reports: Phys. 2000, No. 8. P. 17–20.

162. *Saha B., Shikin G. N.* Nonlinear Spinor Field: Plane-Symmetric Solutions // J. Theor. Math. Comp. Phys. 2002. V. 5, No. 1. P. 54–71.

163. *Saha B., Shikin G. N.* Plane-Symmetric Solitons of Spinor and Scalar Fields // Czech. J. Phys. 2004. V. 54, No. 6. P. 597–620.

164. *Saha B., Shikin G. N.* Static Plane-Symmetric Nonlinear Spinor and Scalar Fields in GR // Intern. J. Theor. Phys. 2005. V. 44, No. 9. P. 1459–1494.

165. *Saha B., Visinescu M.* Bianchi Type-VI Model with Cosmic Strings in the Presence of a Magnetic Field // Rom. J. Phys. 2010. V. 55. P. 1064–1074.

166. *Saha B., Yadav A. K.* Dark Energy Model with Variable q and ω in LRS Bianchi-II Space–Time // Astrophys. Space Sci. 2012. V. 341. P. 651–656.

167. *Sahni V.* Dark Matter and Dark Energy // Lecture Notes on Phys. 2004. V. 653. P. 141–180; astro-ph/0403324.

168. *Sahni V., Starobinsky A. A.* The Case for a Positive Cosmological Λ Term // Intern. J. Mod. Phys. D. 2000. V. 9, No. 4. P. 373–443.

169. *Sahni V. et al.* Statefinder — a New Geometrical Diagnostic of Dark Energy // JETP Lett. 2003. V. 77. P. 243–248.

170. *Sandvik H. et al.* The End of Unified Dark Matter? astro-ph/0212114.

171. *Sen A.* Rolling Tachyon // JHEP. 2002. V. 0204. P. 048.

172. *Sen A.* Field Theory of Tachyon Matter // Mod. Phys. Lett. A. 2002. V. 17. P. 1797–1804.

173. *Setare M. R., Zhang J., Zhang X.* Statefinder Diagnosis in a Nonflat Universe and the Holographic Model of Dark Energy // J. Cosmol. Astropart. Phys. 2007. V. 0703. P. 007.

174. *Shao Y., Gui Y.* Statefinder Parameters for Tachyon Dark Energy Model. arXiv:gr-qc/0703111v1.

175. *Shao Y., Gui Y. X., Wang W.* Parameterization of Tachyon Field // Mod. Phys. Lett. A. 2007. V. 22. P. 1175–1181.

176. *Shikin G. N.* Interacting Scaler and Electromagnetic Fields: Static Cyllindrically-Symmetric Solutions with Gravitation // Problem of Theory of Gravity and Elementary Particles. M.: Atomizdat, 1984. Iss. 14. P. 85–97.

177. *Singh T., Agrawal A. K.* Homogeneous Anisotropic Cosmological Models with Variable Gravitational and Cosmological Constants // Intern. J. Theor. Phys. 1993. V. 32, No. 6. P. 1041–1059.

178. *Socorro J., Medina E. R.* Supersymmetric Quantum Mechanics for Bianchi Class A Models // Phys. Rev. D. 2000. V. 61. P. 087702.

179. *de Souza R. C., Kremer G. M.* Noether Symmetry for Nonminimally Coupled Fermion Fields // Class. Quant. Grav. 2008. V. 25. P. 225006.

180. *Srivastava S. K.* Tachyon as a Dark Energy. arXiv:gr-qc/0409074v4.

181. *Steinhardt P. J., Turok N.* Cosmic Evolution in a Cyclic Universe // Phys. Rev. D. 2002. V. 65. 126003.

182. *Szydlowski M., Czja W.* Stability of FRW Cosmology with Generalized Chaplygin Gas // Phys. Rev. D. 2004. V. 69. P. 023506.

183. *Taub A. H.* Empty Space–Times Admitting a Three-Parameter Group of Motions // Ann. Math. 1951. V. 53, No. 3. P. 472–490.

184. *Taub A. H.* Isentropic Hydrodynamics in Plane Symmetric Space–Times // Phys. Rev. 1956. V. 103. P. 454–467.

185. *Tegmark M. et al.* The 3D Power Spectrum of Galaxies from the SDSS // Astrophys. J. 2004. V. 606. P. 702–740.

186. *Tegmark M. et al.* Cosmological Parameters from SDSS and WMAP // Phys. Rev. D. 2004. V. 69. P. 103501.

187. *Thorne K. S.* Effect of a Primordial Magnetic Field on the Dynamics of the Universe // Bull. Am. Phys. Soc. 1966. V. 11. P. 340.

188. *Thorne K. S.* Primordial Element Formation, Primordial Magnetic Fields, and the Isotropy of the Universe // Astrophys. J. 1967. V. 148, No. 1. P. 51–68.

189. *Tonry J. L. et al.* Cosmological Results from High-z Supernovae // Astrophys. J. 2003. V. 594. P. 1–24.

190. *Vakili B., Sepangi H. R.* Time Reparameterization in Bianchi Type-I Spinor Cosmology // Ann. Phys. 2008. V. 323. P. 548–565.

191. *Vishwakarma R. G.* A Study of Angular Size-Redshift Relation for Models in Which Decays as the Energy Density // Class. Quant. Grav. 2000. V. 17. P. 3833.

192. *Visser M.* Jerk, Snap and the Cosmological Equation of State // Class. Quant. Grav. 2004. V. 21. P. 2603.

193. *Visser M.* Cosmography: Cosmology without the Einstein Equations // Gen. Rel. Grav. 2005. V. 37. P. 1541–1548.

194. *Walker A. G.* On Milne's Theory of World Structure // Proc. of the London Math. Soc. 1937. V. 42. P. 90–127.

195. *Weaver M.* Big-Bang Model without Singularities // Class. Quant. Grav. 2000. V. 17. P. 421–434.

196. *Weaver M.* Dynamics of Magnetic Bianchi VI_0 Cosmologies // Class. Quant. Grav. 2009. V. 17. P. 421.

197. *Weinberg S.* The Cosmological Constant Problem // Rev. Mod. Phys. 1989. V. 61. P. 1–23.

198. *Weller J., Albrecht A.* Future Supernovae Observations as a Probe of Dark Energy // Phys. Rev. D. 2002. V. 65. P. 103512.

199. *Weyl H.* Raum-Zeit-Materie. 1918 (English Translation. 1950).

200. *Will C. M.* Theory and Experiment in Gravitational Physics. Cambridge Univ. Press, 2001; arXiv:gr-qc/0103036.

201. *Yadav A. K., Saha B.* LRS Bianchi-I Anisotropic Cosmological Model with Dominance Dark Energy // Astrophys. Space Sci. 2012. V. 337. P. 759–765.

202. *Yadav A. K., Yadav L.* Bianchi Type-III Anisotropic Dark Energy Models with Constant Deceleration Parameter // Intern. J. Theor. Phys. 2011. V. 50. P. 218–227.

203. *Yadav A. K., Rahaman F., Ray S.* Dark Energy Models with Variable Equation of State Parameter // Ibid. P. 871–881.

204. *Yadav A. K.* Some Anisotropic Dark Energy Models in Bianchi Type-V Space–Time // Astrophys. Space Sci. 2011. V. 335 P. 565–575.

205. *Yadav M. K., Rai A., Pradhan A.* Some Bianchi Type-III String Cosmological Models with Bulk Viscosity // Intern. J. Theor. Phys. 2007. V. 46. P. 2677–2687.

206. *Yadav A. K., Yadav L.* Bianchi Type-III Anisotropic Dark Energy Models with Constant Deceleration Parameter // Intern. J. Theor. Phys. 2011. V. 50. P. 218–227.

207. *Zeyauddin M., Saha B.* Bianchi Type-VI Cosmological Model: A Scale-Covariant Study // Astrophys. Space Sci. 2013. V. 343. P. 445–450; DOI: 10.1007/s 10509-0-12-1228-x.arXiv: 1205.5655 [gr-qc].

208. *Zeldovich Ya. B.* Magnetic Models of the Universe // J. Exp. Theor. Phys. 1970. V. 48. P. 986–988.

209. *Zeldovich Ya. B.* Particle Creation in Cosmology // J. Exp. Theor. Phys. Lett. 1970. V. 12. P. 443–447.

210. *Zlatev I., Wang L., Steinhardt P. J.* Quintessence, Cosmic Coincidence, and the Cosmological Constant // Phys. Rev. Lett. 1999. V. 82, No. 5. P. 896–899.